

CONDUCTIVE POLYMER AND SYNTHETIC POLYMER BASED NANOPARTICLE FOR
REMOVAL OF HEXAVALENT CHROMIUM AND ARSENIDE FROM AQUEOUS SOLUTION

by

NATHANIEL TLOU MOJA

submitted in accordance with the requirements for
the degree of

MASTER OF SCIENCE

In the subject

CHEMISTRY

at the

University of South Africa

Supervisor: Prof Bhardwaj Shivani Mishra

Co-supervisor: Prof Ajay Kumar Mishra

Date submitted: **February 2017**

DEDICATION

I dedicate this research work to my Dad and Mom, Mr David Mashishi Moja and Mrs. Jane Katlego Moja, respectively, for bringing me up to be a complete person. May the Almighty Father in Heaven bless you in everything you do! And to my lovely siblings, Mahlako Mary Moja and Khutso Anna Moja. To my lovely girlfriend, Paballo Felicia Mputle, you are such an amazing figure in my life; I lack words to describe you adequately, many thanks for being there for me always, your patience will pay abundantly, I Love You.

ACKNOWLEDGEMENT

My sincere appreciation goes to the following individuals and institutions for their wonderful contribution towards this research work: My supervisor, Prof. B Shivani. Dr. E Vunain for his encouragement, guidance and criticism of this work, which made me dig deeper and understand the important dimensions of this study. My Co-supervisor, Prof. A.K Mishra who introduced me to nanocomposites and their synthetic methods and for his valuable guidance towards this work. The University of South Africa for offering me an opportunity to study and the National Research Foundation–South Africa (NRF-SA) for their financial support. My colleagues with whom we worked together: Dr Gcina Mamba, Dr Hlengilizwe Nyoni, Ms. Nozipho Nontsikelelo Gumbi, Ms Dineo Anna Bopape, Mr. Jafta Tsiepe, Mr Kamogelo Seema, and Mr Sabastian Mukonza, for their moral support and technical advice.

PUBLICATIONS AND PRESENTATIONS

T.N Moja, B Shivani, A.K Mishra”Fe₃O₄/PPy/PvOH polymer nanocomposite for removal of As(III) from aqueous water. Manuscript in preparation

T.N Moja, B Shivani, A.K Mishra”Fe₃O₄/PPy/PvOH polymer nanocomposite for removal of Cr(VI) from aqueous water. Manuscript in preparation

Conferences and presentations attended:

- **NYRS** (National young research symposium): presented my research titled “The use of conductive polymer and synthetic polymer based nanocomposite for removal of toxic metals from wastewater”. The aim of the talk was to reach out to the science community to alert them about the health risks caused by Cr(VI) and how it can be removed using polymer nanocomposites.
- **FameLab**: presented my research in 5 minutes, to communicate the importance of removing the toxic metals from water and wastewater, and how these contaminants can be introduced into the food chain and our bodies.
- **Taiwan Conference**: presented my research work titled “Synthesis and characterization of conducting polypyrrole/polyvinyl alcohol incorporated with magnetite nanoparticle”. The conference was held at UNISA (Florida Campus).

ABSTRACT

In order to address the issue of water contamination by toxic and carcinogenic hexavalent chromium and arsenite species, a new polymer nanocomposite (PNC) was fabricated with blend of polypyrrole (PPy)/polyvinyl alcohol (PvOH) and reinforcement of magnetite nanoparticles (Fe_3O_4). PNC was designed to selectively remove Cr (VI) and As (III) ions from aqueous solutions using adsorption and magnetic separation technology. The conductive electroactive PPy was synthesized by *in situ* polymerization of pyrrole monomers using FeCl_3 as an oxidant. the PvOH was prepared by hydrolysing polyvinyl acetate dissolved in ethanol with potassium hydroxide and Fe_3O_4 nanoparticle was synthesized by co-precipitation in the presence of Fe (II) and Fe (III) ions as precursors in solution with ration 1:2. Thereafter, the polymer nanocomposite was prepared solution blending method.

The PNC was characterized using fourier transform infrared (FT-IR) to identify the functional groups present in the compound, x-ray diffraction (XRD) to confirm the degree of crystallinity and the crystal orientation, scanning electrode microscope (SEM) to determine the surface morphology, transmission electron microscopy (TEM) for analysis of the internal morphology and braunner emmet tellet (BET) for analysis of the pore size and surface area. The adsorption studies will be carried out after optimization of effect of pH on adsorption kinetics experiment will be conducted by varying adsorbent grade, adsorbent mass and initial Cr (VI) concentration.

Adsorption kinetics studies were performed under batch operation mode and the influence of PvOH polymer and magnetic content in the nanocomposite, individual constituent components, adsorbent dose and initial Cr (VI) concentration were all explored at room temperature and constant pH 12. It was revealed that the ratios of constituent components in the polymer blend significantly increased the adsorption process whereby 56:42 PPy-PvOH nanocomposite performed better [96%, 30 ppm] than 74:26, 64:36, and 52:48 polymer blend. The 56:44 polymer blend performance was exemplary compared to its constituent components. Fe_3O_4 was introduced to the blend in order to increase the polymer blend efficiency. However, a slight decrease in the removal percentage was observed after adding 2% of Fe_3O_4 nanoparticle. This may be due to particle agglomeration of the nanoparticle. Adsorption capacity of the nanocomposite increased

with increase in adsorbent dosage and increase in initial Cr (VI) concentration and reached maximum at 91% removal efficiency. When adsorption kinetic data was fitted to both linear and nonlinear kinetic models, it was established that adsorption of Cr (VI) on PPy-PvOH- Fe₃O₄ is through a chemisorption process and that intra-particles played a key role in controlling the adsorption process in both cases that includes Cr(VI) and As(III). Furthermore, results revealed that by using 10 ml of 30ppm Cr (VI) aqueous solution with 0.12g at 45 minutes and pH 12 optimum conditions, the Cr (VI) removal of was sufficient and achieved 91.3%. And also using 10 ml of 150 ppm of As(III) aqueous solution with 0.10g at 30 minutes and pH 12 optimum conditions. The removal of As(III) from aqueous solution was also sufficient and 100% removal under the optimal conditions.

Keywords: blend, nanocomposite, polypyrrole, polyvinyl alcohol, magnetite, adsorption, removal, arsenic, chromium, isotherms.

LIST OF ABBREVIATION

As - Arsenic
Ch - Chitin
Cr - Chromium
Cu - Copper
ICP – Inductive coupled plasma
MCL-Maximum contaminant level
NC - Nanocomposite
Ni - Nickel
NP - Nanoparticle
PAN - polyacrylonitrile
PANI - Polyaniline
PEG - Polyethylene glycol
PG - phosphogypsum
PNC – Polymer nanocomposite
PPy - Polypyrrole
PVC – Polyvinyl chloride
PvOH – Poly vinyl alcohol
Py - Pyrrole
SD - sawdust
US-EPA- United states – environmental protection agency
WHO – World health organization

LIST OF FIGURES

Figure 2.1: Chemical structure of Trivalent and hexavalent chromium	12
Figure 2.2: A Diagram illustrating the Speciation of Cr (VI) as a function of pH	13
Figure 2.3: Chemical structure of the poisonous arsenic acid and arsenous acid	15
Figure 2.4: A schematic diagram of adsorption technique used to remove Cr(VI) and As(III) by PPy-PvOH-Fe ₃ O ₄	18
Scheme 2.5: Oxidative polymerization of pyrrole to form polypyrrole	20
Figure 2.6: Preparation of PvOH	22
Figure 2. 7: The structure of Magnetite (Fe ₃ O ₄)	25
Figure 2.8: Evolution of magnetic separation technology	25
Figure 2.1: An image of the set up for the preparation of magnetite.....	47
Figure 4.1: FTIR analysis of Fe ₃ O ₄ nanoparticle.....	57
Figure 4.2: FTIR analysis of PPy-PvOH blend, and Fe ₃ O ₄ -PPy-PvOH nanocomposite.....	58
Figure 4.3: TGA analysis of Fe ₃ O ₄ , PPy-PvOH, and Fe ₃ O ₄ -PPy-PvOH.....	59
Figure 4.4: DSC analysis of PPy-PvOH (56:44) polymer blend	60
Figure 4.5: DSC analysis of the PPy-PvOH-Fe ₃ O ₄ (56:42:2) nanocomposites and the filler material	61
Figure 4.6: The Zeta potential of Fe ₃ O ₄ -PPy-PvOH.....	62
Figure 4.7: SEM imaging of (a) 100 nm of PPy-PvOH, (b) 50 nm PPy-PvOH, (c) 100 nm Fe ₃ O ₄ -PPy-PvOH, (d) 50 nm Fe ₃ O ₄ -PPy-PvOH, (e).....	63
Figure 4.8: The XRD pattern of Fe ₃ O ₄	66
Figure 4.9: The XRD pattern of PPy-PvOH polymer blend.....	66
Figure 4.10: The XRD pattern of Fe ₃ O ₄ -PPy-PvOH nanocomposites	67
Figure 4.11: Swelling capacity of PPy-PvOH-Fe ₃ O ₄ nanocomposite with ratio 56:42:2 in deionized water.....	68
Figure 4.12: Swelling capacity of PPy-PvOH-Fe ₃ O ₄ nanocomposite with ratio 56:42:2 with variation of pH	69

Figure 4.13: pH dependent performance characteristics of PPy-PvOH-Fe ₃ O ₄ (56:42:2) nanocomposite, on Cr(VI) and As(III) adsorption, using 0.12g ; 0.10g; and 30 ppm and 150 ppm respectively	70
Figure 4.14: concentration dependent performance characteristics of 74:26, 64:36, 56:44, and 52:48 polymer blend on Cr(VI) adsorption, temp 25 C at pH 2	71
Figure 4.15: Concentration dependent performance characteristics of PPy-PvOH-Fe ₃ O ₄ 56:42:2 nanocomposite, on Cr(VI) and As(III) adsorption, temp 25 C at pH 12	72
Figure 4.16: Dose dependent performance characteristics of PPy-PvOH-Fe ₃ O ₄ 56:42:2 nanocomposite, on Cr(VI) and As(III) adsorption, temp 25 C at 30 ppm and 150 ppm respectively, and pH 12.....	73
Figure 4.17: Variation of Cr(VI) amount adsorbed with time using 56:42:2 PPy-PvOH-Fe ₃ O ₄ nanocomposite.	74
Figure 4.18: Time dependent performance characteristics of 56:42:2 nanocomposite, on Cr(VI) and As(III) adsorption at temp 25 °C, pH 12, 0.12g and 0.10g , 30ppm and 150ppm respectively.	75
Figure 4.19: Linearized fits for (a) Langmuir and (b) Freundlich isotherm 150 ppm of As (III), 0.10 g of 56:42:2 PPy-PvOH-Fe ₃ O ₄ polymer nanocomposites.....	78
Figure 4.20: Linearized fits for Langmuir and Freundlich isotherm 30 ppm of Cr (VI), 0.12 g of 56:42:2 PPy-PvOH-Fe ₃ O ₄ nanocomposite, 25C.....	78
Figure 4.21: First and Second order kinetic model of As(III) removal from aqueous solutions..	82
Figure 4.22: First and Second order kinetic model of Cr(VI) removal from aqueous solutions.....	82

LIST OF TABLES

Table 2.1: The Maximum Contaminant Level (MCL) standards for the most hazardous heavy metals	11
Table 2.2: Advantages and disadvantages of conventional methods for the removal of heavy metals from water	17
Table 3.1: Calculation of the ratio of PvOH and PPy used for the polymer blend.....	46
Table 4.1: Isotherms constants and correlation coefficients for adsorption of Cr(VI) and As(III) from aqueous solution.....	79

Table of Contents

Declaration.....	iii
Dedication.....	iv
Acknowledgements.....	v
Publication and presentation.....	vi
Abstract.....	vii
List of abbreviation.....	xi
List of figures.....	x
List of tables.....	xi
CHAPTER 1	1
1. Introduction.....	1
1.1. Background.....	1
1.2. Problem statement.....	1
1.3. Justification.....	3
<i>1.3.1. Polypyrrole (PPy)</i>	<i>4</i>
<i>1.3.2. Polyvinyl alcohol (PvOH).....</i>	<i>4</i>
<i>1.3.3. Magnetite (Fe₃O₄) nanoparticle.....</i>	<i>4</i>
<i>1.3.4. Modification of magnetite nanoparticles incorporated by a polymer blend (polypyrrole coated with polyvinyl alcohol) polymer nanocomposite</i>	<i>5</i>
1.4. Aim.....	5
1.5. Objectives.....	5
1.6. Outline of the dissertation	6
1.7. References.....	7
CHAPTER 2	10
2. Literature review	10
2.1. Introduction	10

2.2. Arsenic and chromium: General occurrence, toxicity, biological importance and occurrence in aquatic environment	11
2.2.1. <i>Occurrence and toxicity</i>	11
2.2.2. <i>Biological importance of arsenic and chromium</i>	14
2.3. Conventional techniques for the removal of Cr(VI) and As(III) metal ions from aqueous solutions	16
2.3.2.1. Magnetite (Fe ₃ O ₄) nanoparticle.....	24
2.4. Application of nanocomposites, composites and nanomaterials for removal of hexavalent chromium and arsenide	26
2.4.1. <i>Application of polymer nanocomposite in the removal of Cr(VI) from aqueous solutions</i> 26	
2.4.2. <i>Polymer nanocomposite for the removal of As(III)</i>	31
2.5. Polymer nanocomposites	31
2.5.1. <i>Advantages and disadvantages of polymer nanocomposites</i>	32
2.6. References	34
CHAPTER 3	45
3. Experimental	45
3.1. Chemicals and reagents	45
3.2.1. <i>Preparation of the PPy-PvOH polymer blend</i>	45
3.2.2. <i>Preparation of the iron oxide nanoparticles</i>	46
.....	47
3.2.3. <i>Preparation of the Fe₃O₄-PPy-PvOH polymer nanocomposites</i>	47
3.3. Characterization techniques	47
3.3.1. <i>Fourier transform infra-red (FT-IR)</i>	47
3.3.2. <i>Scanning electron microscopy (SEM) and transmission electron microscopy (TEM)</i> ...	48
3.3.3. <i>X-ray diffraction (XRD) studies</i>	48

3.3.4.	<i>Differential scanning calorimetry (DSC)</i>	48
3.3.5.	<i>Brunauer–Emmett–Teller (BET)</i>	48
3.3.6.	<i>Inductive coupled plasma (ICP)</i>	49
3.3.7.	<i>Zeta potential measurements</i>	49
3.4.	Adsorption studies	49
3.4.1.	<i>Preparation of synthetic solutions contaminated with model pollutants of As(III) and Cr(VI)</i> 49	
3.4.2.	<i>Effect of pH</i>	50
3.4.3.	<i>Effect of concentration</i>	50
3.4.4.	<i>Effect of dosage</i>	50
3.4.5.	<i>Effect of time</i>	51
3.5.	Adsorption isotherm models	51
3.6.	Adsorption kinetics models	51
3.7.	Swelling studies of the nanocomposites	51
3.8.	References	53
CHAPTER 4	55
4.	Results and discussion	55
4.1.	Incorporation of Fe₃O₄ particles onto the PPy-PvOH blend to form Fe₃O₄-PPy-PvOH polymeric nanocomposites	55
4.2.	Characterization of the PPy-PvOH polymer blend, Fe₃O₄ and Fe₃O₄-PPy-PvOH polymer nanocomposites	56
4.2.1.	<i>Fourier transform infra-red (FTIR) analysis</i>	56
	58
4.2.2.	<i>Thermo-graphic analysis (TGA) analysis</i>	59
4.2.3.	<i>Differential scanning calorimetry (DSC)</i>	60
4.2.4.	<i>Zeta potential</i>	61

4.2.5.	<i>Scanning electrode microscopy (SEM) analysis</i>	62
4.2.6.	<i>Transmission electrode microscopy (TEM) analysis</i>	64
4.2.7.	<i>Brunauer–Emmett–Teller (BET) analysis</i>	64
4.2.8.	<i>X-ray diffraction (XRD) analysis</i>	65
4.2.9.	<i>Swelling studies of Fe₃O₄-PPy-PvOH nanocomposites</i>	67
4.3.	Adsorption studies	69
4.3.1.	<i>Effect of pH</i>	69
4.3.2.	<i>Effect of pH of Cr(VI) concentration using different polymer blend ratio</i>	70
4.3.3.	<i>Effect of initial concentrations of Cr(VI) and As(III)</i>	72
4.3.4.	<i>Effect of dose</i>	73
4.3.5.	<i>Effect of contact time</i>	74
4.4.	Adsorption isotherm models	75
4.4.1.	<i>Langmuir isotherm model</i>	76
4.4.2.	<i>Freundlich isotherm model</i>	77
4.5.	Adsorption kinetics model	79
4.6.	References	84
CHAPTER 5	86
4.	Conclusions and Recommendations	86
4.1.	Conclusions	86
4.2.	Recommendations	87

CHAPTER 1

1. Introduction

1.1. Background

Wastewater is spent or used water that has been discharged from industrial, domestic and agricultural activities and contains contaminants such as bacteria, heavy metals and fungi. Unlike most organic contaminants, heavy metals such as chromium, mercury, lead and arsenic are not biodegradable and tend to bioaccumulate in living organisms. These toxic metals are known to be mutagenic and carcinogen [1]. Heavy metals are regarded as environmental priority contaminants and are becoming an ecological and environmental problem. Hence, it has become necessary to remove, remediate and minimize the concentration of these metals in wastewater and water in general.

Several techniques have been recommended for the removal of toxic metals from wastewater and these include chemical precipitation, ion exchange, membrane filtration, adsorption and, electrochemical technologies [2]. However, these techniques have specific limitations such as high costs, low efficiency and production of sludge that ultimately requires disposal. Among these techniques, adsorption offers flexibility in design and operation and, in most cases, produces high-quality treated wastewater. As an added advantage, the adsorbents can be regenerated by suitable desorption processes for multiple use. Lastly, many of these desorption processes have low maintenance cost, are highly efficient and are easy to operate [3].

1.2. Problem statement

It is common knowledge that many industries in developed countries such as the United States of America and other European countries discharge their chemicals into ground water sources [4], while developing countries such as most African countries experience agricultural problems of pesticide residues in soil, which run off into water sources. The wastewater from industries and municipalities, which is discharged into the rivers or dams in both partially treated and untreated form, ultimately affects the quality of the ground water. In many instances, this ground water of poor quality is used for many agricultural and domestic purposes. Of the toxic metals that are

found in the groundwater, chromium and arsenic often exceeds the regulatory threshold limit, and thus pose a threat to the immediate environment and aquatic life. Plants irrigated by water contaminated with such pollutants are particularly harmful to animals and human beings. For example, large consumption of contaminated plants may lead to cancer and reproductive disorders in humans [5] [6].

Chromium (Cr) exist in aquatic environment as Cr(III) and Cr(VI). In general Cr(VI) is more toxic than Cr(III), but the human body can convert some amounts of Cr(VI) to Cr(III), since Cr(III) is an essential element in humans at trace level. According to United States Environmental Protection Agency (US-EPA), the average daily intake of chromium from air, water, and food is estimated to be less than 0.2-0.4 $\mu\text{g/L}$, 2.0 $\mu\text{g/L}$, 60 $\mu\text{g/L}$ respectively [7]. The WHO recommends that the maximum concentration of Cr(VI) in drinking water should not exceed 0.05 mg/L in the report published in the year 1996 [8]. Any amounts exceeding the recommended concentrations will lead to diseases that affect the human physiology and thus cause severe health problems that range from skin irritation to lung carcinoma [1].

Arsenic (As) occurs in aquatic environment in two valent states, namely As(III) and As(V). As(III) is considered more toxic than As(V). As(V) acts as a nutrient to humans at trace levels, because it behaves like a soft acid. According to the WHO, the maximum concentration recommended for arsenic in drinking water is 0.01 mg/L [9]. Any amounts exceeding this limit causes severe Osborne diseases such as cancers of the skin, bladder and lungs. Upon long-term exposure to high levels of arsenic through drinking water, the first changes are usually observed in changes to the skin: pigmentation followed by skin lesions, and thereafter hard patches on the palms of the hands and soles of the feet [10].

As already mentioned, techniques that are currently used in the treatment of metal contaminated waste discharges (e.g. coagulation, membrane filtration, centrifugation and reverse osmosis) have disadvantages ranging from the use of expensive equipment to inefficiency in the removal of large amounts of toxic metals. The formation of sludge formation in chemical precipitation and adsorption makes these techniques expensive.

There are certain drawbacks for various separation techniques e.g. membrane filtration process tends to leach and foul. They may absorb relatively large amount of filtrate and introduce metallic ions into the filtrate, and allow viruses and mycoplasmas to pass through. The limitation for

coagulation ranges. Firstly, the performance substantially decreases at lower temperature and also has poor efficiency attracting organic suspended solids. Lastly, determining portions for mixing with inorganic coagulants is a setback due to lack of instrumentation that limits coagulation. With reverse osmosis technique the shortcoming is that its membrane alone does not remove volatile organic chemicals and after removing minerals, the water becomes acidic [11].

The development of nanomaterials and polymer blends for removing toxic metals from wastewater/ synthetic wastewater have proven advantageous as compared to previously used adsorption techniques due to very large surface area, porosity, swelling properties, and short diffusion length [12].

The demand for water is exponentially increasing, while slowly the water source is becoming unfit due to improper waste disposal [13] and not so feasible water treatment technologies.

To address the above stated problem in relation to the shortcoming and limitation of various methods, a new polymer nanocomposite (PNC) has been fabricated with blend of polypyrrole (PPy)/polyvinyl alcohol (PVOH) and reinforcement of magnetite nanoparticles (Fe_3O_4) as a magnetic adsorbent for removing Cr (VI) ions from synthetic wastewater/ aqueous solution. We propose the use of a polymer blend combined with magnetic properties on a pilot scale to try to provide an application of nanomaterials in wastewater/ aqueous solution treatment for Cr(VI) and As(III) removal.

1.3. Justification

In one of the latest review, [14] Muthui studied the removal of Cr(VI) by Fe_3O_4 /polypyrrole nanocomposite with ration constituents in the polymer significantly the adsorption process whereby 49.6:50.4 Fe_3O_4 -PPy nanocomposites was used for the adsorption efficiency. The study was successful with a batch separations indicating that 0.2 L/min was the optimum flow rate with separation efficiency of 80% achievement. The magnetite content in the nanocomposite significantly influenced the separation process whereby high separation efficiency of up to 98% were achieved for 58.50% Fe_3O_4 containing nanocomposite. In 2012, Bhaumik et al. [15] , prepared polypyrrole/polyaniline (PPy/PANI) nanofibers for the removal of the Cr(VI) by

coupling or propagating without template of PPy/PANI free radicals by simultaneous polymerization of pyrrole and PANI. The preparation was a success and yielded excellent results. Earlier in 2008 Hossein [16] identified various adsorbent that could remove toxic metals such as arsenic from wastewater. Adsorbent such as bentonite, activated carbon and the electroactive conductive polypyrrole were used to remove the inorganic arsenic from wastewater. The conductive electroactive polypyrrole was prepared using different surfactants such as poly (vinyl) alcohol (PvOH) and poly (ethylene glycol) (PEG) in the presence of FeCl_3 as an oxidant.

1.3.1. Polypyrrole (PPy)

PPy is a commercial available polymer, synthesized from polymerization of pyrrole monomers. In this study PPy is used as a matrix polymer. PPy is a good organic polymer due to its ability to provide many site for adsorption. It has amine functional groups and conjugated double bonds which assists in the adsorption of heavy metals. Due to its lack of mechanical strength and thermal stability, PPy is often blended with a host polymer that has mechanical strength and thermal stability. Hence in this study, PPy is blended with PvOH. This is because PvOH offer both mechanical strength and thermal stability [18]

1.3.2. Polyvinyl alcohol (PvOH)

PvOH is used together with a PPy to form a polymer blend (56:46, w/w) to enhance the compatibility between the PPy and magnetite for adsorption capacity to remove the toxic metal available in wastewater. PvOH is hydrophilic polymer which has hydroxyl functional group that is available to assists in elimination heavy metals, it is also used as a coat to enhance thermal and chemical stability of PPy for adsorption efficiency [19].

1.3.3. Magnetite (Fe_3O_4) nanoparticle

In this study magnetite nanoparticles are coated with a polymer blend (PPy/PvOH) to create more site for adsorption and enhance adsorption efficiency. The magnetic nanoparticle are functionally capable of adsorbing toxic metal present in wastewater, only when incorporated with stable

polymer or a polymer blend [20]. Encapsulating magnetic nanoparticles within a polymer or a polymer blend not only stabilizes the nanoparticles but also provides various chemical functionalization that enhances adsorption capacity [14].

1.3.4. Modification of magnetite nanoparticles incorporated by a polymer blend (polypyrrole coated with polyvinyl alcohol) polymer nanocomposite

Nanocomposite (NC) are defined as polymer incorporated with a nanomaterial as filler to provide materials with enhanced properties. Polymer nanocomposite (PNC) are synthesized by dispersing a filler material into polymer blend/ composite that form flat platelets or nanopowder [17]. Based on the above rationalization, the following aim and objectives were devised for this study.

1.4. Aim

1.4.1 To incorporate a polymer blend (polypyrrole (PPy)/polyvinyl alcohol (PVOH)) with magnetite nanoparticles for studying the material properties and application to the removal of chromium and arsenic from synthetic waste water.

1.5. Objectives

1.5.1 To synthesis and characterize magnetite (Fe_3O_4) nanoparticle by sol gel method and identify parameters (pH, concentration and time) that control the size of it.

1.5.2 To fabricate polymer nanocomposite using magnetic nanoparticle as filler, which should give rise to improved material properties.

1.5.3 To apply the nanocomposites for uptake hexavalent chromium Cr(VI) from aqueous solution the via adsorption technique.

1.5.4 To study adsorption dynamics and adsorption kinetics based studies will be carried out.

1.5.5 Characterize the resulting material (nanocomposite) using different techniques

1.5.6 To study and evaluate the effectiveness of the synthesized nanocomposite for removal of Cr(VI) from wastewater

1.6. Outline of the dissertation

This dissertation is divided into five chapters, a brief summary of each chapter is given below

Chapter 1 gives the background and the general introduction about Polymers, nanoparticle and nanocomposite. Problem statement, aim and objectives, as well as the dissertation outline are also discussed.

Chapter 2

This chapter gives a summary of the review articles of recently published work for the widely used adsorption methods using PPy, PvOH and Fe_3O_4 for the removal of chromium and arsenic from wastewater.

Chapter 3

This chapter provide the detailed synthesis procedures and characterization of the nanocomposite (PPy-PvOH- Fe_3O_4), polymer blend (PPy-PvOH) and the filler material/ nanomaterial (Fe_3O_4)

Chapter 4

Chapter 4 provides the results of the uptake of hexavalent chromium in optimum conditions, using nanocomposite (PPy-PvOH- Fe_3O_4)

Chapter 5

Chapter 5 presents conclusions and recommendations obtained from the results presented in succeeding chapters. The chapter discusses the successes as they relate to the objectives of the project and future research directions in the field of nanocomposite.

1.7. References

- [1] B. Pan, B. Pan, Z. W.M., L. Lv and Q. Zhang, "Development of polymeric and polymer-based hybrid adsorbents for pollutants removal from waters," *Chemical Engineering Journal*, vol. 12, pp. 19-29, 2009.
- [2] L. Fu and Q. Wang, "Removal of heavy metal ions from wastewaters," *Journal Environment Management*, vol. 3, pp. 407-418, 2009.
- [3] S. Mishra, S. V.K. and D. Tiwari, "Efficient removal of mercury from aqueous solutions by hydrous zirconium oxide," *Application Radiation*, vol. 6, pp. 15-21, 1996.
- [4] P. Chave, G. Howard, P. Bakir and A. S., "Approaches to pollution source," Policy and legal systems to protect, [Online]. Available: http://www.who.int/entity/water_sanitation_health/.../protecting_groundwater_part5.pdf? [Accessed 09 October 2016].
- [5] S. Shankar, U. Shanker and Shikha, "Arsenic contamination of groundwater: A review of sources, prevalence, health risks, and strategies for mitigation," *The Scientific World Journal*, vol. 8, pp. 1-18, 2014.
- [6] D. Pandey and D. Agrawal, "Environmental Vulnerability of Bhandara & Gondia Districts of Maharashtra State," *National Seminar on Water and Environment.*, vol. 2, pp. 1-11, 2011.
- [7] EPA, "United State Environmental Protection Agency.," 1992. [Online]. Available: <http://www.epa.gov/ttnatw01/hlthef/chromium.html>. [Accessed 2015 July 05].
- [8] WHO, "Chromium in Drinking-water," *Guidelines for Drinking-Water Quality*, vol. 2, pp. 1-13, 1996.
- [9] M. Rana, M. Halim, S. Waliul, K. Hasan and M. Hossain, "biosorption of arsenic by prepared and commercial crab shell," *Biotechnology*, vol. 13, p. 8, 2009.

- [10] K. Straif, L. Benbrahim-Tallaa and R. Baan, "Metals, arsenic, dusts, fibres, and ionizing radiation: international agency for research on cancer.," *Journal of Lancet Oncology*, vol. 56, pp. 453-454., 2009.
- [11] UniN, "drinking water treatment," *Reverse Osmosis*, vol. 6, pp. 1-106, 2014.
- [12] M. O. Muthui, "Magnetic adsorption separation process for industrial wastewater treatment using polypyrrole-nanocomposite," *Engineering and Built Environment*, vol. 158, pp. 250-258, 2013.
- [13] M. Rane, R. Sapkal, V. Sapkal, M. Patil and S. Shewale, "Use of naturally available low cost adsorbents for removal of Cr (VI) from wastewater," *International Journal Chemical Science Application*, vol. 5, pp. 1-17, 2010.
- [14] M. Muthiah, I. Park and C. Cho, "Surface modification of iron oxide nanoparticles by biocompatible polymer for tissue imaging and targeting," *Biotechnology*, vol. 8, pp. 1224-1236, 2013.
- [15] M. Bhaumik, A. Maity, V. Srinivasu and M. Onyango, "Enhanced removal of Cr(VI) from aqueous solution using polypyrrole/Fe₃O₄ magnetic nanocomposite," *Journal of Hazard Materials*, vol. 3, pp. 381-390, 2011.
- [16] E. Hossein, "Removal of arsenic in water using polypyrrole and its composites," *World Applied Sciences Journal*, vol. 3, no. 1, pp. 10-13, 2008.
- [17] P. Camargo, "Nanocomposites: synthesis, structure, properties and new application opportunities," *Material Research*, vol. 1, pp. 10-13, 2009.
- [18] M. Krzysztof, "Chemical reactivity of polypyrrole and its relevance to polypyrrole based electrochemical sensors," *Journal of Electroanalysis*, vol. 18, pp. 1537-1551, 2006.
- [19] U. Hafeli, W. Schutt, J. Teller and M. Zborowski, "Scientific and clinical application of magnetic carriers," Plenum press, New York, 1997.

- [20] C. Lemachad, R. Gref and P. Couvreur, "Polysaccharide decorated nanoparticles.," *Europe Journal of Pharmaceutical and Biopharmaceutical*, pp. 327-347, 2004.

CHAPTER 2

2. Literature review

Hexavalent chromium (Cr (VI)) and arsenide (As (III)) contamination poses a serious threat to drinking water quality, which ultimately affects human life and sustainable aquatic biodiversity. Reduced water quality may result from anthropogenic activities, which include mining, disposal of untreated and treated waste effluents containing toxic metals, as well as metal-chelate complexes from different industries such as electrical industries, tanneries, mechanical equipment industries, and steel and thermal power plants. Anthropogenic activities and other natural processes (e.g. weathering and dissolution of minerals) are therefore potential sources of metals in water and sediment. The primary objective of this chapter is to review conventional methods for the removal of hexavalent chromium and arsenide from wastewater.

2.1. Introduction

Environmental pollution is one of the most serious problems in the world. In particular, the presence of toxic metals in drinking water poses a huge challenge to municipalities both in and outside South Africa. Heavy metals are toxic and lethal to plants, animals, human beings and aquatic life, hence the reason why they have attracted so much attention [1]. Sources of heavy metal pollutants include industrial wastewater from the mining, metal processing, and tannery, pharmaceutical and agricultural industries. This is because these metal pollutants are used in various processes such as mining, ore smelting, and pesticide and chloro-alkali production. Most of the major environmental pollutants are, however, from industrial effluents, sewage and farm wastes. These industries typically discharge their metal-containing effluents into dams and rivers without proper treatment and disposal. The toxic metals are thereafter transported by runoff water and end-up polluting water sources downstream from the industrial site.

Heavy metals are the main contaminants in marine, ground, industrial and even treated wastewater. To avoid health hazards, it is critical to remove these toxic heavy metals from wastewater before their disposal. Most of the heavy metals found in industrial and mining effluent are known to be poisonous and carcinogenic, and thus pose a serious threat to the plant, animal, human and aquatic

life [1]. The release of large amounts of poisonous substances into the natural environment has given rise to a number of environmental problems due to their non-biodegradability, persistence, and ability to bio-accumulate in the environment.

2.2. Arsenic and chromium: General occurrence, toxicity, biological importance and occurrence in aquatic environment

2.2.1. Occurrence and toxicity

Heavy metals are mostly considered to be those elements whose density is above 5 g/cm³. A large number of metals fall under this category. The heavy metals listed in the **Table 2.1** are regarded as lethal even at low concentrations.

Table 2.1: The Maximum Contaminant Level (MCL) standards for the most hazardous heavy metals

Heavy metals	Toxicities	MCL (mg/L), permissible limit	Ref
Arsenic	Vascular disease, visceral cancer, skin manifestation	0.05	
Cadmium	Renal disorder, human carcinogenic	0.01	
Chromium	Headache, vomiting, diarrhea, nausea	0.05	
Copper	Liver damages, insomnia, Wilson disease	0.25	[2]
Nickel	Dermatitis, chronic asthma, nausea	0.02	
Mercury	Rheumatoid, arthritis, kidney disease	0.00003	

Arsenic is a semi-metal but it is also regarded as a hazardous heavy metal. Arsenic (As) occurs in aquatic environment in two-valence state as As (III) and As (V); As (III) is considered more toxic

than As (V). As (V) acts as a nutrient at trace levels because it behaves like a soft acid. According to the WHO, the maximum concentration recommended for arsenic in drinking water must not exceed 0.01 mg/L [3]. An amount exceeding the limitation over a high consumption will cause severe Osborne diseases such as cancers of the skin, bladder and lungs. During long-term exposure to high levels of arsenic through drinking water, the initial changes are usually seen in the skin; the pigmentation of the skin changes followed by skin lesions, and hard patches on the palms of the hands and soles of the feet [3].

Chromium is obtained from chromite ore (FeCr_2O_4) and is considered a priority pollutant, which flows into the environment *via* both natural processes of weathering and dissolution of minerals. Chromite ore is one of the leading metals manufactured in South Africa (SA); in 2015, SA held about 70% of the world's total chrome reserves. Metallic chromium is largely used for manufacturing steel and other alloy.

Chromium has oxidation state from 0 up to 6. However, chromium exists mainly in two oxidation states, namely hexavalent Cr (VI) and trivalent Cr(III) states [4]. The chemical structures of Cr(III) and Cr(VI) are shown in **Figure 2.1**.

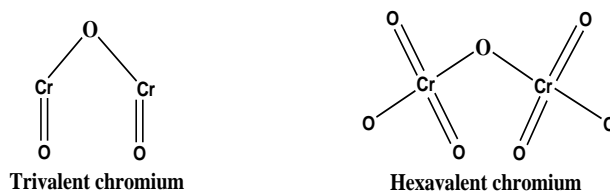


Figure 2.1: Chemical structure of Trivalent and hexavalent chromium

Chromium mixtures are mostly in hexavalent form and are used in chrome coating, as colourants and pigments, and in leather and wood coating. Trivalent chromium is present in cationic form as Cr^{3+} and it is a nutritionally vital component in humans and is frequently added to vitamins as a dietetic enhancement. Cr (III) has moderately low toxicity and would be a worry in portable water only at very high levels of concentration [5].

Cr (VI) is more toxic as compared to the Cr (III), and it poses potential health risk. Societies who drink water having excess total chromium of the maximum contaminant level (MCL) over several years possibly will experience sensitive dermatitis. Cr (VI) is also formed by the industrial

practices and the processing events from steel and pulp mills among others. However, chromium composites have been released into the eco-system by poor storage and leakage of pipes or incorrect discarding practices. Hexavalent chromium (Cr^{6+}) exists as an anion either as chromate (CrO_4^{2-}) or dichromate ($\text{Cr}_2\text{O}_7^{2-}$). Chromate (CrO_4^{2-}) starts to form at pH 8, and it is the only species of chromium that exists at pH 10 [6].

Some of chromium compounds are water insoluble. For example, Cr(III) compounds are water insoluble because they are largely bound to floating particles in water. Cr(III) oxide and Cr(III) hydroxide are the only water soluble chromium compounds. Cr(VI) oxide is an example of a remarkably water soluble chromium compounds, with solubility = 1, 68 mg/L [7]. The speciation of chromium under different pH conditions are shown in **Figure 2.2** below.

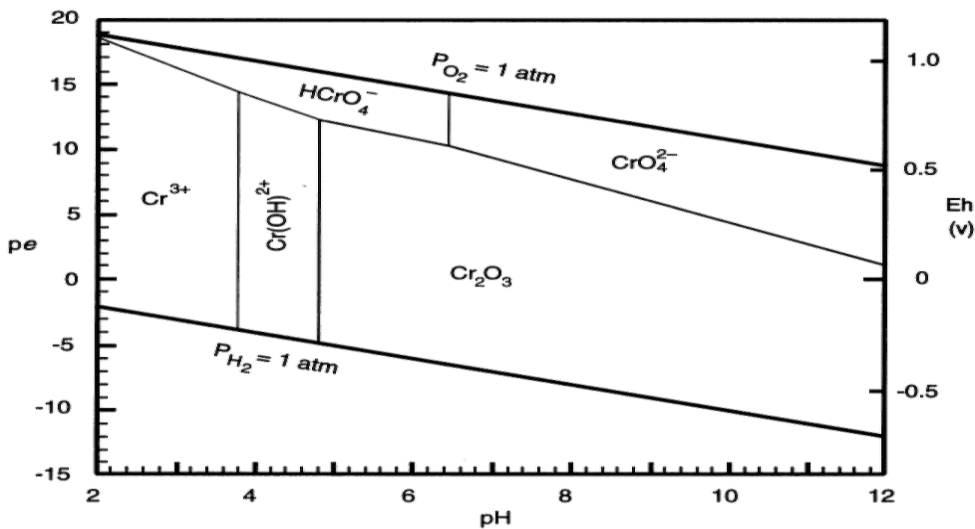


Figure 2.2: A Diagram illustrating the Speciation of Cr (VI) as a function of pH [6].

Although Cr (VI) is more toxic than Cr (III), the human body can detoxify some amount of Cr (VI) to Cr (III), since Cr (III) is an essential element in humans at trace level. According to US-EPA, ‘The average daily intake of chromium from air, water, and food is estimated to be less than 0.2-0.4 $\mu\text{g/L}$, 2.0 $\mu\text{g/L}$, 60 $\mu\text{g/L}$ respectively [5]. The WHO recommends that the maximum concentration of hexavalent chromium in drinking water should not exceed 0.05 mg/L [5]. An amount exceeding the recommended dosage often leads to diseases that affects the human physiology and cause severe health problems ranging from skin irritation to lung cancer [8].

Chromium can be detected in water/ and/or wastewater samples using various types of analytical methods for determination of Cr (VI), Cr (III) or chelating chromium only; methods such as gas chromatography (GC) (with several detection methods), polarography and spectrophotometry can be used [2].

2.2.2. *Biological importance of arsenic and chromium*

Inorganic arsenic and its complexes are increasingly being metabolized to the less toxic form by methylation [9] [10]. The organic complex of arsenic is found in some aquatic foods like fish and algae, and in greater concentrations levels in mushrooms [11]. The typical person's intake of As(III) is about 10–50 µg/day; this amounts to 1000 µg, which is not usual following consumption of fish or mushrooms. However, there is health risk in consuming fish because it contains small amounts of arsenic compound which can be toxic when consumed over a large dosage [12].

In 2008, photosynthetic bacteria that use arsenite ions as electron donors to produce arsenate ions in the absence of oxygen were discovered [13], And have estimated that these photosynthesizing organisms produced the arsenates that permitted the arsenate to decreasing bacteria [14]. Arsenic has been related to epigenetic changes which are transmissible changes in gene appearance that take place without variations in DNA arrangement and contains DNA methylation [15]. Alternately, researchers have found ways in which they can reduce diseases by using arsenic and its derivatives.

Inductive coupled plasma mass spectrometry (ICP-MS) is used to identify accurate levels of intracellular of arsenic, chromium and other heavy metals. During the 19th and towards the 20th centuries, a large amount of arsenic compounds were used as medicines [18], including arsphenamine (by Paul Ehrlich) and arsenic trioxide (by Thomas Fowler). Both Arsphenamine and neosalvarsan (also a synthetic organoarsenic-based drug), which were used for the treatment of syphilis and trypanosomiasis, have been superseded by modern antibiotics [19].

Research has shown that Cr (III) is an essential nutrients at trace level and its biological activity depends on its valence state [20]. In simple salts, Cr (III) has been shown to have some beneficial value in humans. It has been elaborated in some lipids and sugar metabolism. The bioavailability

of Cr (III) salts is known in many food supplements, most especially the liver, such as the American cheese, wheat germs, meat, fish and, fruits. Cr (III) salts have been claimed to have some beneficial effects for patients with diabetes and cardiovascular problems [21]. People with heart diseases and lipprohens deformities may also need Cr (III) salts supplements. However, Cr (VI) is known to be toxic and a mutagenic substance. There has been no carcinogenic reports ascribed for the consumption of Cr (III).

2.2.3. Arsenic and chromium in aquatic environment

Arsenic contaminated water typically contains arsenic acid and arsenous acid (see **Figure 2.3**) or their derivatives [18]. Arsenic acids tend to exist as ions such as $[\text{HAsO}_4]^{2-}$ and $[\text{H}_2\text{AsO}_4]^-$ in neutral water, whereas arsenous acid is not ionized [10].

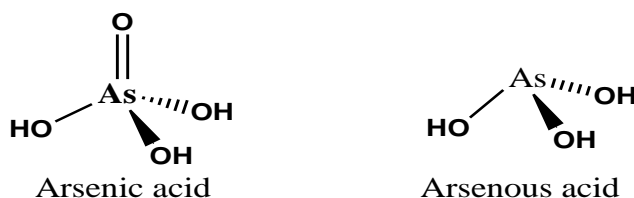


Figure 2.3: Chemical structure of the poisonous arsenic acid and arsenous acid [22]

Concentration of naturally occurring arsenic in groundwater vary regionally due to a combination of climate geographical location [23]. Arsenic released from iron oxide appears to be most common cause of widespread arsenic concentration, which exceeds $10\mu\text{g/L}$ in groundwater. The minimum intake of arsenic in portable water is 0.01 mg/L [24], this are guideline set by WHO and they are similar to those of South African water guidelines [25]. Arsenic is dispersed in groundwater by agricultural uses, where arsenic is being used as an insecticide [26]. Arsenic contamination in groundwater is a high-profile problem due to the use of tube wells for water supply in other areas around the world, causing serious poisoning to a large number of people [26].

In industrial wastewater, arsenic emanates from the electronics manufacturing industry in the production of gallium arsenide wafers and electronic devices [27]. It can also be found in silicon semiconductor operations that use high dose arsenic implants [28]. However, the highly needed

biological properties of arsenic have enabled arsenic derivatives to be used in medicines and wood preservatives and, as a coating material. Arsenate is mostly found in aerobic wastewater, while arsenite is made from the oxidation of arsenate in the presence of oxygen, chlorine or potassium permanganate [29]. The most regularly used technique for the elimination of arsenic and arsenic compounds from wastewater is chemical-precipitation or iron exchange. [30].

Chromium (Cr) generally exist in aquatic environment as Cr (III) and Cr (VI). Cr(VI) being the most toxic as compared to Cr(III). There is a lot of surveys done on the occurrences and toxicity of Cr(VI). There are various ways in which Cr(VI) contaminates aquatic environment and wastewater. Textile, leather tanning and electroplating are some of the good examples of industries that causes water pollution. In most cases the contaminants enters water through improper waste disposal in landfills [31], where the Cr(VI) residence time may be several years. According to USEPA and WHO, the maximum permissible limit for Cr(VI) in surface water is 100 $\mu\text{g/L}$ [32]

In ground water, Cr(VI) has generally been expected to be anthropogenic contamination. Contamination of ground water by Cr(VI) is similar to those of wastewater. Industries such as petroleum refining, water cooling and pulp paper production use chromium to manufacture their products. However, they don't dispose wastewater in their proper disposal, which leads to contamination of groundwater [33]. It has been found that the naturally occurring aqueous Cr(VI) concentration in groundwater has been estimated to 73 $\mu\text{g/L}$. which generally exceeds the value of USEPA and WHO limits for drinking water of 50 $\mu\text{g/L}$ [32]

2.3. Conventional techniques for the removal of Cr(VI) and As(III) metal ions from aqueous solutions

In recent years, various conventional methods such as precipitation, ion exchange, filtration and, coagulation-flocculation have been employed to remove heavy metals from industrial wastewater and other aqueous streams. However, some of these technique (see **Table 2.2**) have significant disadvantages ranging from partial removal of toxic metals, high energy requirement and production of toxic sludge [34]. Amongst these methods, adsorption has been used the most. This is because adsorption is inexpensive, require less energy and can eliminate both inorganic and

organic contaminants from aqueous solution [35]. Various adsorbents such as activated carbon, silicate, natural zeolite, polypyrrole, poly(vinyl)alcohol and chitosan polymers have been used for the removal of heavy metals. [36].

Table 2.2: Advantages and disadvantages of conventional methods for the removal of heavy metals from water

Conventional method	Advantages	Disadvantages
Photocatalysis	<ul style="list-style-type: none"> • Can be improved by increasing the surface area through reducing the size of photocatalysts • Enhancement of the overall quantum productivity of interfacial charge transfer 	<ul style="list-style-type: none"> • In post treatment processes the segregation of residue materials tends to be costly due to labour, time and chemicals utilized for ion exchange and decantation at the end of treatment process. • The subsequent low quantum-yield of this treatment process inhibits the kinetics and efficacy of photocatalysis
Membrane filtration	<ul style="list-style-type: none"> • Benefits of separating discrete cluster of bacteria such as Coliform bacteria from drinking. 	<ul style="list-style-type: none"> • The process is very slow and uses complicated plants, which is very expensive • Critical contaminants are not removed • Period of drying is very high and water is usually acidic (pH below 7.0)

Coagulation and Flocculation

- Does not require addition of alkali to raw water for coagulation, and is much less sensitive to pH, operating within pH 4.5 – 9.5.
- Poor efficiency for attracting organic suspended solids
- Lack of instrumentation for determining relative amounts of organic and inorganic suspended solids in raw water

Adsorption is treated as a adjustment in concentration of a specified substances at all crossing point with respect to its concentration in a majority part of the arrangement. It is the linkage of atoms, ions, or molecules from a gas, liquid, or dissolved solid to a surface [37]. This procedure generates a picture of the adsorbate on the surface of the adsorbent. Moreover the procedure of adsorption contains separation of a material from one point supplemented by its growth or application at the surface of another. The adsorbing material is known as the adsorbent, and the material determined or adsorbed at the surface of that point is the adsorbate. **Figure 2.4** shows a typical adsorption process that involves the extraction of Cr(VI) and As(III) from aqueous solution.

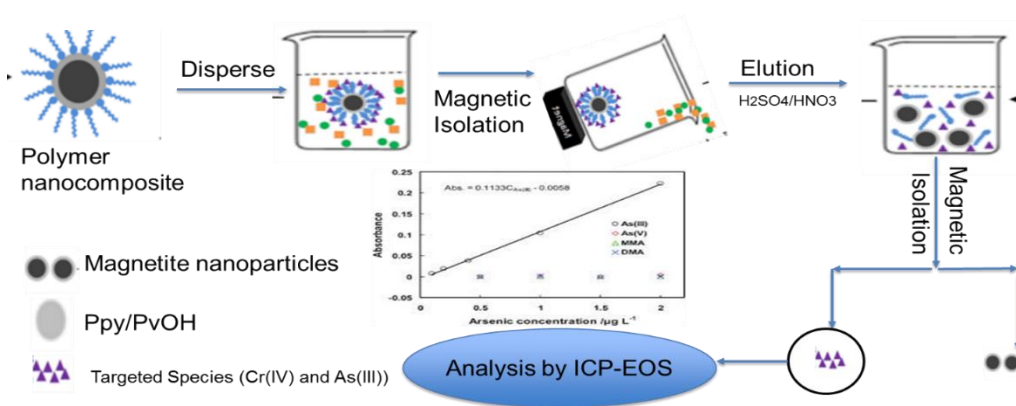


Figure 2.4: A schematic diagram of adsorption technique used to remove Cr(VI) and As(III) by PPy-PvOH-Fe₃O₄

The strategy that was adopted for this study involves blending of a conducting and hydrophilic polymers followed by incorporation of an inorganic material to produce a polymer nanocomposite.

The various components of this polymer nanocomposite are discussed briefly in the following sections.

2.3.1. Organic adsorbents

Various organic adsorbents have been used in the treatment of industrial and agricultural wastewater. Decontamination of water by means of organic adsorbent started in the early 19th centuries [38]. Since then, the application of organic adsorbent such as fly ash, carbon nanotube, conductive polymers, and activated carbon in the removal of toxic contaminants from industrial and agricultural wastewater has attracted a lot of attention from researchers.

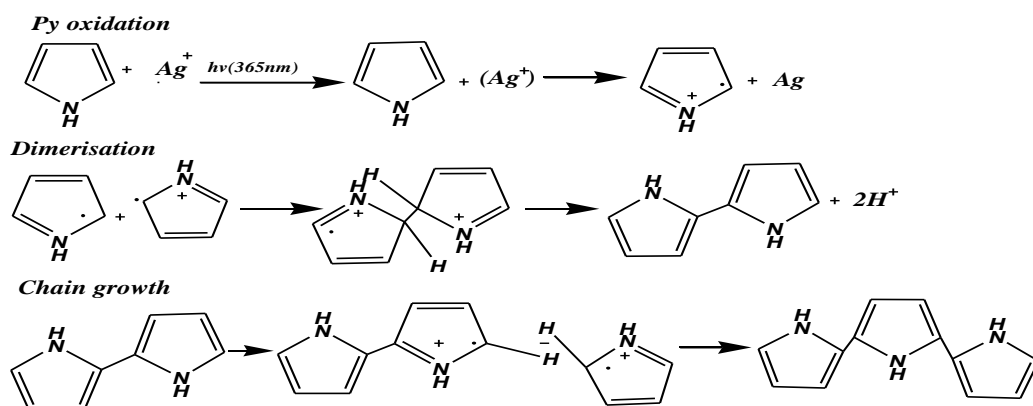
Since the wide scale of coal firing for power generation began in the 1920s, many millions of kilograms of ash and related by-products have been produced. It is approximated that 349 Mt was manufactured in 2000 worldwide [32]. The disposal of fly ash in landfills ash is in due course expected to be expensive if not prohibited by governments [39].

Since then, the application of organic adsorbent such as fly ash, carbon nanotube, conductive polymers, and activated carbon in the removal of toxic contaminants from industrial and agricultural wastewater has attracted a lot of attention from researchers. This study is focussed on conducting polymers and hydrophilic polymer.

2.3.1.1. Conducting polymers

Polymers have attracted a lot of attention from many researchers worldwide. This is due to their flexibility and ability to form materials with different structures. Conducting polymers have many uses. They have been used in corrosion inhibition, compact capacitors, antistatic coating, transistors, organic light-emitting diodes (OLEDs), photovoltaics (OPVs), and thermoelectric materials. They're very cheap and they can be easily synthesized. Electro-conductive polymers such as polypyrrole, polyaniline and many more are mostly used as adsorbent for the removal of contaminants from aqueous and aquatic environment or as coats to stabilize magnetic

nanoparticles. Polypyrrole (PPy) is an electro-conductive polymer from the class of exclusive constituents, which has ionic and semi conductive properties with polymeric features such as elasticity, biocompatibility, greater conductivity, strength and flexibility [40]. They can be used in the transportation of drugs to various parts of the body and can also be used in rechargeable batteries, supercapacitors, anhydrous electrorheological fluids, microwave shielding, and corrosion protection. PPy is formed by oxidative polymerization of pyrrole monomers, which is indicated in the scheme below [41].



Scheme 2.5: Oxidative polymerization of pyrrole to form polypyrrole [42].

PPy is a type of organic polymer formed by oxidative polymerization of pyrrole as shown in **Scheme 2.5**. PPy is used as a polymer matrix for reinforcement for magnetite, to enhance the adsorption capacity by increasing the surface area. The optimum conditions for removal of Cr (VI) was evaluated at pH 5.3, temperature 46.5 °C, initial Cr (VI) concentration of 187.5 mg/L, adsorbent dose of 0.8 g and contact time of 15.4 min. The maximum amount of Cr (VI) removed under optimum concentration was obtained at 89.3% [43].

PPy can be formed chemically or electrochemically through oxidative polymerization of pyrrole monomer, PPy is suitability built on using ionic conductivity and it is dependent on the polymer composition, valence and, ability of reversibly oxidized or reduced

PPy is also accessible commercially. Thus, when PPy is compared to other polymers, PPy is conductive electroactive and water soluble. PPy reactivity can be manifested in various ways;

affecting polymer properties, such as, in modification of conductivity, chemical composition, mechanical strength, the character of voltammetry curves and, open circuit potentials [19]. These methods exerts an unfavourable impact on stability and operation of devices using conductive polymers, for example, polymeric electronic devices or rechargeable batteries

Polypyrrole (PPy) draw unlimited attention due to of their vast potential applications, such as rechargeable batteries [44], gas separation membranes [45], and gas sensors [46] However, their usability remains narrow due to their poor mechanical properties. PPy is an easily synthesized polymer hence its study is vast. The main limitation in the study of PPy is the mechanical properties [47] which arises from their irregular structure. To improve the structural, physical, and mechanical properties, several efforts have been made to synthesize blends or composite materials containing PPy [48].

The chemical methods containing PPy can be attributed to some functional groups, since conductive polymers are redox-active [49], these methods can either be oxidation/ reduction by other components existing in the adjacent medium, e.g., metal ions, OH⁻ ions, H₂O molecules that leads to the degradation of the polymer. The other groups of reactions is associated with acid/base properties, addition of protonation/deprotonation of polymer chains especially important for polypyrrole and its by-products complexes of metal ions from the medium by ligands included in the polymer phases. Ion exchange or adsorption it the last group of interfaces can be incorporated in the medium of the polymer phase components [49].

2.3.1.2. Hydrophilic polymers

Water-soluble polymers such as polyethylene glycol, polyacrylamides, polyacrylic acid copolymer, and polyvinyl alcohol are organic polymers that dissolve, disperse, or swell in water and consequently change the physical properties of aqueous systems undergoing gelation or thickening. The water-soluble polymers carry out a variety of functions in aqueous media, which include: dispersing and suspending agents, stabilizers, thickeners, flocculants and coagulants, film-formers, humectants, binders, and lubricants.

They can be achieved from a wide range of sources. Moreover, they can be classified as natural (isolated from plant, or animal sources), semisynthetic, or synthetic polymers. Natural water-

soluble polymers may be used as is or can be modified. Semisynthetic water-soluble polymers are derived from chemical alteration of natural polymers or from microbial sources. A large number of natural and semisynthetic water-soluble polymers are polysaccharides, which may differ greatly in their basic sugar units, linkages, and substituents. **Figure 2.6** shows poly(vinyl) alcohol is accessed.

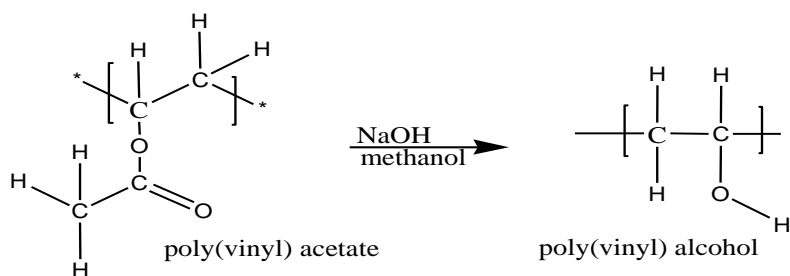


Figure 2.6: Preparation of PvOH [50]

Polyvinyl alcohol (PvOH) is a water-soluble synthetic polymer. It is prepared by hydrolyzing polyvinyl acetate in ethanol with potassium hydroxide (see **Figure 2.6**). PvOH is a large volume produced polymer with high tensile strength and hydrophilic. The hydroxyl groups on partial hydrolyzed PvOH are expected to interact with the hydrophilic surfaces and the residual vinyl acetate groups with the hydrophobic. A study for the possibility to use PvOH together with a PPy blend (50:50, w/w) to enhance the compatibility between the PPy and magnetite for adsorption capacity to remove the toxic metal available in wastewater. The calculated maximum amount under optimum conditions for the removal of arsenic is 22112 mg/kg [51]. PvOH is used as a coat to enhance thermal and chemical stability of PPy for adsorption efficiency.

Combining PPy with thermoplastic or water soluble polymers is one the ways to enhance their processibility [52]. Moreover, mechanical behavior is improved by the preparation of grafted copolymers having conventional and conducting sequences [53]. This is accomplished by polymeric initiators with functional groups along the chain, which is polymerized in the presence of the monomer of the conducting polymer. By introducing PPy in polymer matrix, researchers have improved the limitation of PPy making it composite polymer with new characteristics. The well-known matrixes of PPy studied include; poly(vinyl alcohol), PvOH [54], poly(acrylamide) [55], and poly(vinyl chloride), PVC [56].

The combination of polymer matrices changes the physical properties of the polymer blend, which make the samples more resistive to chemicals, ambient and physical action.

Because of the water soluble, good polarity and good mechanical strength of PvOH has been the main focus to be used as matrix in this study. Improvements were expected from composite materials in which the PPy provides the required porous characteristics, while the PvOH polymer enhances its mechanical properties [57]. In other words, a combination of a conventional polymer such as PvOH with PPy allows the creation of new polymeric materials with specific Porosity and good mechanical properties. The goal of the present work is to develop a multifunctional composite with porous, swell-able, and enhanced physical properties; conducting polyvinyl alcohol (PVA), which ensures suitable mechanical properties.

PvOH is widely used for diverse application such as adhesives of paper, coating etc. PvOH is used for coating because it prevent interparticle agglomeration by reducing the crystalline surface tension, to provide the particle with necessary functionality and in some cases, the coating layer can also protect magnetite from attacks of corrosive media such as acidic and alkaline conditions [58].

2.3.1.3. Swelling studies of organic polymers

Hydrogels may be described as hydrophilic polymers that do not dissolve in water. Furthermore, they can also be described as three dimensional hybrid polymeric structures that are able to swell in an aqueous solution. However, many naturally occurring polymers may be used to produce these types of materials. The synthetic hydrogels have distinctive properties, which in turn makes them have enhanced practical utility. Due to properties such as swellability in water, hydrophilicity, lack of toxicity and biocompatibility, hydrogels have been used in pharmaceutical and biological environmental application [59]

2.3.2. Inorganic adsorbents

Inorganic adsorbents such as polymeric adsorbents have gained popular awareness in water decontamination recently. In modern assessment on inorganic adsorbent, there are suggestion of detailed studies to explore the feasibility of changing activated carbon with low cost inorganic adsorbent such as modified zeolites, nano metal oxides, functionalized inorganic polymers and, modified clay for water and wastewater treatment that can be used for removal of metals and or trace organics. The recent growth of inorganic, coated compounds, and nanomaterial adsorbent for uses in removal organics and inorganics pollutants have been discussed by, demonstrating the advantages of low dosage and high rate for nanomaterial as adsorbents. [60]

2.3.2.1. Magnetite (Fe_3O_4) nanoparticle

Magnetite can be categorised as one of the promising adsorbent for toxic metals removal from wastewater due to its large surface areas, which increases their adsorption capacity caused by the size-quantization effect. Nevertheless, as the size of metal oxides decreases from micrometer to nanometer quantities, the amplified surface energy leads to their poor stability [61].

Magnetite is a ferromagnetic nanoparticle derived from precursors of FeCl_3 and FeCl_2 using co-precipitation. Fe_3O_4 differs in size ranging from 22 to 56 nm, and it is synthesized chemically by a modified sol gel or chemical precipitation. Magnetite targets certain elements (toxic metal) in wastewater and removes them sufficiently using its good magnetism properties. Element such as Ni, Cr, As and Cu are targeted and a large amount of the trace metals are removed [62].

The mixture of Fe_3O_4 -(γ - Fe_2O_3) was used for removal of Cr (VI) and As (III), 'the results of the study showed 96-99% arsenic and chromium uptake under controlled pH conditions. The maximum arsenic adsorption occurred at pH 2 with values of 3.69 mg/g for As (III) and 3.71 mg/g for As (V). Magnetite nanoparticles present a higher performance in terms of chemical stability and biocompatibility compared with the other metallic nanoparticles [63]. In addition, Magnetite has advantages ranging from large surface area [64], no secondary pollutants are produced, commercially available and reduces the risks of particle aggregation [65]. Moreover, the magnetic nanoparticles are used for bio-applications which are usually made from biocompatible materials

such as magnetite (Fe_3O_4) for which are susceptibility large [66]. **Figure 2.7** shows the structure of magnetite

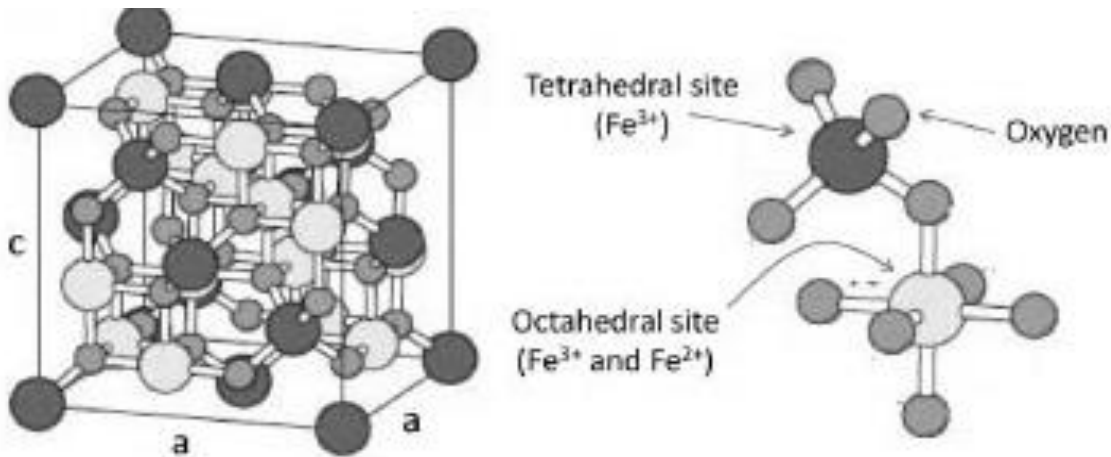


Figure 2. 7: The structure of Magnetite (Fe_3O_4) [85]

The understanding about magnetism dates back in 6th century even though separation by magnetic field has been a mystery until late 18th century [68]. The achievement of an English patent for separating iron ore using magnetic filtration in 1792 by W. Fullerton led to practical importance of magnetic attraction. **Figure2.8** below shows the timeline of magnetic separation technology.

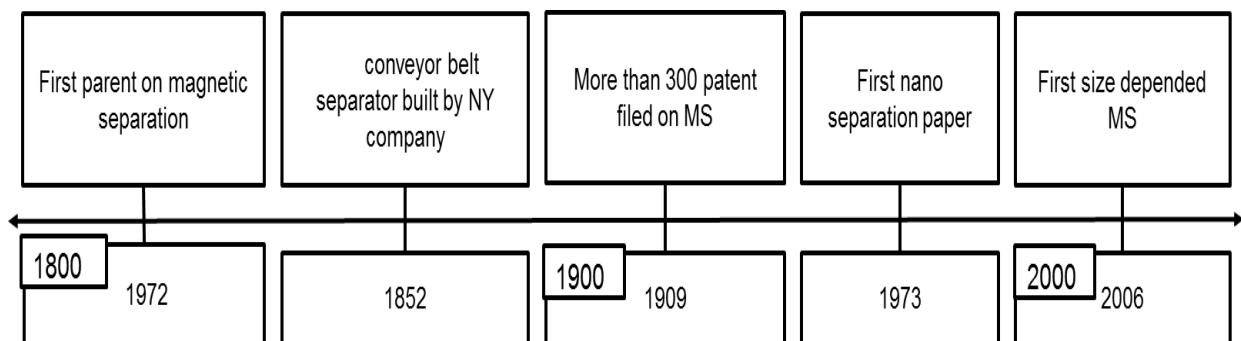


Figure 2.8: Evolution of magnetic separation technology

The procedure of eliminating metal based on a magnetically enhanced separation technology as an alternative to existing methods for separation of the targeted pollutants from waste water stream is a usually applied in technique of recent water treatment. This technology uses specifically

tailored exterior modified magnetic nanoparticles that have a high attraction for the target impurities (trace metals, organic compounds etc.). These particles have a magnetic core that enables their recovery, a shell that provides stability, shield from oxidation and a surface to which contaminant specific ligands are attached. The benefits of this alternative are that it uses low cost chemicals and magnets, can be applied in a continuous manner and can be target specific.

Developments in nanomaterial (NM) preparations enable the accurate control of surface active sites by developing monodisperse and shape controlled iron oxide nanomaterials [69]. Some developing techniques, like fungi or proteins refereed biological method and sono-chemical method, which have expanded widely over the years. Studies in the future aim to address different challenges to offer new efficient and specific magnetic nanomaterials. Moreover, the improvement of iron oxide nanomaterials into a field scale may give useful range of exploration, and more research is required to explore the uses of potential of these novel nanomaterials. Commonly, NM's must be stable to prevent accumulation and endow a low deposition rate [70], in order to assure their reactivity and flexibility. In one of the latest review, Muthui et al studied the removal of Cr (VI) by Fe₃O₄-PPy nanocomposite with ratio constituents in the polymer significantly the adsorption process whereby 49.6:50.4 ratio of Fe₃O₄-PPy nanocomposites was used for adsorption. The study was successful with 'batch separations indicating that 0.2 L/min was the optimum flow rate with separation efficiency of 80% achievement and the magnetite content in the nanocomposite significantly influenced the separation process whereby high separation efficiency of up to 98% where achieved for 58.50% Fe₃O₄ containing nanocomposite [71].

2.4. Application of nanocomposites, composites and nanomaterials for removal of hexavalent chromium and arsenide

2.4.1. Application of polymer nanocomposite in the removal of Cr(VI) from aqueous solutions

In one of the latest review, Muthui et al [72] studied the removal of Cr(VI) by Fe₃O₄-PPy nanocomposite with ration constituents in the polymer significantly the adsorption process whereby 49.6:50.4 ratio of Fe₃O₄-PPy nanocomposites was used for adsorption. The study was

successful with 'batch separations indicating that 0.2 L/min was the optimum flow rate with separation efficiency of 80% achievement' and the magnetite content in the nanocomposite significantly influenced the separation process whereby high separation efficiency of up to 98% where achieved for 58.50% Fe₃O₄ containing nanocomposite.

Lo et al [73], reported the removal of heavy metals from industrial wastewater using maghemite nanoparticle with a diameter of about 10 nm. The removal efficiency was highly dependent on pH effect. The optimum pH for the removal of Cr(VI), Cu(II) and, Ni(II) was reached at 2.5, 6.5 and, 8.5 respectively resulting with a removal percentage of about 100% for Cr(VI), 96.2% for Cu(II) and, about 100% for Ni(II). Recovery studies were made with 0.01 M NaOH as an eluent for Cr(VI) for desorption and 0.05 M HCl as an eluent for both Cu(II) and Ni(II) desorption. 92 % of Cr(IV) was recovered and 94 % of Cu(II) and Ni(II) was recovered. Maghemite nanoparticles were able to remove heavy metal from wastewater, which reduced the waste discharge, pollution and, be recovered for reuse purposes [74].

Mahmud et al reviewed composites of polypyrrole for removal Cr(VI). One of the study reviewed was Polypyrrole-Chitin (PPy/Ch) composites [75]. The composite was prepared in situ via polymerization and batch tests were carried out to observe the adsorption efficiency of Cr(VI) ions under different parameters. The study exhibited a maximum adsorption capacity of 35.22 mg/g for an initial concentration of 50 mg/L at 323 K and pH= 4.8 within 60 minutes of contact time and 0.1 g adsorption dosage. When chitin is used alone as an adsorbent for toxic metals removal, it appears to be insufficient because of its poor solubility in common solvents, low sorption capacity and poor stability. As a result, it is hosted by polypyrrole structure to increase the sorption efficiency of conducting polymer-based bio-adsorbent [76].

The adsorption of Cr(VI) with polypyrrole-glycol (PPy-gly) was also reviewed by Mahmud et al. The sorption was highly dependent on pH. The optimal adsorption efficiency of PPy-gly was observed at 217 mg/g, pH 2.0 and, 298 K. It is much better than the other reported polymer-based materials [75]. A similar study was accomplished by Ballav et al. [77] using Fe₃O₄ coated glycine doped polypyrrole magnetic nanocomposite for the elimination of Cr(VI). The experiment reached an adsorption efficiency of 238 mg/g with the optimal removal percentage of 99.91%. pH was

highly regarded in the experiment. External magnetic field was used to elute the adsorbent from the solution.

In the latest studies, Hsing-Lin Wang [78] reported the electro-conductive polymer blends of polypyrrole and other various insulating polymers with the aim of the study was to enhance the miscibility and homogeneity of the material, however in 2013 a similar study was reported, ‘the removal of Ni(II) from water by PPy/ PvOH composite’ which attained good results. Furthermore, the optimal conditions of sorption were investigated and reported 0.4g sorbent dose in 100 ml of Ni(II) contact time of 14 min, pH 3 for the Ni (II). The results obtained from this investigation were well described by the theoretical Freundlich. The kinetic showed that the adsorption process was controlled by pseudo-second order equation.

In the present study by Mohammad Al-Hwaiti [79], an attempt to utilize a less expensive adsorbent system for the elimination of metals including arsenic ions from phosphogypsum (PG) using *Polyethylene glycol* (PEG) and poly(vinyl alcohol (PvOH)). The objective of the study was to examine the performance of two polymers blends (PEG and PvOH) in eradicating heavy metal from PG with a batch reaction approach. The batch experiments’ result obtained showed that the removal of Cd, Cr, Cu, Pb, Zn and Mo in these samples ranged from 57% to 70%, 80% to 94%, 90% to 96%, 7% to 11%, 55% to 74%, and 81% to 94%, respectively for PEG, and from 70% to 84%, 80% to 91%, 89% to 95%, 7% to 10%, 55% to 78%, and 82% to 93%, respectively for PvOH. These results indicated that Cd, Cr, Cu, Pb, and Zn content removal using PEG-PvOH polymers were of great importance in environmental applications, and they can be considered a very suitable safe use of PG in agriculture and soil amendment.

Terrence Burks [80].reported the removal of Cr (VI) by an application of surface modified superparamagnetic iron oxide nanoparticles, separation science and technology. The adsorbent used to modify the surface was polyacrylonitrile (PAN) nanofibers. The adsorption was highly dependent on the pH. The experiment showed excellent results with maximum removal of Cr (VI) at pH 2 and the equilibrium was reached at 90 minutes. Thus the experimental results followed the pseudo-second order showing a chemisorption process.

Kai Wang [81] experimented on the Removal of Cr(VI) from wastewater using Fe₃O₄ polymer microspheres functionalized with amino groups. The outcomes showed that the initial solutions pH had an effect on the adsorption capacity and the optimal pH measurement for Cr(VI) adsorption was obtained at pH 2. It was shown that adsorption process was a pseudo-second-order reaction with an equilibrium establishment of 120 minutes. Langmuir isotherm model was an excellent agreement with the experimental data and the maximum adsorption measurements was valued at 236.9 mg/g at 298 K.

The need to selectively segregate metal ions from a variety of pollutants is a fast rate development and preparation of adsorbents that has been investigated in modern days. In the past, researchers have seen that the unprotected iron oxide nanoparticles are prone to air oxidation and they easily aggregate in aqueous solution systems. Thus, for these nanoparticles to be applicable in many potential fields their stabilization by surface modification is essential. Due to these reasons the main focus shifted on magnetic particles coated with functional polymer especially conducting polymers which include among others polystyrene, polyaniline, poly (N-isopropylacrylamide) and polypyrrole. These polymers have a spectrum of applications such as in batteries, molecular electronics, separation material ion exchangers and chemical sensors. The works of Pyun gave a detailed discussion on the preparation methods and properties of organic-inorganic hybrid materials comprised of polymers and magnetic materials. Among the discussion, the functionalization and modification of these nanocomposites materials surface using different surfactants are used to improve their adsorption properties.

Bhaumik *et al* [82] worked on demonstrating the bench scale removal of Cr(VI) from aqueous solution by use of PPy/Fe₃O₄ which had been prepared by using 0.8 ml of Py and 0.4 g of Fe₃O₄. Even though good withdrawal results were achieved, the study needed to be advanced to magnetic separation in a flowing stream to suit industrial application. In addition, Bhaumik *et al*, prepared polypyrrole/polyaniline (PPy/PANI) nanofiber for the removal of the Cr(VI) by coupling or propagating without template of PPy/PANI⁺ free radicals by simultaneous polymerization of Pyrrole and PANI. The preparation was a success and yielded excellent results.

In the latest review, Karunakaran K [83], used polypyrrole/sawdust (PPy/SD) composite to remove hexavalent chromium and other heavy metals from industrial wastewater. The high efficiency of

the removal of hexavalent chromium is seen only under acidic condition for sawdust and has a pH range of 1-2, but for the condition of PPy/SD composite reaches pH 10. The Cr (VI) was not affected by the pH in the test solution. The optimal pH used for elimination of hexavalent chromium by SD was established at pH 5 (see **Table 2.3**). This is because under alkaline conditions, Cr (VI) elimination is insignificant. According to Karunakaran, the results showed that the optimal pH is stationary at 50 mg due to the quality of Fe (III) uptake. The total optimal pH is stable at pH4 because of the removal of all Fe (III) and the optimal time fixed was obtained at 30 min

Table 2.3: Effect on pH on removal of heavy metals form aqueous solutions.by PPy/SD

Metal	Contact time in minutes	Metal concentration	Adsorbent dose	pH range	Optimal pH	Current work
Cr(VI)	60 minutes	50ppm	0.60 g	1-10	5	High efficiency removal observed at pH 5 [84]
As(III)	30 minutes	5 mg/L	0.25g with 30 m/ As	-	-	Good results in such condition [85]
Fe(III)	30 minutes	50 ppm	50-250 mg	2-6	4	Unique results seen at pH 4, but ranges from 2-6 [86]
Cr(VI)	30-180 minutes	200 ppm	0.1 g with 50 m/ Cr(VI)	2-11	2	Removal is more effective at pH 2 and gives 73.5% removal, when the pH increases the removal % decrease to 57% [82]

In 2010, Zhao et al [87] prepared characterized and applied magnetics polymers functionalized with ethylene diamine on the elimination of Cr(VI) from industrial wastewater. The batch equilibrium and kinetic studies indicated that the materials was effective in removing Cr(VI) from aqueous solution. VSM characterization results indicated the magnetic property of the polymer magnetic nanocomposite was less compared to that of naked magnetite.

2.4.2. *Polymer nanocomposite for the removal of As(III)*

Recently, arsenic occurrence in drinking water is regarded as a serious threat to human health [88]. The long term consumption of the highly concentrated arsenic contaminated water leads to diseases such as cardiovascular, diabetes and cancer of the bladder. Several articles have been published for the removal of trivalent arsenic from waste water. In one of the recent publications, K Simoenidis et al [89] reported the magnetic separation of hematite-coated Fe_3O_4 particles for adsorption of As(III) . The results obtained were efficient and reduced the level of arsenic below the international regulation limit (0.01 mg/L) having an adsorption capacity of 2.1 g/mg. Feng L et al [90] reported the removal of arsenic using superparamagnetic Fe_3O_4 nanoparticles as adsorbents. Fe_3O_4 nanomaterials presented excellent ability to remove arsenic ions in aqueous solutions. They obtained maximum adsorption capacity of 16.56 mg/g for arsenic (V), and 46.06 mg/g for arsenic (III). In one of the latest publications, Peng B et al [91] studied the removal of arsenic using facile synthesized $\text{Fe}_3\text{O}_4\text{-Cu(OH)}_2$ composites. The results indicated that adsorption capacity was increased about 10 times from 3.58 to 35.71 mg/g, which was greater than most of the reported magnetic sorbents in literature. However, in 2015 Sadrolhosseini et al [92] reported Surface plasmon resonance sensor for detecting arsenic in aqueous solution using polypyrrole-chitosan-cobalt ferrite nanoparticles composite. The PPy-Chi/CoFe₂O₄-NPs composite adsorbed about 93.20% of As(V) in aqueous solution. Moreover, Zhao et al [93] studied the removal of arsenic by zirconium/polyvinyl alcohol modified flat-sheet polyvinylidene fluoride membrane. The maximum adsorption capacity of 128 mg-As/g was achieved at acidic condition at pH 2.0 which reached equilibrium at $t = 24$ hrs.

2.5. **Polymer nanocomposites**

Polymer nanocomposites (PNC) are commonly defined as combination of a polymer matrix and a filler material that has a dimension in the 10^{-9} m range. The nanomaterial is in one-dimension; two-dimensional, three-dimensional such as nanotubes, layered silicate minerals and, spherical nanoparticles, respectively. [94]

2.5.1. *Advantages and disadvantages of polymer nanocomposites*

Nanoparticles poses a large high surface area to volume ratio [95], which changes their properties when compared to their bulk sized proportionate. It also changes the way in which the nanoparticles bond with the bulk material [95]. The result is that the composite can be many times improved with respect to the component parts.

Nanoparticles have a few disadvantages [96], such as toughness and impact performance. However, in recent work researchers have shown that modification of polymers such as polyamides could even decrease impact performance of the nanoparticle. Hence, there is a need for better understanding of structure and property relationships to dispersion of the nanoparticle. The advantages and the disadvantages of the nanocomposites are shown in **Table 2.4**.

Table 2.4: Characteristics of nanocomposites Source [96]

Advantages	Disadvantages	Reference
Thermal expansion and thermal conductivity	Viscosity increase (limits process ability)	[96]
Mechanical properties (tensile strength, stiffness, toughness)	Black color when different carbon containing nanoparticles are used	
Gas barrier and properties	Improved	
Synergistic flame retardant additive	Optical issues	
Ablation resistance	Dispersion difficulties	
Dimensional stability		

Ideally applications for nanocomposites are coming slowly [96], and these is due this to the new technology cost and variability in the quality of some of the products. Another challenge faced by researchers and manufactures of nanocomposite is pre-polymerization and post polymerization for preparing nanocomposites [95]. At industrial level, pre-polymerization preparations can disturb

the polymerization process, which is critical and requires time and expense to achieve good yields, and post polymerization requires a lot of time to achieve a good dispersion of the nanoparticles in the composite. This then becomes an expensive and low cost-competitive process.

2.6. References

- [1] S. Srivastava and P. Goyal, Decontamination of toxic metals from wastewater, Berlin Heidelberg: *Environmental Science*, Vol 8, pp. 23-34, 2010.
- [2] R. Michalski, "Ion Chromatography Method for the Determination of trace level Chromium in water," *Polish Journal of Environmental Studies*, Vol. 12, pp. 73-77, 2004.
- [3] K. Straif, L. Benbrahim-Tallaa and R. Baan, "Metals, arsenic, dusts, and fibres. Lyon, International Agency for Research on Cancer," *The Lancet Oncology*, Vol. 6, pp. 453-454., 2009.
- [4] M. Mothui, M. Onyango and A. Maity, "Magnetic adsorption separation process for industrial waste water treatment using polypyrrole-magnetite nanocomposite," *Journal of Chemistry and Metallurgical Engineering*, Vol. 158, pp. 250-258, 2013.
- [5] EPA, "United State Environmental protection agency," 1992. [Online]. Available: <http://www.epa.gov/ttnatwo1/hlthef/chromium>.
- [6] Dionex, "Determination of Cr(VI) in water, wastewater, solidwasterextraction," 1996. [Online]. Available: www.dionex.com/en-US/webdocs/4428tn26pdf. [Accessed 16 November 2015].
- [7] Lenntech, "Chromium and water: reaction mechanisms, environmental impact and health effects," 2010. [Online]. Available: www.lenntech.com/periodic/water/chromium/chromium-and-water.htm. [Accessed 07 June 2016].
- [8] N. Oyaro, O. Juddy, E. Murago and E. Gitonga, " The contents of Pb, Cu, Zn and Cd in meat in Nairobi, Kenya," *International Journal Food Agriculture Environment*, Vol. 6, pp. 119-121., 2007.
- [9] P. Finnegan, "Arsenic toxicity effect on plant metabolism," *Frontiers In Physiology*, Vol. 8, pp. 115-124, 2012.

- [10] R. Bentley, "Microbial methylation of metalloids arsenic, antimony and bismuth," *Microbiology and Molecular Biology*, Vol. 4, pp. 250-271, 2002.
- [11] P. Tchounwou, "Metal toxicity and the environment," *HHS Public Access*, Vol. 12, pp. 133-164, 2012.
- [12] J. Akan, "determination of heavy metal in blood, urine and water sample by ICP-AES and Fluoride using ion selective electrode," *Analytical and Bioanalytical*, Vol. 24, pp. 1-7, 2014.
- [13] H. Fountain, "In lakes, photosynthesis relies on arsenic," *The New York Times*, New York, 2008.
- [14] E. Ruben, "Regression analysis of dissolved heavy metals in storm waters runoff from electrical roadways," *University of New Orleans Theses and Dissertations*, Vol. 4, pp. 150, 2005.
- [15] U. M.-. Najar, "Epigenetic control of aging," *Antioxidant and REDOX Signaling*, Vol. 9, pp. 241-259, 2011.
- [16] A. Arita, "Epigenetic in metal carcinogenic: Nickel, Arsenic, Chromium and Cadmium," *HHS Public Access*, Vol. 16, pp. 222-228, 2009.
- [17] M. Patel, "Advances in reprogramming somatic cells to induce pluripotent stem cells," *HHS Public Access*, Vol. 15, pp. 367-380, 2010.
- [18] S. B. K. G. S Gupta, "Advancements in medical electronics," *Bioengineering*, Vol. 6, pp 8-16, 2015.
- [19] P. Soria, "Role of In-Utero and chromium arsenate exposure in the development of adult cardiovascular photosynthesis," *Pharmacology and Toxicology*, Vol. 7, pp 83-94, 2013.
- [20] M. Shadrack, "Chromium, an essential nutrient and pollutant," *African Journal of Pure and Applied Chemistry*, Vol. 3, pp 1-12, 2013.

- [21] G. borries, "Safety and effeciency of chromium methionine as food active for all species," *EFSA Journal*, Vol. 5, pp. 1-69, 2009.
- [22] P. Most and P. j., "Possible Roles of Plant Sulfurtransferases in Detoxification of Cyanide, Reactive Oxygen Species, Selected Heavy Metals and Arsenate," *Molecules*, Vol. 20, no. 1 , pp. 1410-1423, 2015.
- [23] D. K. PL Smedley, "Sources and behaviour of arsenic in natural waters," *British Geological Survey*, Vol. 8, pp 12, 2014.
- [24] N. Nevetha Yogarajaha and S. Tsai, "Detection of trace arsenic in drinking water: challenges and opportunities for microfluidics," *Environmental Science: Water Research and Technology*, Vol. 1, pp. 426-447, 2015.
- [25] B. Mamba, L. Rietveld and J. Verberk, "S.A drinking water under the microscope," *The Water Wheel*, vol. 7, pp. 24-27, 2008.
- [26] M. S. R. Rane, V. Sapkal, P. M. B. and s. S.P., "Use of Naturally Available Low Cost Adsorbents for Removal of Cr (VI) from Wastewater," *International Journal Chemical Science Application.*, Vol. 18, pp. 119-132, 2010.
- [27] EHS, "Environmental, health, and safety giudelines for semiconductors and other electronical manufactures," 2007. [Online]. Available: <http://www.ifc.org/wps/wcm>. [Accessed 05 March 2016].
- [28] D. McCannon, "Semocondutors thermistors," *Journal of Physics*, Vol. 6, pp. 2-26, 2005.
- [29] H. Korjus, "Polluted soil restoration," *Estonian University Pile Science*, Vol. 2, pp 1-25, 2014.
- [30] D. Lakherwal, "Adsorption of heavy metal," *Indian Publications*, Vol. 8, pp. 41-44, 2007.
- [31] G. Witmann and U. Forstner, Metal pollution in aquatic environment, New York: Springer study edition, 1983.

- [32] WHO, "Trends in maternal mortality: 1990 to 2015," Switzerland, World health organization, 2015, pp. 1-92.
- [33] C. Oze, S. Fendorf and D. Bird, "chromium geochemistry of sepentine soils," *International Geology Review*, vol. 46, pp. 97-126, 2010.
- [34] L. Raa, "Removal of heavy metals by biosorption," *Technical Journal*, Vol. 23, pp. 1-6, 2011.
- [35] M. Rashed, "Adsorption for removal of organic pollutants form water and wastewater," *Journal of Hazards materials*, Vol. 6, pp. 1-14, 2013.
- [36] H. Mahmud and S. Hosseini, "Polymer adsorbent for the removal of lead ions from aqueous solutions," *International Journal of Technical Research*, Vol. 12, pp. 23-29, 2014.
- [37] T. Wanchun, "Adsorption of nitrogen and Phosphorus on natural zeolite and influencing factors," *Intelligent Environmental Monitoring*, Vol.18, pp. 1949-1952, 2011.
- [38] J. Cha, M. Cui, M. Jang, S. Cho, D. Moon and J. Khim, "Kinetic and mechanism studies of the adsorption of lead onto waste cow bone powder (WCBP) surfaces," *Environmental Geochemistry and Health*, Vol. 33, p. 81–89, 2011.
- [39] J. Spiegel and L. Maystre, *Environmental pollution control*, 5th ed., encyclopedia of occupational health and safety, 2010.
- [40] J. Ge, E. Neofytou, T. Cahill, R. Beygui and Z. R.N., "Drug release from electric-field-responsive nanoparticles," *Journal of American Chemical Society*, Vol. 1, pp. 1-7, 2011.
- [41] H. N. M. E. Mahmud, H. S and R. B. Yahya, "Polymer adsorbent for the removal of lead ions from aqueous solution," *International Journal of Technical Research and Applications*, Vol. 7, pp. 4-8, 2014.
- [42] A. Singh, Z. Salamib, N. Joshi, P. Jha, P. Decorse and H. Lecoq, "Electrochemical investigation of free-standing polypyrrole–silver nanocomposite films: a substrate free

- electrode material for supercapacitors," *Journal of Royal Society of Chemistry*, vol. 3, pp. 24567-24575, 2013.
- [43] K. Reza, O. Seyed, H. Ehsan, F. Maysam, M. Seyed and A. Hossien, "United State Environmental Protection Agency. Retrieved from aqueous solution using polypyrrole," *Environmental Engineering and Management Journal*, Vol. 14, pp. 17-28, 1992.
- [44] S. Veenstra, J. Loos and J. Kroon, "Nanoscale structure of solar cells based on pure conjugated polymer blends," *Journal of Photovoltaic Res. Application*, Vol. 15, p. 727–740., 2007.
- [45] M. Anderson, B. Matters, H. Reis and R. Kaner, "Conjugated polymer films for gas separations," *Science*, Vol. 252, p. 1412–1415, 1991.
- [46] H. Eisazadeh and H. Khorshidi, "Preparation and characterization of PAn-HPC/Fe₃O₄ and PAn-HPC/Fe₂O₃ nanocomposite using hydroxypropylcellulose as a steric stabilizer," *Journal of Polymer Plasma Technology Engineering*, vol. 49, p. 1591–1596, 2010.
- [47] J. Yang, Y. Yang, J. Hou, X. Zhang, W. Zhu, M. Xu and M. Wan, "Polypyrrole—polypropylene composite films: preparation and properties," *Polymer 1996*, vol. 37, p. 793–798, 1996.
- [48] T. Li, X. Zeng and J. Xu, "Preparation and characterization of conductive polypyrrole/organophilic montmorillonite nanocomposite. Polym," *Journal of Polymer Plastic Technology Engineering*, vol. 46, p. 751–757, 2007.
- [49] M. Krzysztof, "Chemical reactivity of polypyrrole and its relevance to polypyrrole based electrochemical sensors," *Journal of Electroanalysis*, vol. 18, pp. 1537-1551, 2006.
- [50] S. Saxena, "Polyvinyl alcohol (PVA)," *Chemical and Technical Assessment*, Vol. 12, pp. 1-3, 2004.

- [51] S. Chowdhury and E. Yanful, "Arsenic and chromium removal by mixed magnetite-magnetite nanoparticles and the effect of phosphate on removal," *Environmental Management Journal*, Vol. 11, pp. 2238-2247., 2010.
- [52] B. Aydınli, L. Toppare and T. Tincer, "A conducting composite of polypyrrole with ultrahigh molecular weight polyethylene foam," *Journal of Application of Polymer Science*, vol. 72, p. 1843–1850, 1999.
- [53] S. Alkan, L. Toppare, Y. Hepuzer and Y. Yagci, "Block copolymers of thiophene-capped poly(methyl methacrylate) with pyrrole," *Journal of Polymer Science* , vol. 37, p. 4218–4225, 1999.
- [54] E. Benseddik, M. Makhlouki, J. Bernede, S. Lefrant and A. Pron, "XPS studies of environmental stability of polypyrrole-poly(vinyl) alcohol composites," *Journal of Synthesized Materials*, vol. 72, p. 237–242, 1995.
- [55] B. Corbacioglu, O. Ismail, Z. Altyn, S. Keyf and S. Erturan, "Conducting polymer composites of polythiophene and polyacrylamide," *International journal of Polymer Material*, vol. 54, p. 607–617, 2005.
- [56] V. Mano, M. Felisberti, T. Matencio and M. De Paoli, "Thermalmechanical and electrochemical behaviour of poly(vinyl chloride)/polypyrrole blends (PVC/PPy)," *Journal of Polymer*, vol. 37, p. 5165–5170, 1996.
- [57] M. Ramesan, "In situ synthesis, characterization and conductivity of copper sulphide/polypyrrole/polyvinyl alcohol blend nanocomposite," *Journal of Polymer-Plastics Technology and Engineering*, vol. 51, p. 1223–1229, 2012.
- [58] U. Hafeli, W. Schutt, J. Teller and M. Zborowski, " Scientific and clinical application of magnetic carriers," Plenum press, New York, 1997.
- [59] E. Karada and S. D., "Swelling studies of super water retainer acrylamide/crotonic acid hydrogels crosslinked by trimethylolpropane triacrylate and 1,4- butanediol dimethacrylate," *PolymerBulletin*, pp. 299-307, 2002.

- [60] V. Ranade and V. Bhandari, *Industrial wastewater treatment, recycling and reuse*, Oxford: Elsevier, 2014.
- [61] T. Pradeep and Anshup., "Noble metal nanoparticles for water purification," *Thin Solid Films*, vol. 12, pp. 6441-6478., 2009.
- [62] T. Lindgren, J. Mwabora, E. Avendano, J. Jonsson, A. Hoel, C. Granqvist and S. Lindquist, "The chemistry of nanostructured materials," *Physical Chemistry*, vol. 18, pp. 5709-5716, 2003.
- [63] A. Gupta and M. Gupta, "Synthesis and surface engineering of iron oxide nanoparticles for biomedical applications," *Biomaterials*, vol. 26, pp. 3995-4021, 2005.
- [64] P. Tartaj, M. del Puerto Morales and S. Veintemillas-Verdaguer, "The preparation of magnetic nanoparticles for applications in biomedicine," *Applied Physics*, vol. 36, pp. 182-197, 2003.
- [65] J. Arias, V. Gallaro, M. Ruiz and A. Delgado, "Magnetite/poly (alkyl cyanoacrylate) (core/shell) nanoparticles as 5-Fluorouracil delivery systems for active targeting," *Europe Journal of Pharmaceutical*, Vol. 40, pp. 54-63, 2008.
- [66] S. Shaw, Y. Chen, J. Ou and L. Ho, "Preparation and characterization of Pseudomonas putida esterase immobilized on magnetic nanoparticles," *Enzyme microbe. Technology*, Vol. 26, pp. 1089-1095, 2006.
- [67] P. TeixeiraI, C. TristãoII, M. AraujoI and L. OliveiraI, "A versatile element to produce materials for environmental applications," *Journal of the Brazilian Chemical Society*, Vol. 23, pp. 1579-1593, 2012.
- [68] D. Cox and M. Maple, "Electronic pairing in exotic superconductors," *Physics Today*, vol. 1, pp. 32-40, 195.

- [69] E. Busseron, Y. Ruff, E. Moulin and N. Giuseppone, "Supramolecular self-assemblies as functional nanomaterials," *Journal of Royal Society of Chemistry*, vol. 5, pp. 7098-7140, 2013.
- [70] W. Che, Y. Wu, Y. Yue, J. Liu, W. Zhang, X. Yang, H. Chen, E. Bi, I. Ashraful, M. Grätzel and L. Han, "Efficient and stable large-area perovskite solar cells with inorganic charge extraction layers," *Scienceexpress*, vol. 5, pp. 1-11, 2015.
- [71] M. M., P. I.K. and C. C.S., "Surface modification of iron oxide nanoparticles by biocompatible polymer for tissue imaging and targeting," *Biotechnology Adv*, pp. 1224-1236, 2013.
- [72] M. O. Muthui, "Magnetic adsorption separation process for industrial wastewater treatment using polypyrrole-nanocomposite," *Journal of Engineering and Biult Environment*, Vol. 12, pp. 4-5, 2013.
- [73] I. Lo, J. Hu, G. Chen and M. Asce, "Selective removal of heavy metals from industrial wastewater using maghemite nanoparticle: performance and mechanisms," *Journal of Environmental Engineering* , vol. 132, no. 7, pp. 1-6, 2006.
- [74] J. C. G. a. L. I. Hu, ". "Selective Removal of Heavy Metals from Industrial Wastewater Using Maghemite Nanoparticle: Performance and Mechanisms," *Journal of Environmental Engineering*, pp. 709-715., 2006.
- [75] H. N. M. E. Mahmud, H. A. K. Obidul and Y. Rosiyah binti, "The removal of heavy metal ions from wastewater/aqueous solution using polypyrrole based adsorbents," *Royal Society of Chemistry Advanced*, vol. 6, no. 14776, pp. 1-12, 2016.
- [76] R. K. a. S. Meenakshi, "Synthesis of conductive-biopolymer composites," *Matetials*, vol. 181, p. 198, 2014.
- [77] N. Ballav, N. Choi, S. Mishra and A. Maity, "Synthesis, characterization of Fe₃O₄@glycine doped polypyrrole magnetic nanocomposites and their potential

- performance to remove toxic Cr(VI)," *Journal of Industrial and Engineering Chemistry*, vol. 20, p. 4085–4093, 2014.
- [78] H. Wang and J. Fernandez, "Blends of polypyrrole and poly(vinyl alcohol)," *Macromolecules*, vol. 26, pp. 3336-3339, 1993.
- [79] M. Al-Hwaitia, K. A. Ibrahim and M. Harrarad, "Removal of heavy metals from waste phosphogypsum materials using polyethylene glycol and polyvinyl alcohol polymers," *Arabian Journal of Chemistry*, vol. 9, pp. 2-27, 2015.
- [80] T. Burks and U. Abedusalam, "Removal of Cr (VI) by using of surface modified superparamagnetic iron oxide nanoparticles," *Separation Science and Technology*, vol. 48, no. 8, 2015.
- [81] K. Wang, Q. Guangming, H. Cao and J. Ruifa, "Removal of Chromium(VI) from Aqueous Solutions using magnetite polymer microspheres functionalized with amino acids groups," *materials*, Vol. 13, pp. 1-14, 2015.
- [82] M. Bhaumik, A. Maity, V. Srinivasu and M. Onyango, "Enhanced removal of Cr(VI) from aqueous solution using polypyrrole/Fe₃O₄ magnetic nanocomposite.," *Journal of Hazard Materials*, vol. 3, pp. 381-390, 2011.
- [83] A. Bablu, A. Srivastava and J. Srivastava, "Adsorption of heavy metals from industrial downstream using polypyrrole as a polycomposite material," *Novus International Journal of Engineering & Technology*, Vol. 15, pp. 34-42, 2014.
- [84] R. Ansari and F. Khoshbakht, "application of polypyrrole coated wood sawdust for removal of Cr(VI) ions from aqueous solution," *Reactive and Functional Polymers*, Vol. 20, pp. 26-35, 2007.
- [85] H. Eisazadeh, "Effect of various agent on removal of nickel from aqueous solution using polypyrrole as an adsorbent," *Journal of Science, Engineering and Technology*, Vol 12, pp. 540-550, 2012.

- [86] k. Karunakaran and P. Thamilarasi, "Removal of Fe(III) form aqueous solution using ricinus communi seed shell and polypyrrole coated ricinus communi seed activated carbon," *International Journal off Chem Tech Research*, Vol. 8, pp. 26-35, 2010.
- [87] Y. Zhao, H. Shen and S. Pan, "Preparation and characterization of amino-functionalized nano-Fe₃O₄ magnetic polymer adsorbents for removal of chromium(VI) ions," *Journal of Materials Science*, vol. 19, no. 45, p. 5291–5301, 2010.
- [88] P. Smedley and D. Kinniburgh, "A review of the source, behaviour and distribution of arsenic in natural waters," *Journal of Applied Geochemistry*, vol. 17, pp. 517-568, 2002.
- [89] K. Simeonidisa, T. Gkinisa, S. Tresintsi, C. Martinez-Boubetac and G. Vourliasa, "Magnetic separation of hematite-coated Fe₃O₄ particles used as arsenic adsorbent," *Journal of Chemical Engineering*, vol. 168, p. 1008–1015, 2011.
- [90] L. Fenga, M. Caoa, X. Maa, Y. Zhua and J. Hua, "Superparamagnetic high-surface-area Fe₃O₄ nanoparticles as adsorbents for arsenic removal," *Journal of Hazard Materials*, vol. 218, p. 439– 446, 2012.
- [91] B. Peng, T. Song, T. Wang, L. Chai, W. Yang, X. Li and C. Li, "Facile synthesis of Fe₃O₄@Cu(OH)₂ composites and their arsenic adsorption application," *journal of Chemical Engineering*, vol. 299, pp. 15-22, 2016.
- [92] A. Sadrolhosseini, M. Naseri and M. Kamari, "Surface plasm on resonance sensor for detecting arsenic in aqueous solution using polypyrrole-chitosan-cobalt ferrite nanoparticles composite," *Journal of Optics Communications*, vol. 383, p. 132–137, 2017.
- [93] D. Zhao, Y. Yu and J. Chen, "Zirconium/polyvinyl alcohol modified flat-sheet polyvinylidene fluoride membrane for decontamination of arsenic: Material design and optimization, study of mechanisms, and application prospects," *Journal of Chemosphere*, vol. 155, pp. 630-639, 2016.
- [94] S. Sinha, "Polymer nanocomposites," CSIR, [Online]. Available: <http://www.csir.co.za/nano/pn.html>. [Accessed 12 September 2016].

- [95] C. Okpala, "The benefits and application of nanocomposites," *International Journal of Advanced Engineering Technology*, Vol. 23, pp. 12-18, 2014.

CHAPTER 3

3. Experimental

In this chapter, an overview of the experimental procedures that were adopted in pursuance of this study is presented. Specifically, the preparation and characterization of the nanocomposites that are used for the extraction of the targeted pollutants is documented. The chapter concludes with a description of a study on the extraction of Cr(VI) and As(III) from aqueous solutions using the synthesized nanocomposites.

3.1. Chemicals and reagents

Pyrrole monomer (98%) with density $0,967\text{g/cm}^3$, poly(vinyl)alcohol (PvOH), ammonium hydroxide (NH_4OH), potassium dichromate ($\text{K}_2\text{Cr}_2\text{O}_7$), ferric chloride (FeCl_3), ferrous chloride (FeCl_2) and NaAsO_2 were purchased from Sigma Aldrich, South Africa. Deionized water was collected from the lab. Pyrrole was stored in a dark place prior to use. All chemicals used in the experiment were of analytical grade.

3.2. Synthetic procedures

3.2.1. Preparation of the PPy-PvOH polymer blend

Different masses (1.0, 2.0, 3.0, and 4.0 g) of the PvOH were accurately weighed using an analytical weighing balance (HR 250 A MODEL) as illustrated in **Table 2.1** and dispensed into 50ml of distilled water for 1 h at 90°C . The solution was then cooled down to room temperature using cool water bath. To this mixture, of pyrrole (0.6 ml) was syringed using a micropipette and hand shaken for 2 minutes. To initiate co-polymerization, anhydrous ferric chloride (5g) of was added to the mixture, while shaking and this resulted in the formation of a black precipitate of polypyrrole-polyvinyl alcohol blend. The black mixture was left for 5 hrs at room temperature for completion of the polymerization process [2].

Table 3.1: Calculation of the ratio of PvOH and PPy used for the polymer blend.

Pyrrole (ml)	PvOH (g)	PPy loading (g)	PPy/PvOH (total)	Ratio (PPy: PvOH)
0.6 ml	1 g	2.79g	3.79g	74:26
0.6 ml	2 g	3.49g	5.49g	64:36
0.6 ml	3 g	3.84g	6.84g	56:44
0.6 ml	4 g	4.365g	8.365g	52:48

The following equation was used for calculating the exact amount of PPy available in PPy/PvOH blend

$$PPy = (PPyPvOH \text{ total}) - PvOH$$
$$PPy \text{ loading} = \frac{PPy}{PPy+PvOH} \times 100 \quad \text{OR} \quad PPy \text{ loading} = 100 - \left(\frac{PvOH}{PPy+PvOH} 100 \right) \quad (3.1)$$

3.2.2. Preparation of the iron oxide nanoparticles

Fe₃O₄ nanoparticles (NPs) were prepared by using a method described in the literature [1]. About 200 cm³ of distilled water was measured and placed into a three necked flask. Nitrogen gas was bubbled into this solution throughout the experiment. A 1:2 ratio of FeCl₃ (5.2 g) and FeCl₂ (2.0 g), respectively, were dissolved in deaerated water (200 mL) and stirred for a period of 30 minutes. This was followed by a drop-wise addition of the 1.5 mol/L solution of NH₄OH (40 ml) under inert and stirring conditions. The pH of the solution was monitored using a universal pH paper. When the pH of 9 was reached, the solution was allowed to settle for 3 hours and the precipitate was isolated using external magnetic field, followed by the decanting of the supernatant liquid. The resulting wet nanogel was rinsed twice with water followed by freeze-drying for 24 hours to obtain the nanocrystals. **Figure 3.1** shows the experimental set-up for the preparation of the iron oxide nanoparticles.

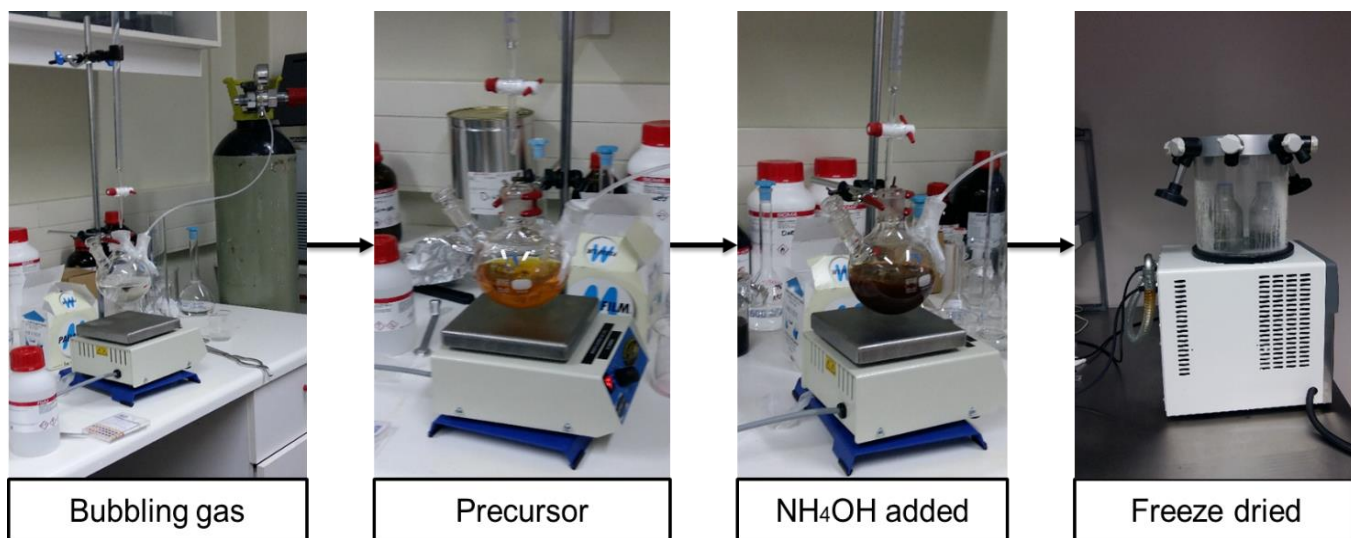


Figure 3.1: An image of the set up for the preparation of magnetite

3.2.3. Preparation of the Fe_3O_4 -PPy-PvOH polymer nanocomposites

To fabricate the nanocomposites, a previously synthesized magnetite nano-powder (0.4g) was dispensed into the PPy-PvOH polymer blend during copolymerization and thereafter ultrasonicated (Sciencetech, South Africa) for 30 minutes in order to achieve better dispersion of the nanoparticles [1]. The precipitate of PPy-PvOH- Fe_3O_4 nanocomposite was washed repeatedly and sequentially with distilled water and acetone to purify the material by removing any residual oligomers. The resultant nanocomposites powder was freeze-dried for 24 hrs.

3.3.Characterization techniques

3.3.1. Fourier transform infra-red (FT-IR)

Fourier Transform Infra-Red (FT-IR) was used to evaluate the structures of compounds that were synthesized and were measured using a Perkin–Elmer PE 1600 FTIR spectrophotometer [4]. The KBr pellets were used to take the spectra in the range of $4000-400\text{ cm}^{-1}$.

3.3.2. *Scanning electron microscopy (SEM) and transmission electron microscopy (TEM)*

The morphology of the PPy-PvOH-Fe₃O₄ polymer nanocomposite was studied using scanning electron microscopy (SEM), (JEOL model JSM 6260 LE) [5] and transmission electron microscopy (TEM), (JEOL JEM-2100F) [6]. The SEM and TEM were operated with accelerating voltage of 20 KV and 90 KV, respectively. The samples were coated with carbon for SEM analysis.

3.3.3. *X-ray diffraction (XRD) studies*

The crystalline and amorphous character of the Fe₃O₄ nanoparticles and the PPy-PvOH-Fe₃O₄ nanocomposite were investigated by using the Rigaku Ultima IV diffractometer. The XRD data were collected at a 2θ range of 20° to 90°.

3.3.4. *Differential scanning calorimetry (DSC)*

Differential scanning calorimetry (DSC) (SDT-Q600) was used to study the thermal decomposition of the samples. Thermal studies were conducted in a temperature range of 0 °C to 900 °C in a nitrogen atmosphere and a heating rate 10°C/min [7].

3.3.5. *Brunauer–Emmett–Teller (BET)*

The changes in the surface area, pore size, and pore volume of the polymer matrix after the formation of nanocomposite were monitored using the surface area and porosity analyzer (Micromeritics, ASAP 2020) [8]. Measurements were taken through the nitrogen isothermal adsorption technique.

3.3.6. *Inductive coupled plasma (ICP)*

ICP-EOS is an analytical method utilized to detect trace metals such as Cr, As, Pb, and many others [9]. The post adsorption concentration for both As(III) and Cr(VI) were analysed by ICP-OES (700 series, Agilent technology) using Cr(VI) standard solution of wavelength 37,868 nm corresponding to the maximum absorbance of Cr(VI) and As(III) standard with a wavelength 193 nm corresponding the maximum absorbance of As(III)

3.3.7. *Zeta potential measurements*

The Zetasizer is used to measure the zeta potential and electrophoretic mobility in aqueous and non-aqueous dispersions using Laser Doppler Micro-Electrophoresis. The charge on the surface of an adsorbent is very important in order to explain the mechanism of interaction between the adsorbent and the dye and it was calculated using zeta potential measurements at different pH using Zetasizer Nano-ZS, ZEN3600 (Malvern Instruments Limited)[10].

3.4. Adsorption studies

3.4.1. *Preparation of synthetic solutions contaminated with model pollutants of As(III) and Cr(VI)*

To prepare the As(III) sample solution, a 100 ppm stock solution of As(III) was prepared by dissolving NaAsO₂ (3.745 g) in deionized water (1000 ml). Similarly, the 100 ppm stock solution of Cr(VI) was prepared by dissolving K₂Cr₂O₇ (4.9 g) in deionized water (1000 ml). From the stock solution 50 ppm to 150 ppm were prepared for As(III) and 10 ppm to 50 ppm standards were prepared for Cr(VI). The post adsorption concentrations of As(III) and Cr(VI) were determined by ICP-EOS at their respective wavelength of 193 nm (corresponding to the maximum absorbance of As(III)) and 37,868 nm (corresponding to the maximum wavelength of Cr(VI))

To analyze the As(III) and Cr(VI) absorbance, 0.10 g and 0.12 g of PPy-PvOH-Fe₃O₄ nanocomposite was added to 10 ml of the different standards, respectively. The adsorbent was

measured against the calibration standards. The adsorption efficiency of PPy-PvOH-Fe₃O₄ nanocomposite towards the Cr(VI) ions were calculated by using the following equation.

$$\% Cr(VI)removal = \frac{(C_0 - C_t)}{C_0} \times 100 \quad (3.1)$$

PPy-PvOH-Fe₃O₄ nanocomposite where C_0 initial concentration of the Cr(VI) ions and C_t is the equilibrium concentration of Cr(VI) at time t

3.4.2. Effect of pH

The adsorption capacity of the PPy-PvOH-Fe₃O₄ nanocomposite was determined by varying the pH of the Cr(VI) and As(III) solution at a range of 2,4,8, and 12 while the other parameters were maintained as explained in abovementioned experiment. The solutions used to control pH of the solution were 0.125 M HCl and 0.125 M NaOH.

3.4.3. Effect of concentration

The effect of the initial concentration of the model pollutants on the adsorption capacity of the PPy-PvOH-Fe₃O₄ nanocomposite was studied by varying the initial concentrations of As(III) and Cr(VI) ions from 50-150 ppm and 10-50 ppm respectively. The respective optimum masses of the adsorbent, which were found to be 0.10 g and 0.12 g for As(III) and Cr(VI) , where kept constant throughout the experiment. Furthermore, the experiment were conducted at pH 12 and reaction time of 30 and 45 minutes for As(III) and Cr(VI) experiments, respectively.

3.4.4. Effect of dosage

In order to investigate the effect of adsorbent mass on the rate of adsorption, 150 ppm of As(III) and 30 ppm Cr(VI) solution were used as initial concentration at pH 12. To initiate the adsorption process, PPy-PvOH-Fe₃O₄ nanocomposites (0.12g and 0.10g) were added into the 30 ppm solution of Cr(VI) and 150 ppm solution of As(III), respectively. The post adsorption concentration of each

nanocomposite sample, the sample was then removed from the aqueous solution filtration using Whatmann filter paper) and thereafter analyzed for the model pollutant at 5 minute intervals from time $t=0$ up to time $t=60$ minutes. This experiment was subsequently repeated under similar conditions using 0.01g, 0.02g, 0.03g, 0.04g, 0.10g, and 0.12g of PPy-PvOH-Fe₃O₄ nanocomposites

3.4.5. *Effect of time*

Time was also varied for adsorption capacity using PPy-PvOH-Fe₃O₄ nanocomposite with ratio 56:42:2 respectively. Time range of 5 15 3. 45 120 240 minutes was used.

3.5. **Adsorption isotherm models**

An adsorption isotherm study was carried out using two isotherm models, namely Langmuir and Freundlich isotherms models. More details are provided in the relevant discussion section in chapter.

3.6. **Adsorption kinetics models**

Adsorption kinetics studies consist of theoretical studies and gas adsorptions. The purpose of the present work is to develop pseudo-first-order and pseudo-second-order models for sorption processes from aqueous solutions by a general kinetic method.

3.7. **Swelling studies of the nanocomposites**

The swelling properties of the PPy-PvOH-Fe₃O₄ nanocomposites were determined by immersing the nanocomposite in distilled water at variable pH and time periods. 0.12g of nanocomposite sample was accurately weighed and dispersed in 10ml deionised water over a period of time [3]. The swelling [S%] of the nanocomposite was calculated using the following equation:

$$S\% = \frac{M_t - M_o}{M_o} 100 \quad (3.5)$$

where M_t is the mass of the swollen gel at time t and M_o is the dry gel at time 0.

3.8.References

- [1] M. Muthui, A. Muliwa and M. Onyango, “agnetic adsorption separation process for industrial wastewater treatment using polypyrrole-magnetite nanocomposite,” *Journal of Hazard Materials*, vol. 158, pp. 250-258, 2013.
- [2] T. Ramesan, “In Situ Synthesis, Characterization and Conductivity of Copper Sulphide/Polypyrrole/Polyvinyl alcohol nanocomposites,” *Polymer-Plastics Technology and Engineering*, vol. 51, p. 1223–1229, 2012.
- [3] E. Karada and D. SaraydÖn, “Swelling studies of super water retainer acrylamide/crotonic acid hydrogels crosslinked by trimethylolpropane triacrylate and 1,4- butanediol dimethacrylate,” *Polymer Bulletin*, vol. 48, pp. 299-307, 2002.
- [4] Nicolite, “Information to Fourier Transformation Infrared Spaectroscopy,” *FTIR Introduction*, vol. 14, pp.1-45, 2001.
- [5] R. Pool, “Nanowires delivery drugs on target,” *Biomedical Engeenering*, vol. 26, pp. 1-9, 2015.
- [6] H. Rose, “Layout of optical component in a basic T.E.M,”*Science and Technology Advanced Materials*, vol. 9, pp. 1-31, 2008 .
- [7] R. Usamentiaga, P. Venegas, L. Vega, J. Molleda and F. Bulnes, “Infrared Thermography for Temperature Measurement and Non-Destructive Testing,” *Sensors*, vol. 14, no. 7, pp. 12305–12348, 2014.
- [8] L. Neal, “Surface area and porosity,” Cma analytical, *New York*, 2012.
- [9] G. de Gennaro, B. Daresta, P. Ielpo and P. M., “Analytical methods for determination of metals in environmental samples,” *Laboratory of Environmental Sustainability*, vol. 6, pp. 1-46, 2016.

[10] W. Tscharnuter, "Mobility measurements by phase analysis," *Applied Optics*, vol. 40, pp. 1-9, 2001.

CHAPTER 4

4. Results and discussion

This chapter involves a discussion of results of this study. Specifically, the synthesis, characterization and application of PPy-PvOH-Fe₃O₄ nanocomposites in the extraction of Cr(VI) and As(III) from aqueous solutions are discussed.

4.1. Incorporation of Fe₃O₄ particles onto the PPy-PvOH blend to form Fe₃O₄-PPy-PvOH polymeric nanocomposites

- Synthesis of PPy-PvOH blend

PPy-PvOH polymer blend were synthesized by co-polymerization in the presence of FeCl₃ as an oxidant.

- Synthesis of Fe₃O₄ particles

Fe₃O₄ nanoparticles (NPs) were prepared by using a method described in the literature [1]. About 200 cm³ of distilled water was measured and placed into a three necked flask. Nitrogen gas was bubbled into this solution throughout the experiment. FeCl₃ and FeCl₂ were used as pre-cursors to initiate the synthesis.

- Incorporation of Fe₃O₄ particles onto the PPy-PvOH blend to produce the Fe₃O₄-PPy-PvOH polymeric nanocomposites

Prepared magnetite nano-powder was dispensed into the PPy-PvOH polymer blend during co-polymerization and thereafter ultra-sonicated (Sciencetech, South Africa) for 30 minutes in order to achieve better dispersion of the nanoparticles

4.2. Characterization of the PPy-PvOH polymer blend, Fe₃O₄ and Fe₃O₄-PPy-PvOH polymer nanocomposites

4.2.1. Fourier transform infra-red (FTIR) analysis

The results from FTIR analysis of magnetite (Fe₃O₄) nanoparticle illustrated in **Figure 4.1**, PPy-PvOH polymer blend, and Fe₃O₄-PPy-PvOH nanocomposite are shown in figure 4.2 above. A strong adsorption peak of Fe₃O₄ is observed at 554 cm⁻¹ in the figure corresponds to Fe-O stretching [1]. In **Figure 4.2** FTIR analysis of PPy-PvOH was determined to observe the functional group of the samples in which provided information regarding the formation of blend. At 1044 cm⁻¹ the peak can be assigned to the C=C formation related to aromatic ring of PPy. The peaks at 1450 cm⁻¹ (C-N stretching vibration), 1292 cm⁻¹ (C-H in-plane deformation), 3185 cm⁻¹ (N-H in-plane deformation), and at 3402 cm⁻¹ there is an overlap assigned to OH-functional group [2].

The FTIR spectra of PPy-PvOH-Fe₃O₄ was also analysed, the samples exhibit the characteristic peaks of PPy-PvOH blend, of which a strong vibration band about 3185 and 3402 cm⁻¹ corresponds to the overlapping absorption of NH and OH group of the blend composite respectively. It can be noticed that the incorporation of Fe₃O₄ to blend causes some observable changes in the spectrum of composites. It brings new absorption bands at 667 cm⁻¹ which exhibits Fe-O group and small shift in the intensity of some absorption bands. The new absorption bands may be correlated to defects brought by the ligand to metal charge-transfer reaction between the blend chains and Fe₃O₄ nanoparticle. From the results it can be concluded that the polymerization was carried out and the Fe₃O₄ nanoparticles were successfully incorporated in the blend.

Table: 4.1 Summary table of IR spectra

In **Table 4.1**, the wavenumber of Fe_3O_4 and $\text{PvOH-PPy-Fe}_3\text{O}_4$ nanocomposites are illustrated with their corresponding

Compound	Wavenumber (cm^{-1}) and Band Assignment			
Fe_3O_4	1641 $\nu\text{C}=\text{N}$ str	1568 $\nu\text{N-H}$ bend	-	-
$\text{PvOH-PPy-Fe}_3\text{O}_4$	3206-3210 $\nu\text{N-H}$ str	1631-1629 $\nu\text{C}=\text{N}$ str	1531-1536 $\nu\text{N-H}$ bend	3338 $\nu\text{N-H}$ str

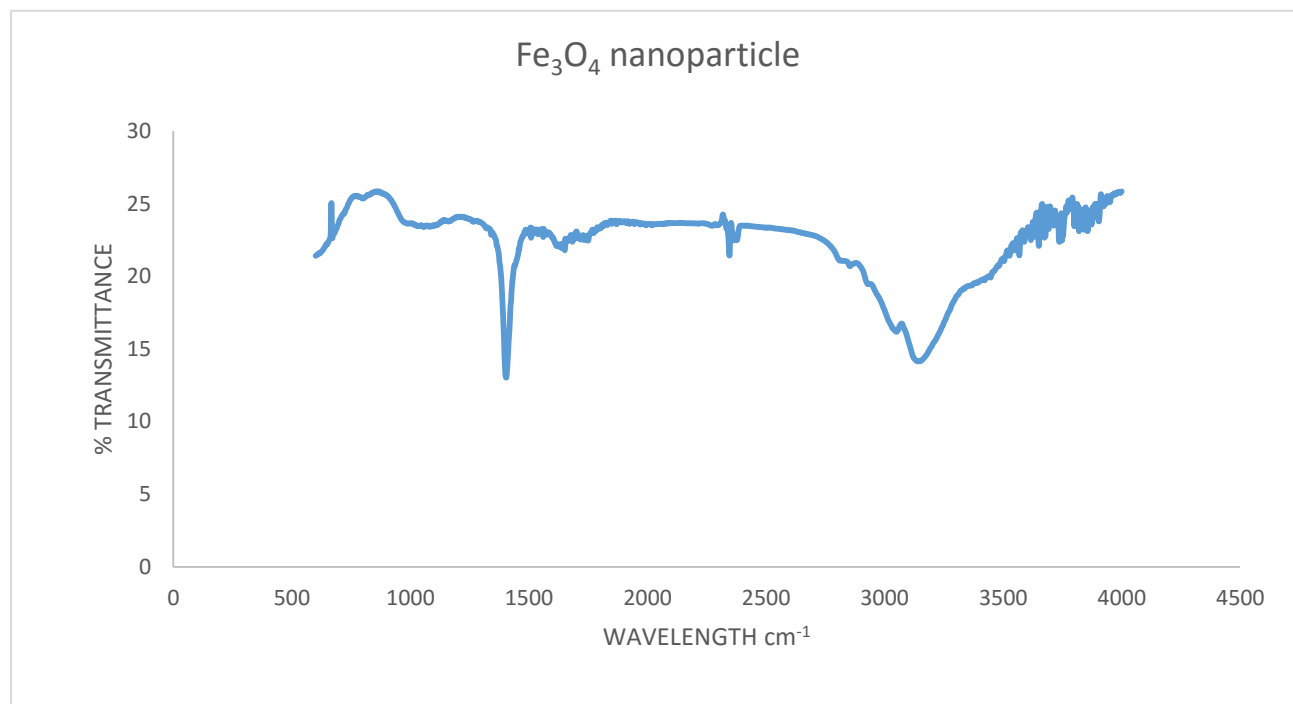


Figure 4.1: FTIR analysis of Fe_3O_4 nanoparticle

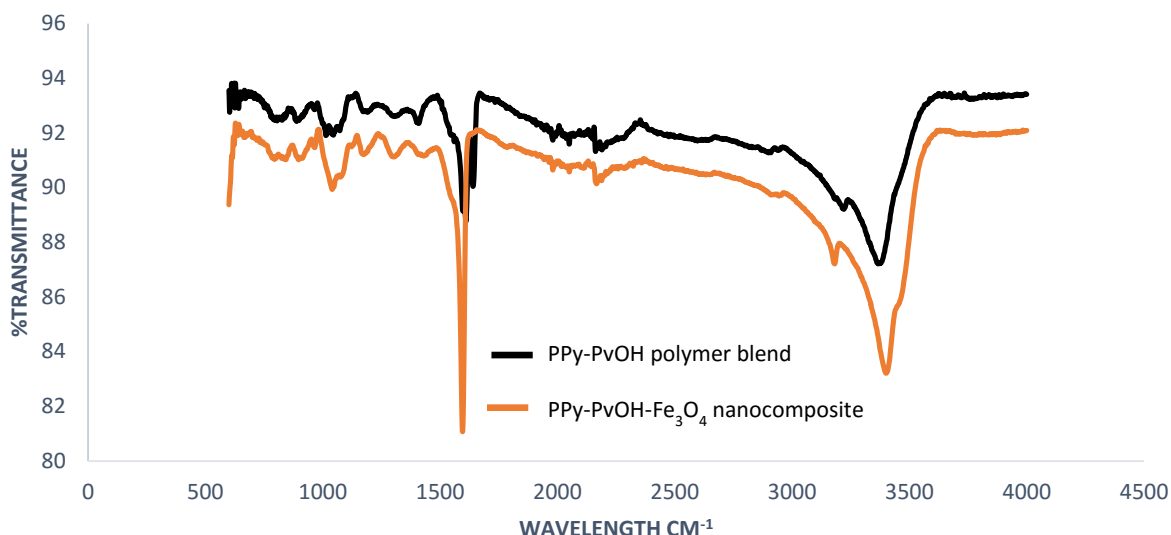


Figure 4.2: FTIR analysis of PPy-PvOH blend, and Fe₃O₄-PPy-PvOH nanocomposite

Figure 4.3 illustrate the TGA analysis of Fe₃O₄ nanoparticle, PPy-PvOH polymer blend, and Fe₃O₄-PPy-PvOH nanocomposite. The <10 nm sample of Magnetite (Fe₃O₄) is also indicated in in Figure 4.3 with an indication of two degradation occurring in the stages at two different temperature. The initial stage is observed at the region of 60 to 100°C with the weight loss of 2 %, which is attributed to the loss of moisture. The second step of degradation at the range of 150 to 300°C attributes to the structural backbone, the elimination of the Fe-O, and Fe-OH functional groups. From 300 to 900°C shows the residual of Fe₃O₄ nanoparticle that is left is around 55%

The PPy-PvOH (56:44) polymer blend thermal stability was also measured. The composite showed similar characteristics at the first stage of degradation, with a gradual weight loss assigned to the evaporation of water molecules at a range of 70 to 100°C. The second weight loss is at a range of 100 to 300°C which is assigned to degradation of the composite functional groups, including OH, N-H, and C=C. The final stage of the (PPy-PvOH) polymer composite is attributed to the structural back bone, with the elimination of C-H and C-C bonds.

Finally PPy-PvOH-Fe₃O₄ (56:42:2) nanocomposite does not show any loss of water molecules but instead, starts degrading at a high temperature of 320°C. The degradation of Fe-O, OH, N-H and, C=C functional groups is observed at 320 to 650°C with a mass loss of 57% and no composition is noticeable after 650°C, and residual left is around 40%. From the results it can be concluded that the incorporation of the Fe₃O₄ nanoparticle into the blend brought thermal stability to the composite. Observations from figure 4.3 illustrates the thermal stability of the composite, which shows that after the incorporation of the Fe₃O₄ nanoparticle, the composite degrades at a high temperature of 330°C.

4.2.2. Thermo-graphic analysis (TGA) analysis

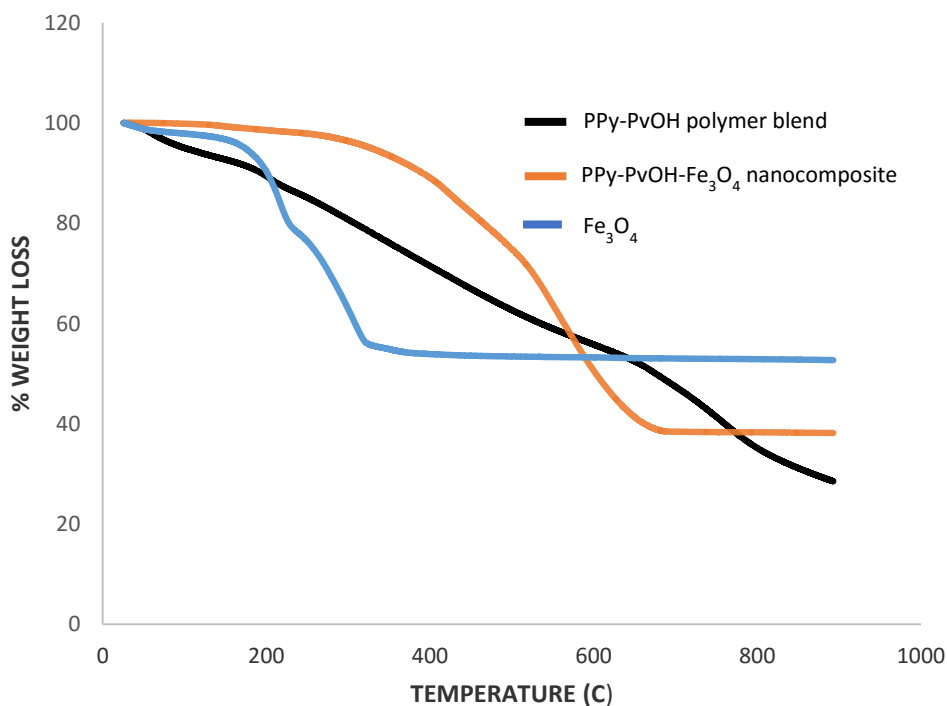


Figure 4.3: TGA analysis of Fe₃O₄, PPy-PvOH, and Fe₃O₄-PPy-PvOH

4.2.3. Differential scanning calorimetry (DSC)

The results of measurement of the PPy-PvOH-Fe₃O₄ nanocomposite containing ratio with 2% of magnetite present in the nanocomposite and the results of Fe₃O₄ are measured by means of DSC method are presented in Figure 4.5 above. The DSC curve of Fe₃O₄ shows the low temperature maximum at 70 °C which can be related to the elimination of absorbed water, whereas the two maxima at higher temperatures of 225 °C and 323 °C are assigned to melting and the decomposition of the functional groups (Fe-O and Fe-OH). The PPy-PvOH-Fe₃O₄ nanocomposite does not show any low temperature maximum but the DSC curve of nanocomposite exhibits endothermic maxima at about 417°C, 466 °C and 554 °C[3].

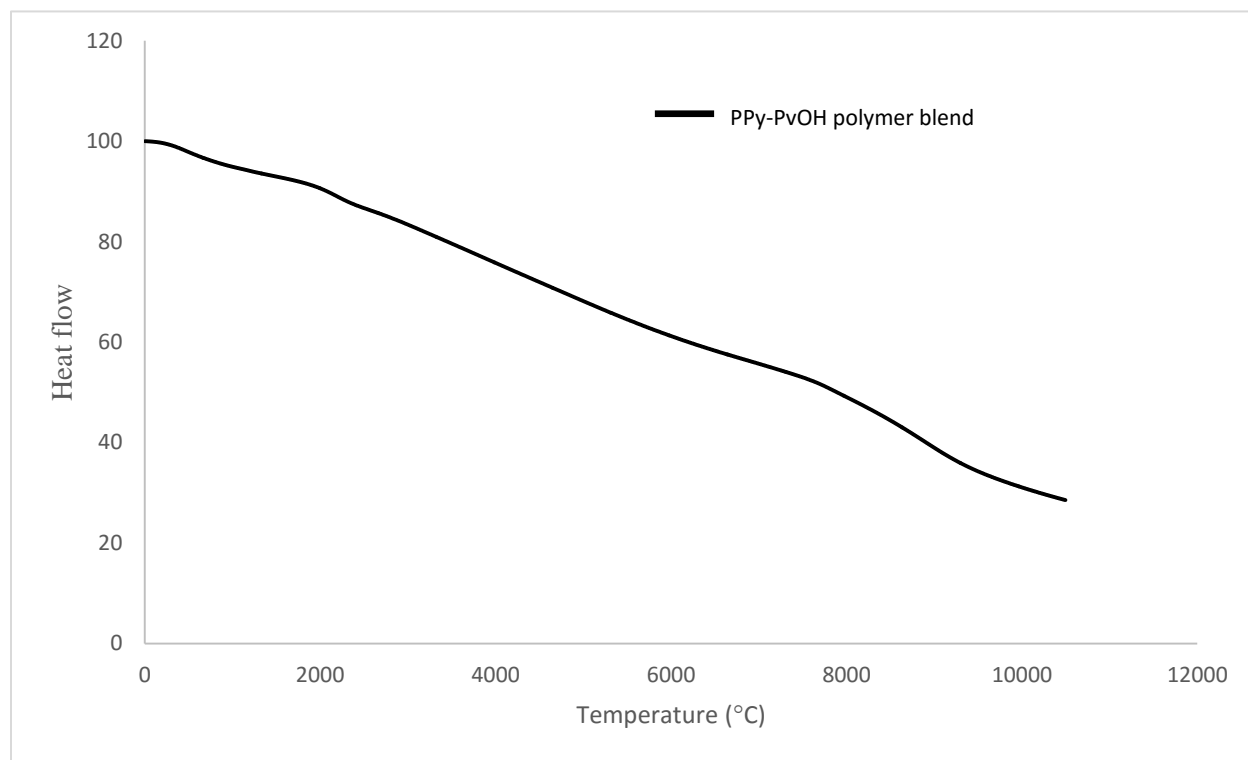


Figure 4.1: DSC analysis of PPy-PvOH (56:44) polymer blend

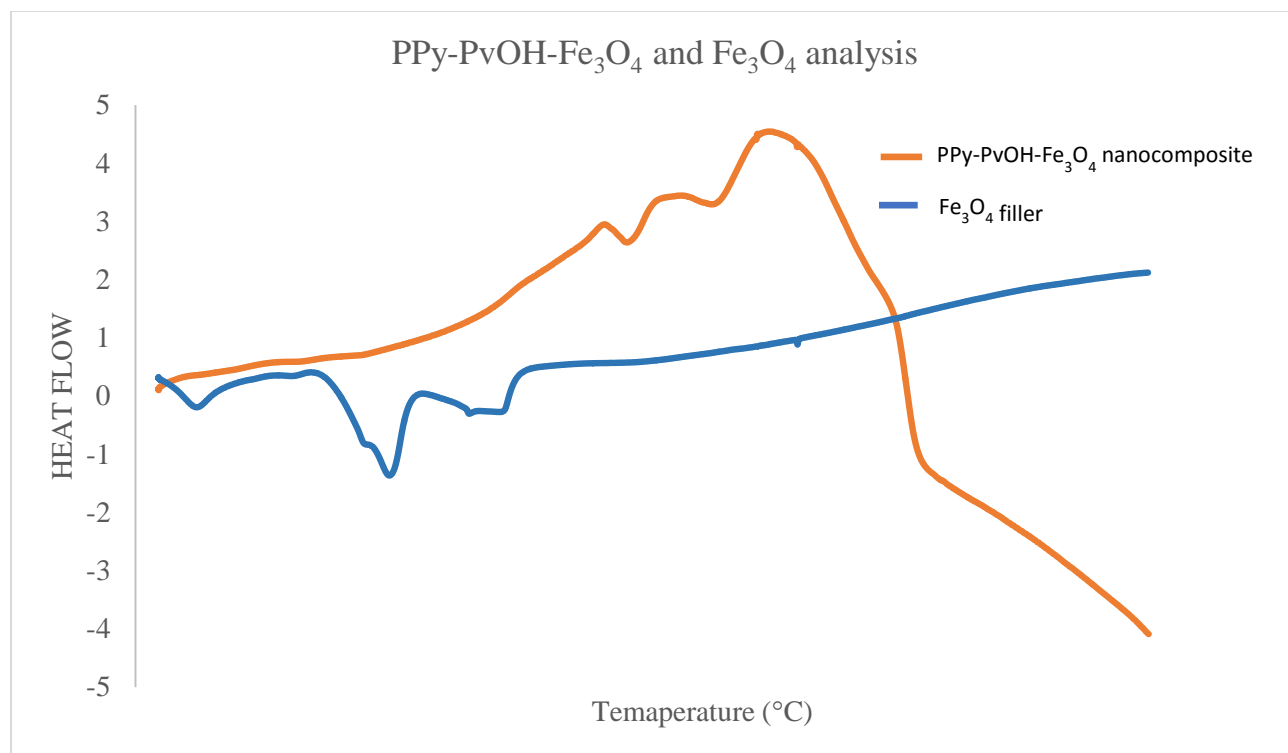


Figure 4.2: DSC analysis of the PPy-PvOH-Fe₃O₄ (56:42:2) nanocomposites and the filler material

4.2.4. Zeta potential

The observed results of surface charge clearly indicate that with the increase in pH, the surface charge of Fe₃O₄-PPy-PvOH nanocomposite decreases. The surface becomes more negative as the pH increases. At pH 2 the zeta potential is measured to be -0.2 mV. At pH 12 zeta potential is recorded to be -4.1 mV. To initiate adsorption, the adsorbent should be highly negative in order to attract positively charged ions from the aqueous solution. Fe₃O₄-PPy-PvOH nanocomposite is expected to yield good efficiency at pH 12 for the removal of Cr(VI) and As(III) since it has a high negative charge at that point.

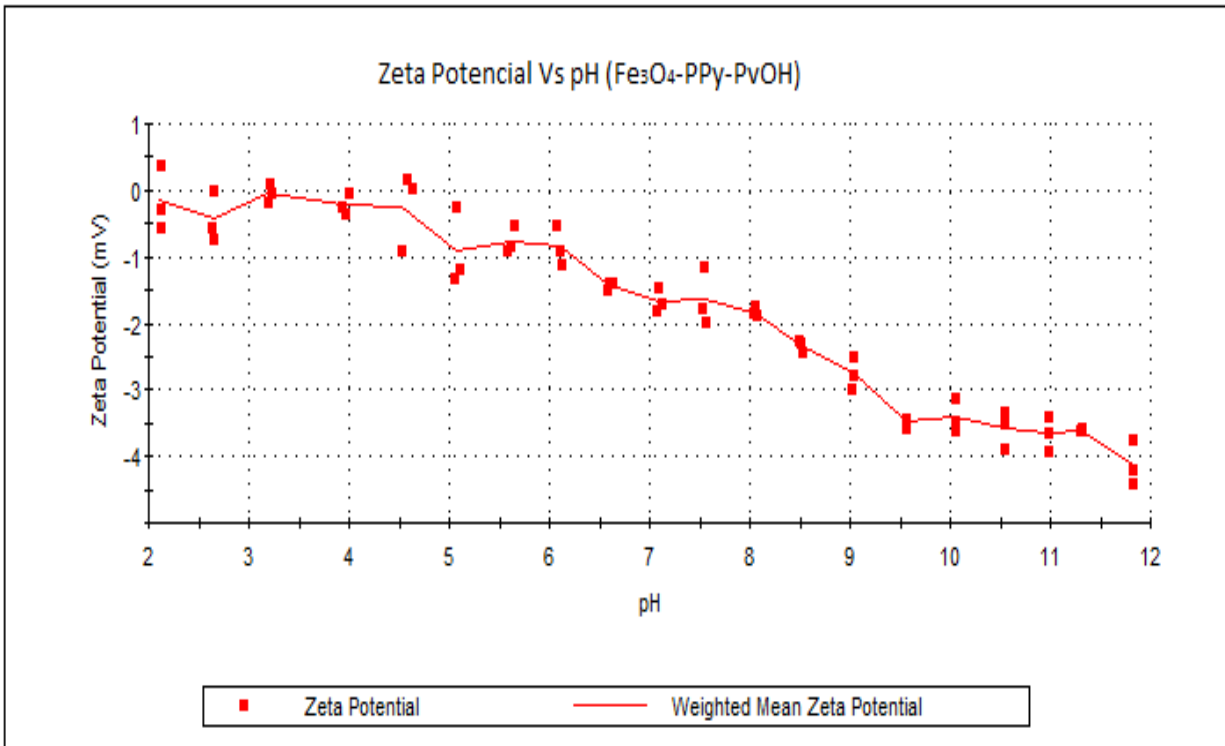


Figure 4.1: The Zeta potential of Fe₃O₄-PPy-PvOH

4.2.5. Scanning electrode microscopy (SEM) analysis

Figure 4.7 shows the surface morphology of the synthesized (a) PPy-PvOH polymer blend and (b) Fe₃O₄-PPy-PvOH nanocomposites. The images shows the flake like particles with holes in between, clearly observed in image (c). The figure4.7 indicates rough surface morphology with porous exhibition and good uniformity and adhesiveness samples. However, after the incorporation of the Fe₃O₄ nanoparticle, small white spots were observed and can be related to the Fe₃O₄ nanoparticles dispersed in the PPy-PvOH matrix. Fe₃O₄-PPy-PvOH nanocomposites showed uniform distribution of the nanoparticle on the surface of the blend [3]. Figure 4.7.1 below shows the EDS obtained for Fe₃O₄-PPy-PvOH nanocomposites which clearly indicated the presence of all components (elements) for the formation of Fe₃O₄-PPy-PvOH nanocomposites.

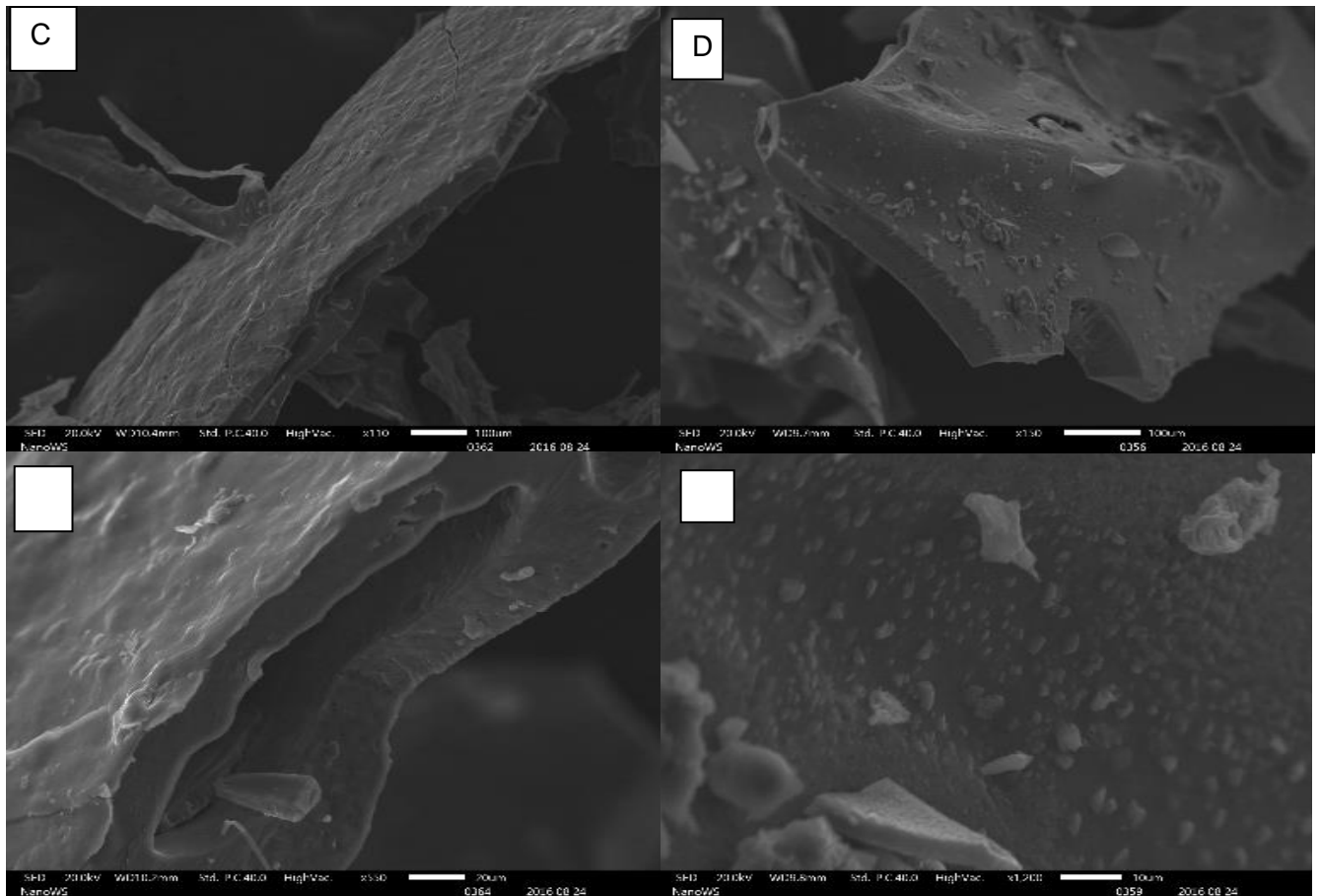


Figure 4.1: SEM imaging of (a) 100 nm of PPy-PvOH, (b) 50 nm PPy-PvOH, (c) 100 nm Fe₃O₄-PPy-PvOH, (d) 50 nm Fe₃O₄-PPy-PvOH, (e)

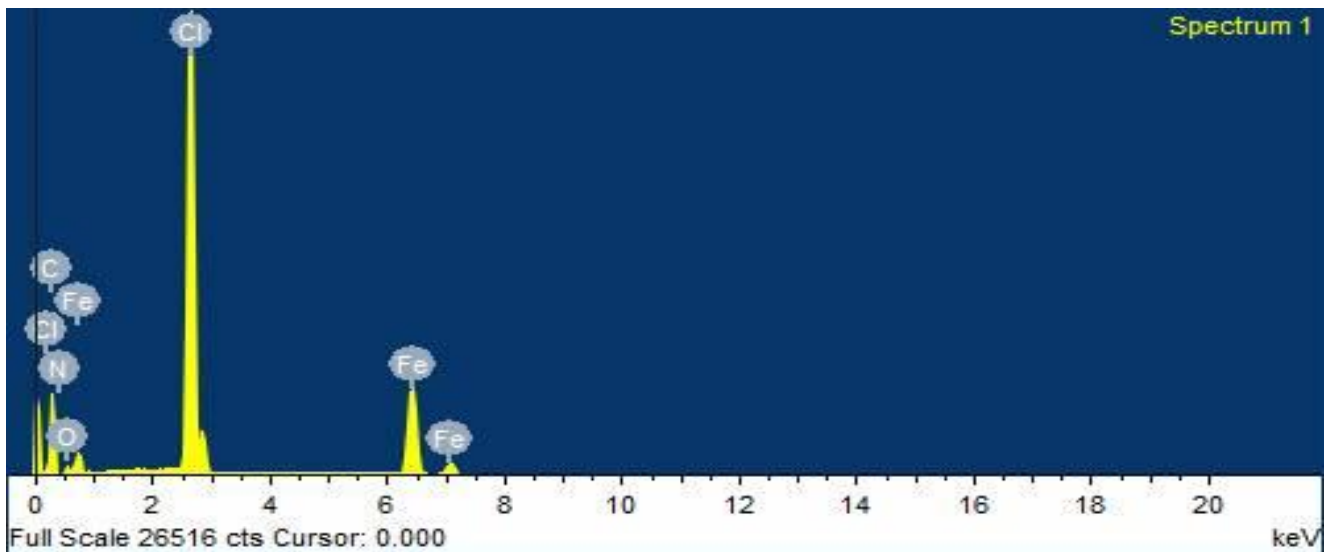


Figure 4.7. 1: An EDS image of Fe₃O₄-PPy-PvOH

4.2.6. Transmission electrode microscopy (TEM) analysis

Figure 4.8 shows the TEM imaging of Fe₃O₄-PPy-PvOH nanocomposite. In the image PPy-PvOH forms two types of structures, one is neatly spherical which appears as light spots and the other has semi-dark spots which can be attributed to PPy and PvOH respectively. PPy polymer seems to have formed an inter-connection network to each other, and the PvOH assists in the formation of the network. The darker spots observed in Fe₃O₄-PPy-PvOH nanoparticle image can be due to the presence of Fe₃O₄ nanoparticle.

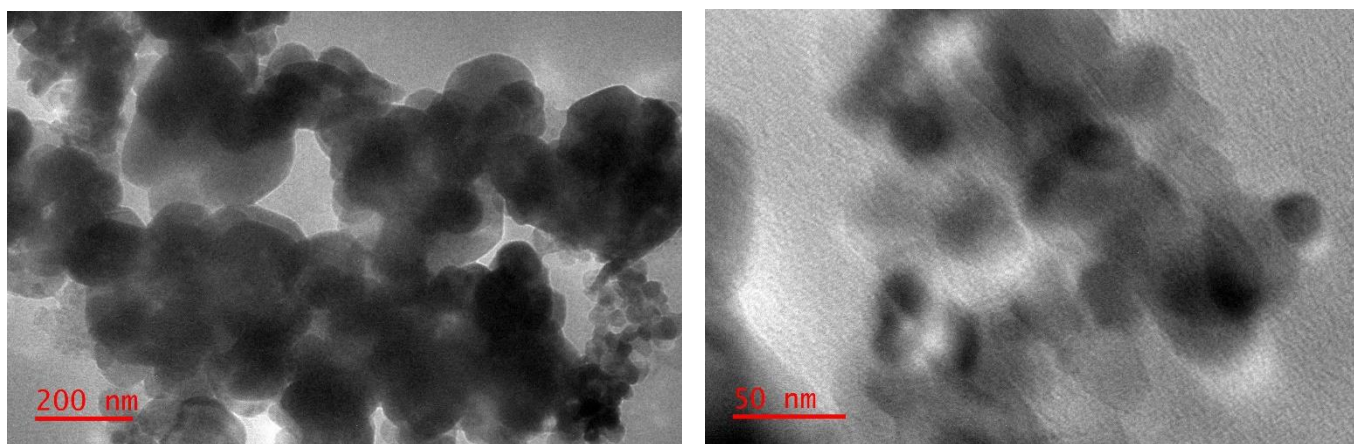


Figure 4.8 1 TEM imaging (a) 200 nm Fe₃O₄-PPy-PvOH, and (b) 50 nm Fe₃O₄-PPy-PvOH

4.2.7. Brunauer–Emmett–Teller (BET) analysis

The surface area and the particle size of Fe₃O₄ nanoparticles and Fe₃O₄-PPy-PvOH nanocomposites were achieved using BET analysis. The particles size was measured to be <10 nm at pH 9 using 1.5 M NH₄OH. The surface area of Fe₃O₄ nanoparticles was achieved at 50 m²/g. Surface area of the polymer blend was found to be 0.2356 m²/g with Adsorption average pore width (4V/A by BET) of 126.7589 (see **Table 4.2**). With the addition of Fe₃O₄ to the blend, there was an increase of the surface area and pore size of the Fe₃O₄-PPy-PvOH nanocomposite. The surface area of the Fe₃O₄-PPy-PvOH nanocomposite was found to be 1.2646 m²/g with Adsorption average pore width (4V/A by BET) 130.7667 Å

Table 4.2: BET analysis showing the values obtained for surface area, pore size, and pore volume of Fe₃O₄ filler, PPy-PvOH polymer blend and Fe₃O₄-PPy-PvOH nanocomposites

Sample	Surface area	Pore size	Pore volume
Fe ₃ O ₄ nanoparticle	50 m ² g ⁻¹	300.537 Å	0.034270 cm ³ /g
PPy-PvOH polymer blend	0.2356 m ² g ⁻¹	490.413 Å	0.000747 cm ³ /g
Fe ₃ O ₄ -PPy-PvOH nanocomposites	1.2646 m ² g ⁻¹	417.470 Å	0.004134 cm ³ /g

4.2.8. X-ray diffraction (XRD) analysis

X-ray diffraction analysis was carried out to approve the crystalline nature of the Fe₃O₄ nanoparticles. The comparison of the XRD spectrum with the standard XRD data for bulk of magnetite was confirmed from literature that the magnetite particles formed in our experiments were in the form of nanocrystals, as proved by the peaks at 2θ values of 23.13°, 32.88°, 35.76°, 47.03°, 54.59°, 58.45° and 63.34° equivalent to (111), (220), (311), (222), (400), (422) and (511) [1] Bragg's reflections. The XRD results clearly show that the Fe₃O₄ nanoparticles formed by co-precipitation method are crystalline in nature. It was found that the average size from XRD data and using Debye-Scherrer equation was approximately 10 nm. The average particle size of magnetite nanoparticles synthesized by co-precipitation was measured using the Debye-Scherrer equation:

$$d = \frac{K\lambda}{\beta \cos \theta}$$

Where d is the mean diameter of nanoparticles, β is the full width at half-maximum value of XRD diffraction lines, λ is the wavelength of X-ray radiation source 0.15405 nm, θ is the half diffraction angle –Bragg angle, and K is the Scherrer constant with value from 0.9 to 1.

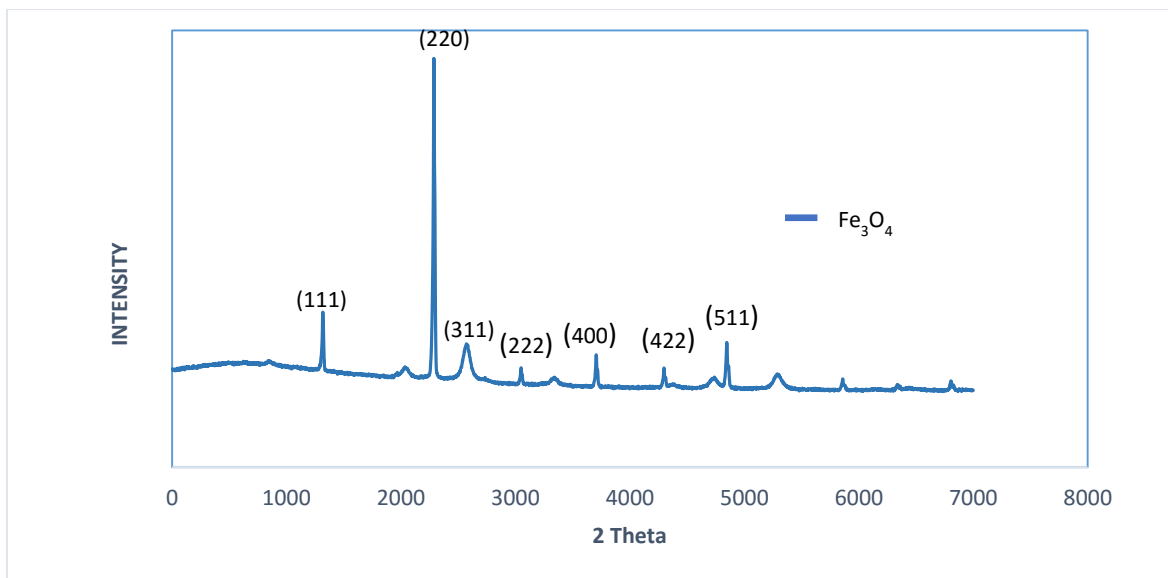


Figure 4.9: The XRD pattern of Fe₃O₄

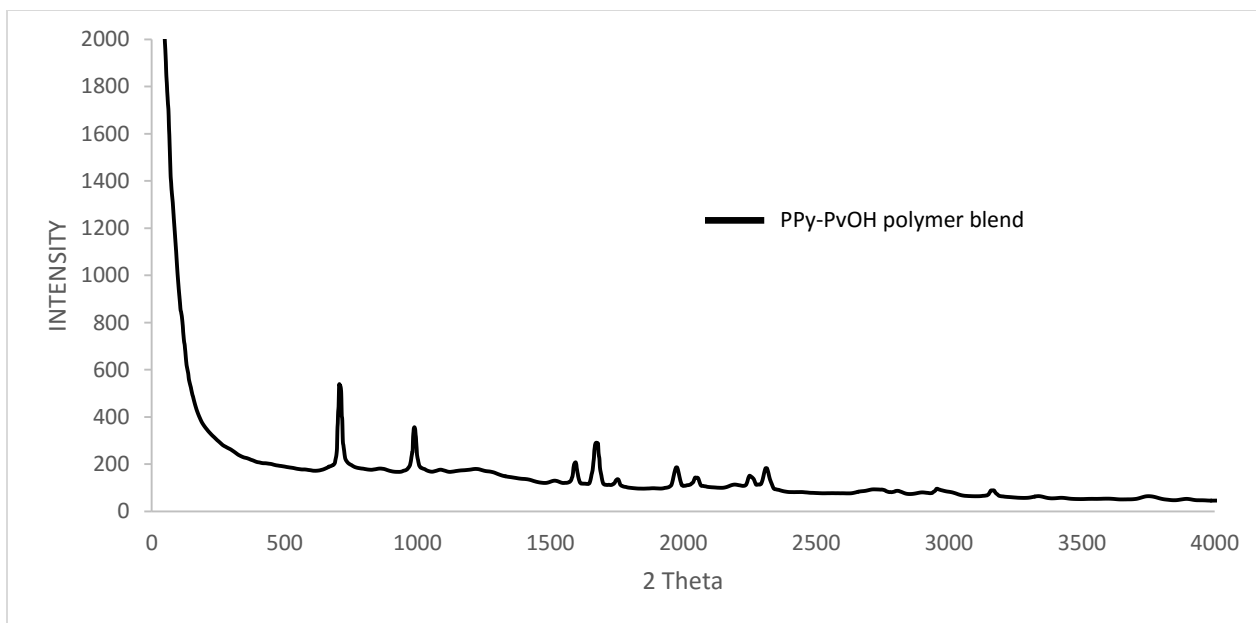


Figure 4.10: The XRD pattern of PPy-PvOH polymer blend

The XRD pattern of Fe₃O₄-PPy-PvOH in figure 3.10 show some additional peak around $2\theta = 16.8^\circ$, 20.9° , 32° , 30.3° and 43.3° as reported in literature suggesting that the crystalline nature of Fe₃O₄ imparts crystallinity to the semi-crystalline PPy-PvOH chains by the strong intermolecular interaction between Fe₃O₄ chains and PPy-PvOH through the intermolecular hydrogen bonding

[4]. The incorporated Fe_3O_4 nanoparticle showed all the peak in the polymer along with the characteristic peak of PPy-PvOH [3].

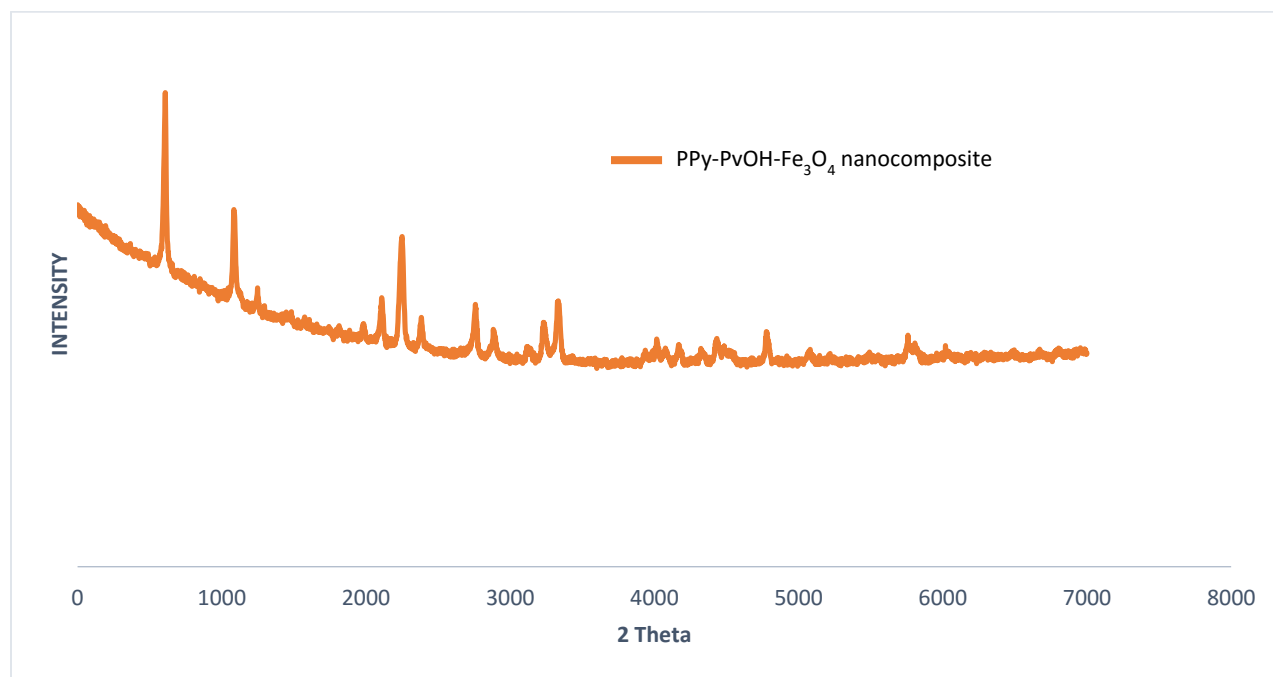


Figure 4.11: The XRD pattern of Fe_3O_4 -PPy-PvOH nanocomposites

4.2.9. Swelling studies of Fe_3O_4 -PPy-PvOH nanocomposites

In Figure 4.11, PPy-PvOH- Fe_3O_4 nanocomposite with ratio 56:42:2 was introduced to distilled water in order to measure the swelling capacity of the material. The sample was measured over time in hours. The analysis indicated a gradual increase at time range of 4 hours to 12 hours, with an increase of about 270% of the swelling capacity. From 12 to 24 hours the nanocomposite swellability increased drastically. The optimum swellability was reached at 24 hours. The improvement in water solubility are due to the solubility of the complex formed during polymerization of PPy and due to the binding of NH_3^+ species which contributes to swelling and the strong hydroxyl groups located on the polymer crystallite surfaces

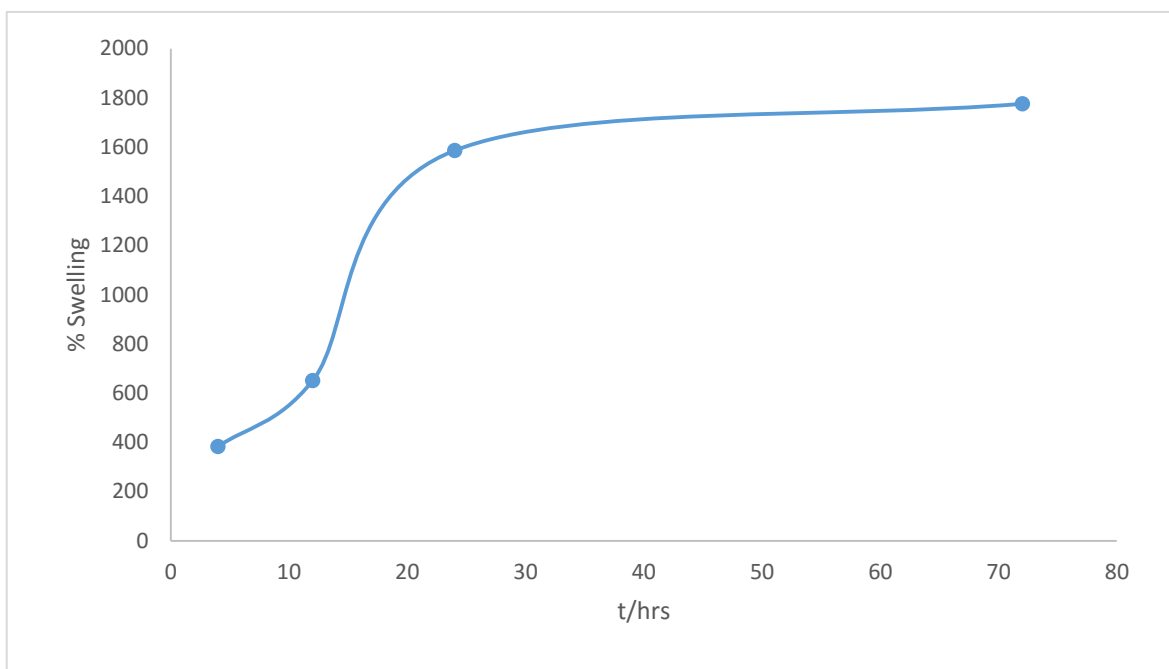


Figure 4.11: Swelling capacity of PPy-PvOH-Fe₃O₄ nanocomposite with ratio 56:42:2 in deionized water

Figure 4.12 shows the swelling of PPy-PvOH-Fe₃O₄ nanocomposite prepared at different alkalinity in water [5]. The figure indicates that there is an overall increase in the swelling percentage in the pH range 2 to 12. This may be due to the addition of hydrophilic polymer (PPy) to PvOH which increases the water absorption due to binding of NH₃⁺ species which contributes to swelling. Swelling is maximum at pH 12 and reach minimum swellability at pH 2. At low pH, the high swellability can be due to amine groups (NH₃⁺) of PPy being protonated; which favours the chain [6]. At high pH, high swelling capacity may be due to the hydration water bonding, which involves two kinds (strong and weak); the strong one contains OH⁻ groups sited on the polymer crystallite surfaces, and the weak one contains other available OH⁻ groups. Water that has not bonded with polymer OH⁻ groups forms a condensation water species; it is located in the polymer with an enhanced equilibrium swellability.

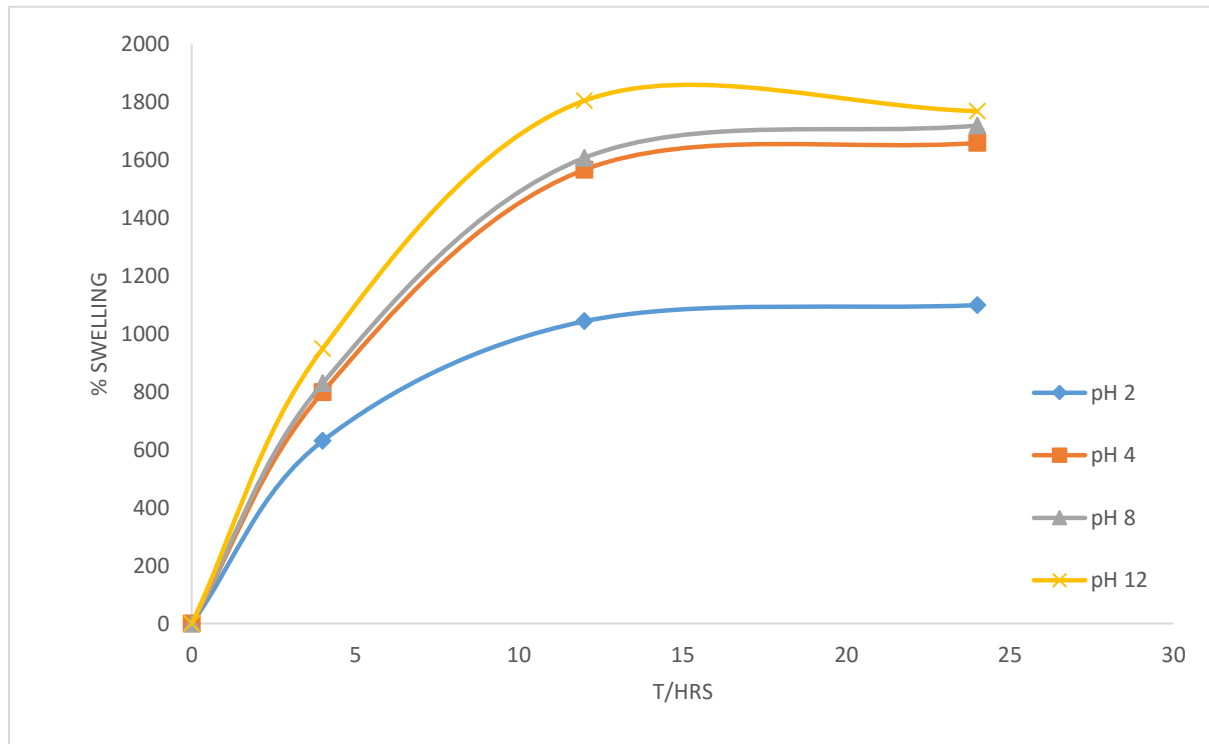


Figure 4.12: Swelling capacity of PPy-PvOH-Fe₃O₄ nanocomposite with ratio 56:42:2 with variation of pH

4.3. Adsorption studies

4.3.1. Effect of pH

Figure 4.13 illustrates the variation of pH in Cr(VI) metal ions removal at 30ppm, contact time of 45 min. pH variation is one of the most important parameters controlling removal of metallic ions from aqueous solutions

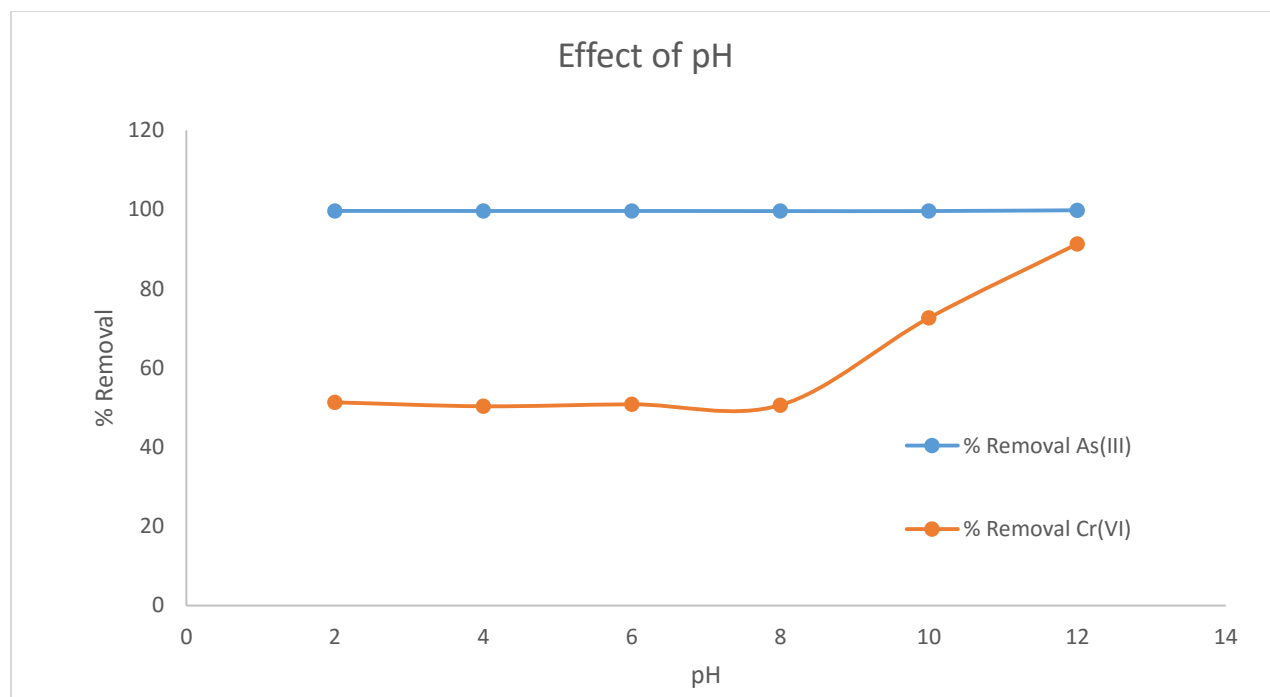


Figure 4.13: pH dependent performance characteristics of PPy-PvOH-Fe₃O₄ (56:42:2) nanocomposite, on Cr(VI) and As(III) adsorption, using 0.12g ; 0.10g; and 30 ppm and 150 ppm respectively

Fig. 4.13 shows the effect of pH on As(III) and Cr(VI) metals removal efficiencies using PPy-PvOH-Fe₃O₄ nanocomposites adsorbent. The percentage of adsorption increases with pH to attain a maximum at pH 12 for both metal ions. However, as pH decreases there is a drastic drop in the adsorption efficiency. The maximum removals of Cr(VI) ions at pH 12 were found to be 91.3% and the maximum removal of As(III) was also obtained at pH 12 with 99.8 %. This may be due to the swellability and the porosity of PPy-PvOH-Fe₃O₄ nanocomposites at pH 12.

4.3.2. Effect of pH of Cr(VI) concentration using different polymer blend ratio

The effect of concentration was estimated using various ratio. The ratio was a combination of PvOH polymer on PPy loading in the prepared polymer blend [7]. The sample was weighed and the percentage was accurately calculated based on final mass weighed, indicated in figure 4.14. The figure 4.14 above shows the percentage removal of Cr(VI). The polymer blend was labelled based on the ratio of PPy to PvOH (wt %) as 74:26, 64:36, 56:44, and 52:48. These results were

similar with a study of Muliwa et al (2016) [7], where by Py was used at 0.6 ml while the nanoparticle content was varied at different masses. The effect of concentration was measured at 0.12g adsorbent dose, pH 2 and 45 min contact time. The effect of initial concentration on the percentage elimination of Cr(VI) by PPy/PvOH polymer blend is illustrated in Figure 4.14. It can be observed from the figure that the percentage elimination efficiency increases with the increase of initial metal ions concentration, the percentage of removal is highly effective on 50 ppm initial concentration after which percentage removal decreases slowly to below 60%. At lower initial concentrations Cr(VI) metals have lower percentage removal. At higher initial concentrations of metal ions, sufficient sites for adsorption are available for the uptake of the heavy metals ions. Hence, the fractional adsorption is independent of initial metal ion concentration. The maximum removal of Chromium is 96% at 50 ppm concentration using ratio 56:44

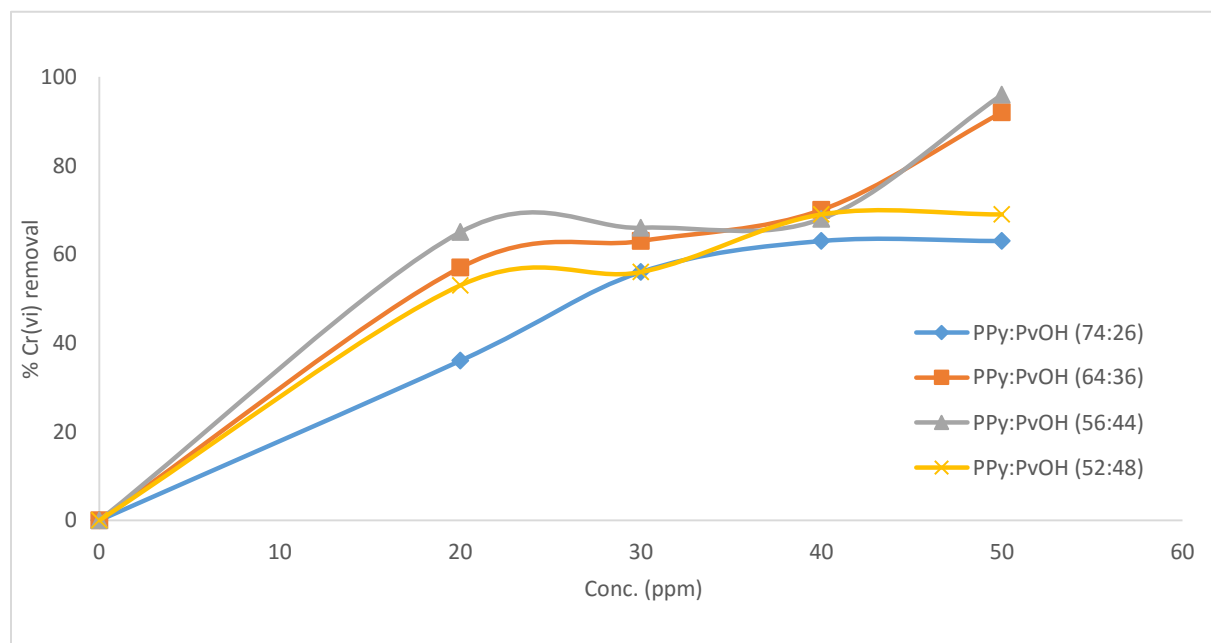


Figure 4.14: concentration dependent performance characteristics of 74:26, 64:36, 56:44, and 52:48 polymer blend on Cr(VI) adsorption, temp 25 C at pH 2

4.3.3. Effect of initial concentrations of Cr(VI) and As(III)

The effect of concentration at 0.12g and 0.10g adsorbent doses for Cr(VI) and As(III) respectively was observed at pH 12 and 45 min contact time is shown in Fig 4.15. The effect of initial concentration on the percentage removal of Cr(VI) and As(III) by PPy-PvOH-Fe₃O₄ nanocomposites is shown in **Figure 4.15**. It can be seen from the figure that the percentage removal of every dose increases with the increase in initial Cr(VI) ion concentration, the percentage removal is highly effective on the 30 ppm initial concentration after which percentage removal decreases as the concentration gradually decrease to an efficiency below 75% at dose 0.12g, this is due to sufficient adsorption sites available for adsorption of the Cr(VI) metal ions at high concentration and the adsorbent being negatively charged. At higher initial concentrations Cr(VI) metals drastically increase in percentage removal and at low initial metal ion concentrations. The maximum removal of Cr(VI) ion is 90.3% at 30 ppm concentration. However, As(III) shows a major drop in percentage removal at 100 ppm and reaches optimal at 150 ppm with 100% removal efficiency when the concentration is increased.

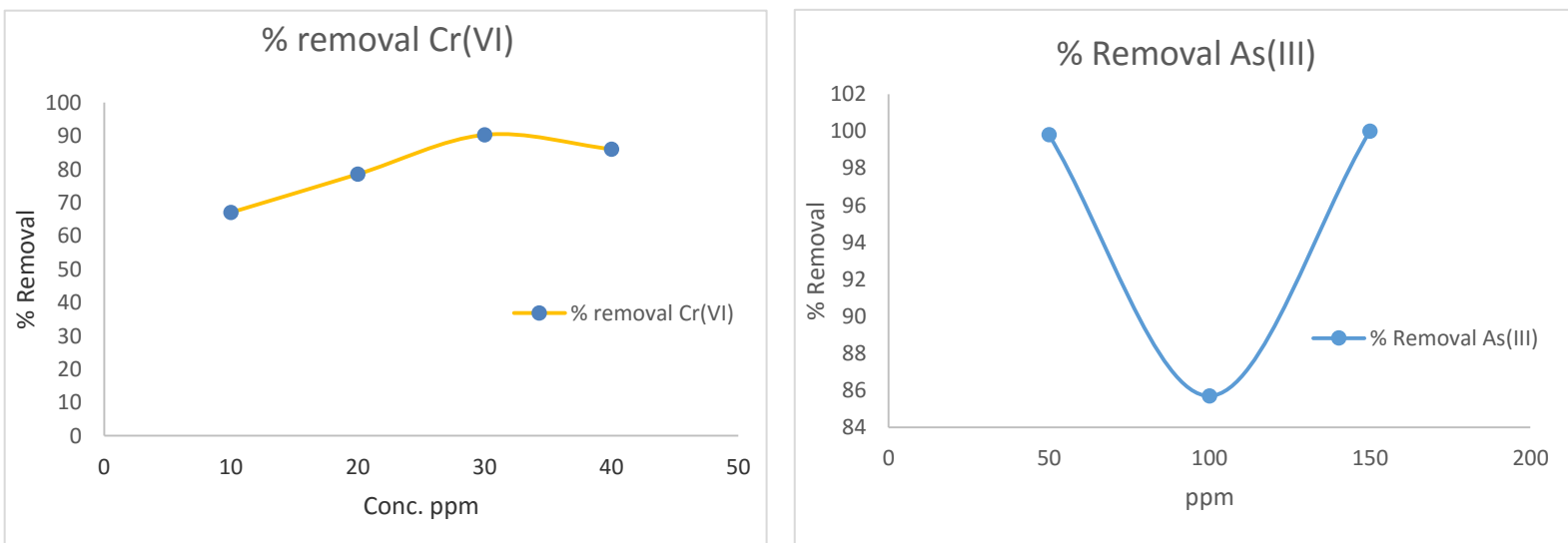


Figure 4.15: Concentration dependent performance characteristics of PPy-PvOH-Fe₃O₄ 56:42:2 nanocomposite, on Cr(VI) and As(III) adsorption, temp 25 C at pH 12

4.3.4. Effect of dose

The results for adsorptive removal of heavy metals with respect to adsorbent dose are shown in Fig.4.16 over the range 0.02 to 0.12g, at pH 12 and 45 minutes contact time for Cr(VI) and for As(III) ion the range of dose and pH were kept the same but other parameters were different from Cr(VI) ions. The concentration was 150 ppm with contact time of 30 min. The percentage removal of Cr(VI) metal ions is observed to increase with the increase of adsorbent dose. There is a gradual increase in percentage removal from 0.04 to 0.12g with adsorbent dose for Cr(VI) metal ions. The optimum removal of Cr(VI) is 90.3% at 0.12 g dose amount of PPy-PvOH-Fe₃O₄ nanocomposites adsorbent. The percentage removal of As(III) reached optimal at 0.10g with percentage removal of 97.5%. It is apparent that the percent removal of heavy metals increases rapidly with increase in the dose of the adsorbents due to the greater availability of the exchangeable sites and swellability characteristics. In figure 4.17 the graph illustrates the amount of Cr(VI) adsorbed in mg/g . The amount of Cr(VI) adsorbed increases gradually with time and reach optimum at 45 min with 1.2 mg/g.

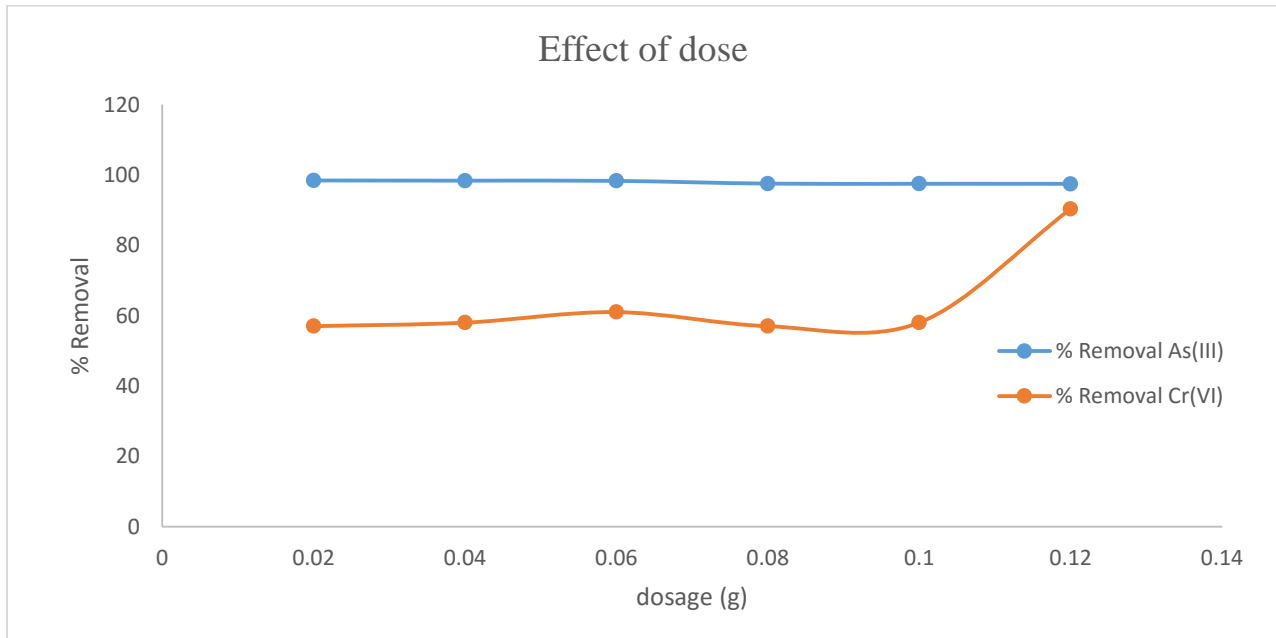


Figure 4.16: Dose dependent performance characteristics of PPy-PvOH-Fe₃O₄ 56:42:2 nanocomposite, on Cr(VI) and As(III) adsorption, temp 25 C at 30 ppm and 150 ppm respectively, and pH 12

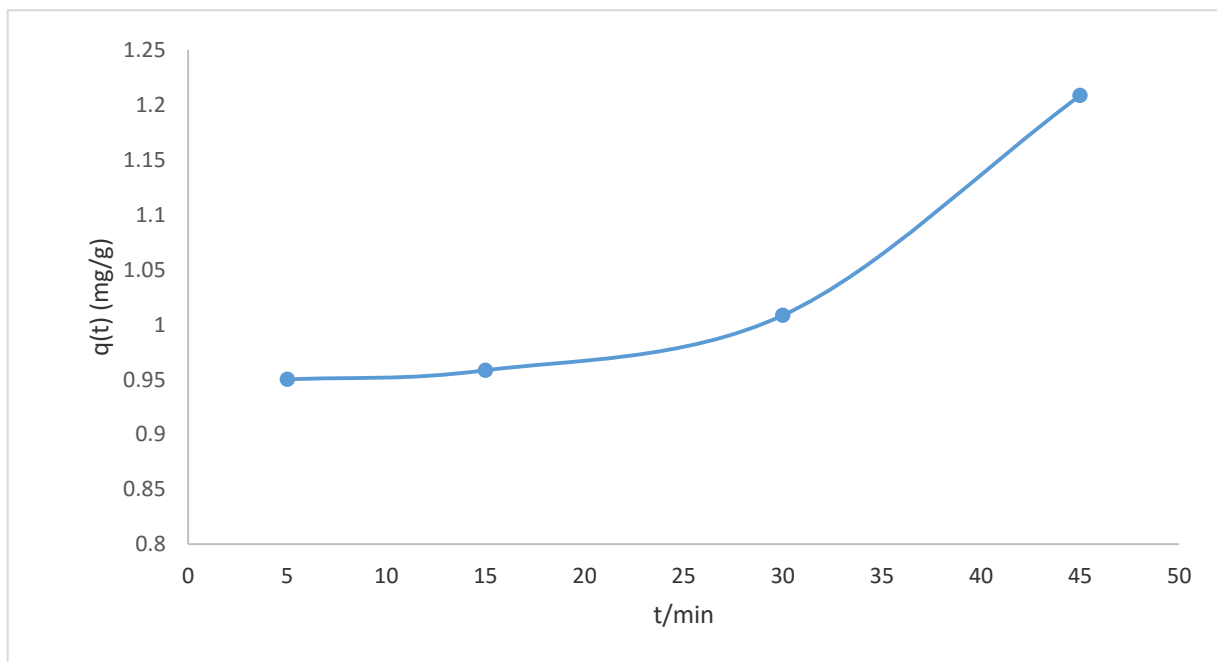


Figure 4.17: Variation of Cr(VI) amount adsorbed with time using 56:42:2 PPy-PvOH-Fe₃O₄ nanocomposite.

4.3.5. Effect of contact time

Fig.4.18 shows the variation in the percentage removal of Cr(VI) and As(III) over a period of time range (5, 15, 30, 45, 60 min) using 0.12 g for Cr(VI) and 0.10g for As(III) of Fe₃O₄-PPy-PvOH nanocomposites adsorbent at pH 12 and 30 ppm Cr(VI) initial concentration and 150 ppm of As(III). From figure 4.18 it can be observed that maximum removal of Cr(VI) ions were nearly 91,3% in 60 min at pH 12. The graph shows that as the time is increased the percentage removal increases. For As(III) there is no much change in the in the removal efficiency. At 5 min the percentage removal is about 95.6% and at optimal time the percentage only increased with 1% to reach 96.8%.

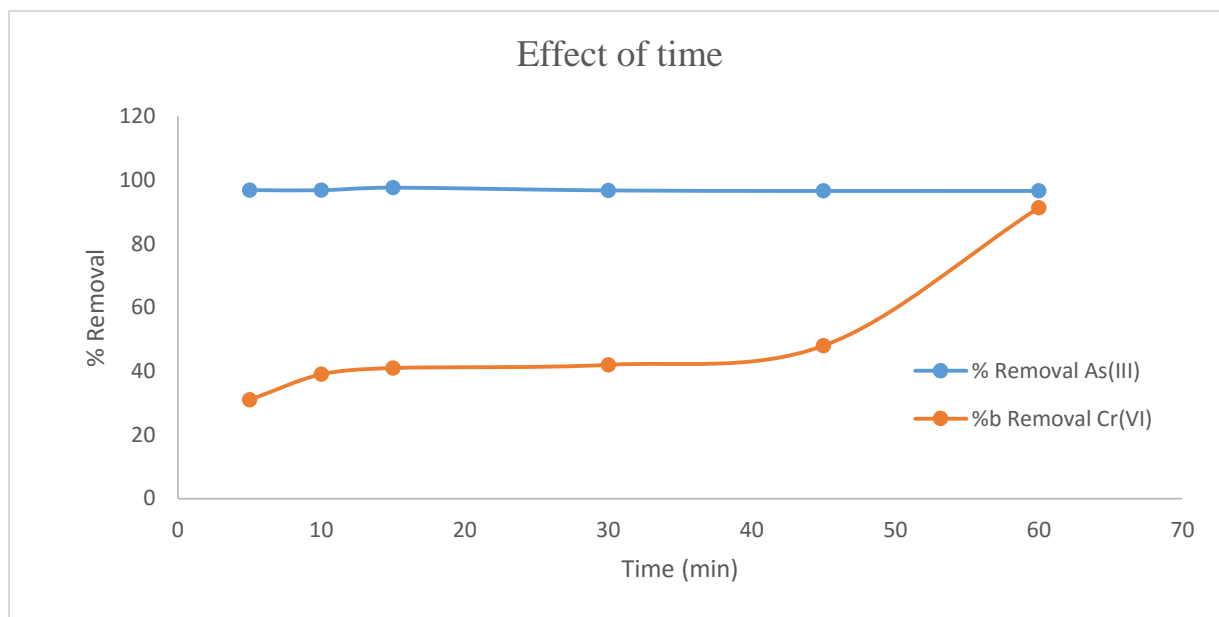


Figure 4.18: Time dependent performance characteristics of 56:42:2 nanocomposite, on Cr(VI) and As(III) adsorption at temp 25 °C, pH 12, 0.12g and 0.10g , 30ppm and 150ppm respectively.

4.4. Adsorption isotherm models

Some of the adsorptions transformation processes of various solid phases are time dependent. To understand the dynamic interactions of Cr(VI) with Fe₃O₄-PPy-PvOH nanocomposite and to calculate their outcome with time, understanding the kinetics of these processes is essential. Various kinetic models, for example, Lagergren rate expression and pseudo second order models have been utilized with the experimental adsorption data for the Cr and As(III) onto Fe₃O₄-PPy-PvOH nanocomposite. Hence, kinetic can be studied from the remaining metal ions concentration in the aqueous solution. The study of adsorption kinetics defines the solution removal rate. To examine the change in the concentration of Cr(VI) and As(III) onto Fe₃O₄-PPy-PvOH nanocomposite with shaking time, the kinetic data of Cr(VI) and As(III) ions sorption onto Fe₃O₄-PPy-PvOH nanocomposite were subjected to Lagergren rate expression and pseudo second order models

4.4.1. Langmuir isotherm model

The Langmuir model is based on the assumption that maximum adsorption occurs when a saturated monolayer of solute molecules is present on the adsorbent surface, that the energy of adsorption is constant and that there is no migration of adsorbate molecules in the surface plane. The nonlinear form of Langmuir isotherm is given by Gupta and Babu as:

$$\frac{1}{qe} = \frac{1}{Q^{\circ}K} + \frac{1}{KQ^{\circ}Ce} \quad (4.0)$$

Where Ce is the equilibrium concentration of metal in solution (mg/L), qe is the amount absorbed at equilibrium, and K is the Langmuir constants, representing the maximum adsorption capacity for the solid phase loading and the energy constant related to the heat of adsorption, respectively. The constants in the Langmuir isotherm can be determined by plotting $1/qe$ versus $1/Ce$ which gives a linear plot whereby Langmuir parameters can be extracted.

The equilibrium behaviour of adsorption processes has been widely described by the Langmuir model. The Langmuir isotherm is useable only for monolayer sorption because it has a surface with a finite number of identical sites [8]. A linear form of the Langmuir isotherm [9] is given by equation 4.1 below

$$\frac{Ce}{qe} = \frac{Ce}{k} + \frac{1}{kQ_0} \quad (4.1)$$

Where the constant Q_0 can be assigned for the adsorption capacity (mg/g), and k is the energy of adsorption (L/mg) [9]. Whenever the plot fits a Langmuir isotherm, a plot of Ce/qe versus Ce is linear Fig. 4.18 (a). The R^2 values show that the adsorption data for PPy/PvOH follows the Langmuir model. The correlation coefficients are given in Fig. 4.18 (b) where N-H and O-H functional groups have been applied for the uptake of Cr(VI) from aqueous solutions; and, the results thoroughly followed the Langmuir adsorption model [10]. The important feature of the Langmuir sorption model is the R_L . R_L a dimensionless constant stated to as an equilibrium parameter for calculating whether a sorption system is satisfactory or disapproving [11]. The constant R_L is calculated from the initial concentration by equation 4.2 below [12]. Since R_L ranges

between 0 and 1, the adsorption is classified as favourable [12]. Favourable adsorption means that adsorption takes place at specific homogeneous sites within the adsorbent [12].

$$RL = \frac{1}{1+KCo} \quad (4.2)$$

Where K is related to the energy of adsorption (L/mg) and Co is the initial concentration.

4.4.2. Freundlich isotherm model

The Freundlich isotherm model is obtained from a correlation relating the adsorption of solutes from a liquid to a solid surface and assumes that the adsorbent surface is heterogeneous, (e.g. different sites with numerous adsorption energies are involved). The nonlinear form of Freundlich isotherm is given by Choy, McKay and Porter as:

$$qe = KfCe^{1/n} \quad (4.3)$$

Logarithmically equation (2.2) above can be transformed to:

$$\log qe = \log Kf + \frac{1}{n} \log Ce \quad (4.4)$$

Where K_f and n are the Freundlich constants. A plot of $\log Ce$ vs. $\log qe$ yields a linear curve with the intercept value of K_f and the slope of n . K_f Value shows the adsorption capacity of the adsorbent; the slope $1/n$ specifies adsorption intensity. Freundlich isotherm model is commonly used but does not provide much information on the monolayer adsorption capacity in contrast to the Langmuir model.

The linearized logarithmic form of the Freundlich model is given by equation 3.4 [13];

$$\text{Log} qe = \log Kf + \frac{1}{n} \log Ce \quad (4.4)$$

Where K_F is the Freundlich constant and n is a dimensionless constant indicating the extent of nonlinearity between analyte concentration and adsorption. A plot of $\log q_e$ vs. $\log C_e$ is shown in Fig. 4.19 (b) PPy/PvOH polymer blend and 4.20 (b) PPy-PvOH-Fe₃O₄ nanocomposites. The linear plots with good correlation coefficients (>0.900) indicate that the adsorption conformed to the Freundlich isotherm model.

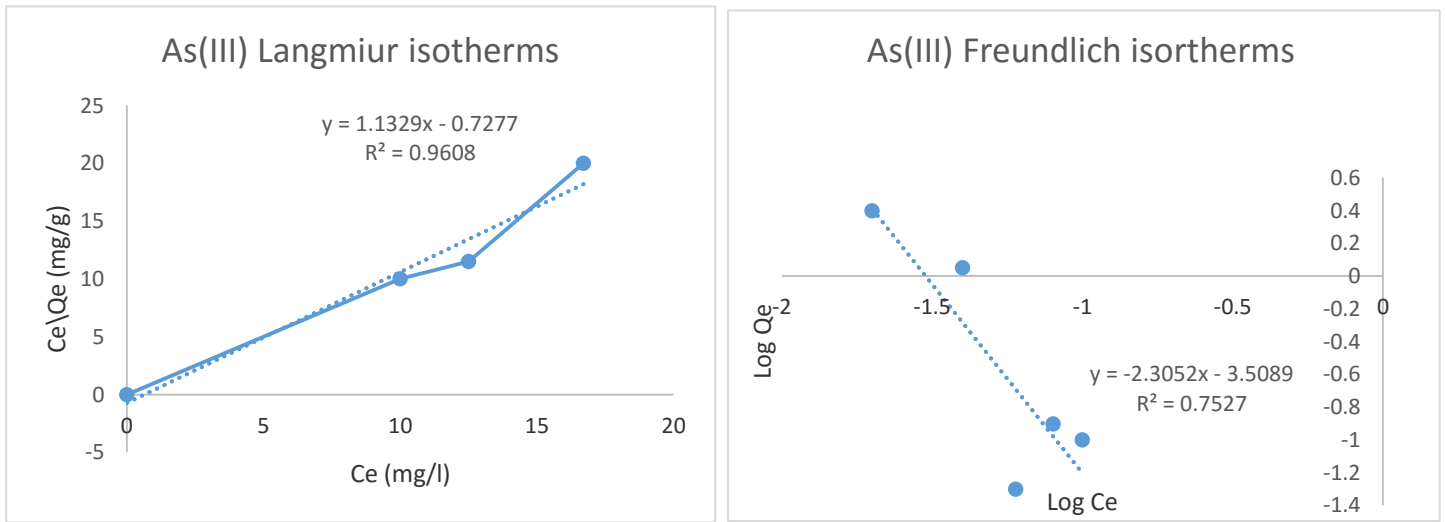


Figure 4.19: Linearized fits for (a) Langmuir and (b) Freundlich isotherm 150 ppm of As (III), 0.10 g of 56:42:2 PPy-PvOH-Fe₃O₄ polymer nanocomposites

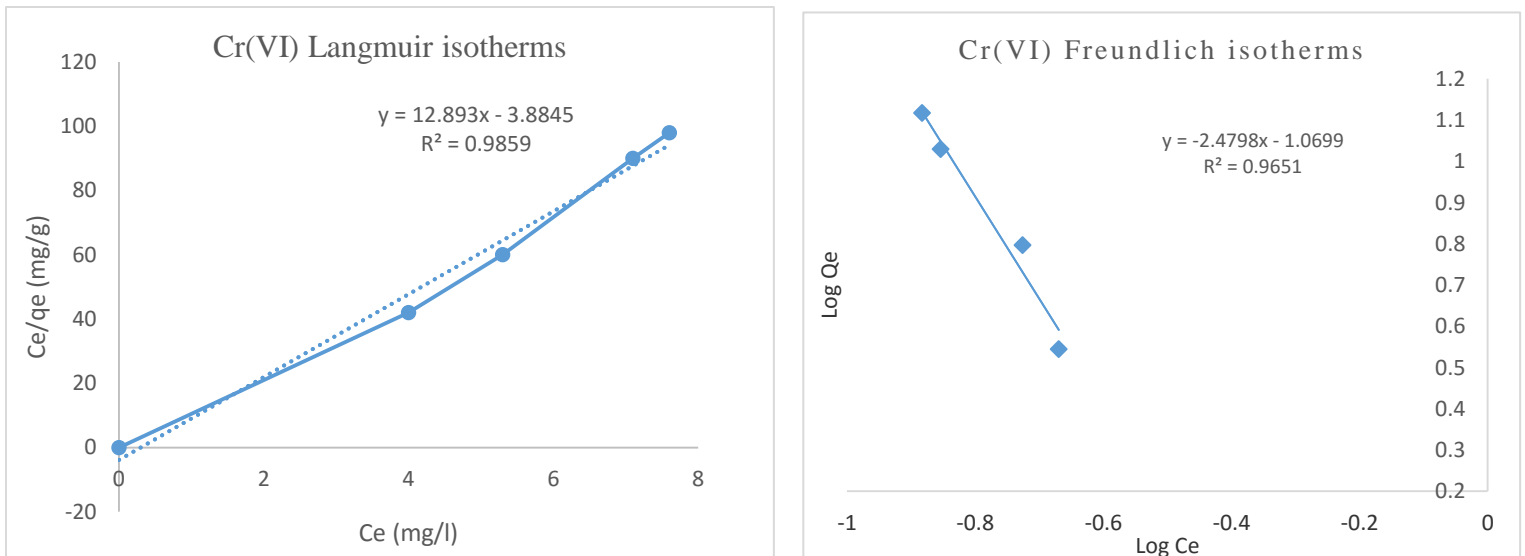


Figure 4.20: Linearized fits for Langmuir and Freundlich isotherm 30 ppm of Cr (VI), 0.12 g of 56:42:2 PPy-PvOH-Fe₃O₄ nanocomposite, 25C

Table 4.1: Isotherms constants and correlation coefficients for adsorption of Cr(VI) and As(III) from aqueous solution

Sample	Langmuir model				Freundlich model		
	Q _o	K	R _L	R ²	K _f	N	R ²
PPy(56%) PvOH (44%) Polymer composite for Cr(VI)	1.4	0.08	0.294	0.9981	1.13	0.16	0.9979
PPy (56%) PvOH (42%) Fe ₃ O ₄ (2%) Nanocomposites for Cr(VI)	3.31	0.257	0.115	0.9859	0.082	0.403	0.9651
PPy (56%) PvOH (42%) Fe ₃ O ₄ (2%) Nanocomposites for As(III)	1.55	0.374	0.005	1	2.915	0.403	0.7525

4.5. Adsorption kinetics model

The adsorption kinetics of the pollutant uptake by the adsorbent in aqueous medium depends on the contact time between the pollutant and the adsorbent. The adsorption process constitutes the movement of the pollutant from aqueous solution to the external surface of adsorbent and then from the adsorbent surface into the inner sites that are responsible for pore diffusion. The pseudo first-order, pseudo second-order and intra-particle diffusion models were employed to understand the adsorption mechanism.

The pseudo first-order kinetic rate [14] equation is expressed as follows:

$$\log(q_e - q_t) = \log q_e - \frac{K_1}{2.303} t \quad (4.5)$$

where q_e is adsorption capacity of pollutant onto adsorbent at equilibrium, q_t is adsorption capacity of the pollutant onto the adsorbent at time t , K_1 (min^{-1}) is the pseudo-first-order kinetic rate constant.

The pseudo second-order kinetic model is given by the following equation:

$$\frac{t}{q_t} = \frac{1}{K_2 q_e^2} + \frac{t}{q_e} \quad (4.6)$$

where K_2 is pseudo second-order kinetic adsorption rate constant.

The pseudo first-order parameters K_1 , q_e and correlation coefficient (R_2) were calculated from Figure 4.5 and are described in Table 4.2. The inapplicability of this model was confirmed by the disagreement between the estimated q_e values and experimental values. The pseudo second-order parameters K_2 , q_e and R_2 were examined from the linear plot of t/q_t vs t (Figure 4.21b) and they are listed in Table 4.2. The good agreement of the pseudo second-order kinetic model is supported by the high R_2 values and the similarity between the calculated and experimental adsorption capacities. It can be seen that pseudo second-order rate constant decreases with an increase in the initial pollutant concentration, which may be due to the competition amongst the pollutant molecules for the nanocomposite surface active sites at a high initial pollutant concentration.

The transfer of pollutant from the outside surface to the pores of the adsorbent can be explained by using the intra-particle diffusion model. The linear form of intra-particle diffusion kinetic model is given as:

$$q_t = K_3 t^{1/2} + C \quad (4.7)$$

where K_3 is rate constant of intraparticle diffusion kinetic model, C is equal to the thickness of the boundary layer.

First order is a reaction rate that depends on a single reactant and the value of the exponent is one, it is expressed as

$$r = K[A]$$

For a reaction to be second order the overall order should be two. One concentration squared may be proportional to the rate of a second-order reaction $r = k[A]^2$, or generally to the product of two concentrations $r=k[A][B]$

The linear form of Lagergren et al, equation was used for pseudo-first-order as:

$$\log(q_e - q_t) = \log q_e - \frac{K_{ad}}{2.303} t \quad (4.8)$$

Where q_e and q_t refer to the amounts of Cr(VI) and As(III) (ppm) adsorbed on the nanocomposites at equilibrium time and time t (min), K_{ad} representing the pseudo-first-order constant (min^{-1}). The rate constant, K_{ad} and correlation coefficients for different concentrations of the Cr(VI) and As(III) ions were calculated from the linear plots of $\log (q_e - q_t)$ versus t . A best fit line was plotted and the correlation coefficient (R^2) was obtained as shown in Fig.4.20 and Fig 4.21. The correlation coefficient did not fit, which indicated that the adsorption of Cr(VI) ions onto polymer nanocomposites could not obey pseudo-first order kinetics on both occasion of As(III) and Cr(VI) adsorbate. The pseudo-second-order equation is expressed as [14]:

$$\frac{1}{q_t} = \frac{1}{h} + \frac{1}{q_e} t \quad (4.9)$$

Where $h = kq_e^2$ (mg/g min) and k (g/mg min) is the pseudo second- order rate constant of adsorption.

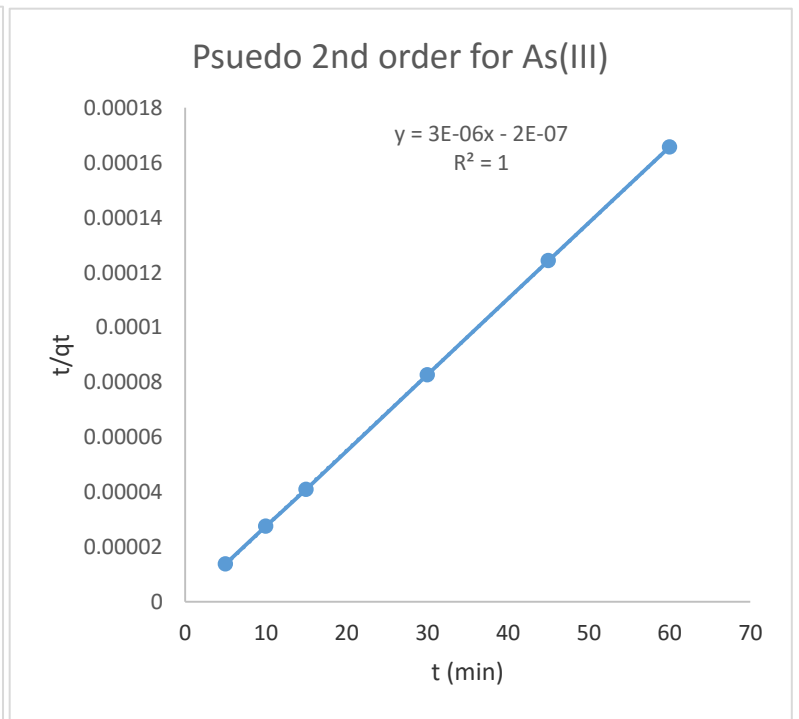
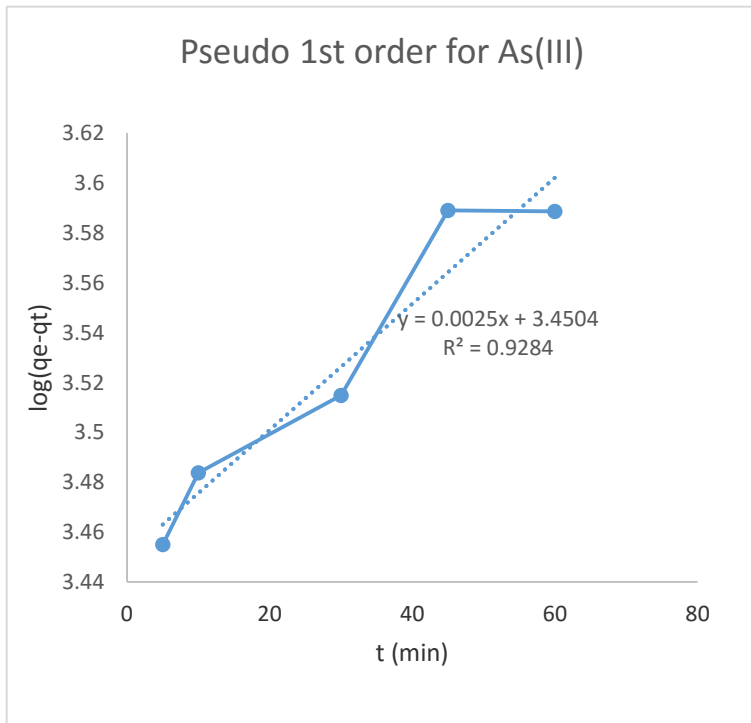


Figure 4.21: First and Second order kinetic model of As(III) removal from aqueous solutions

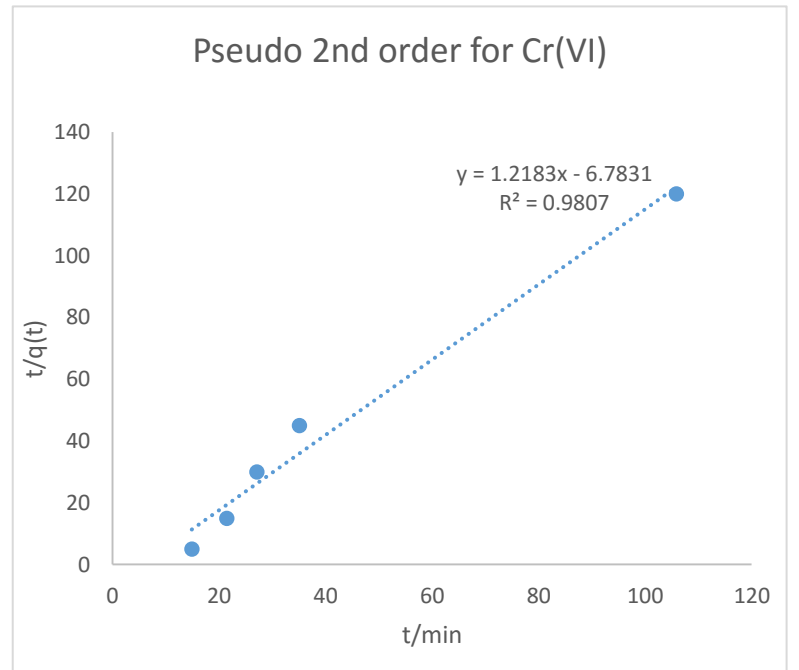
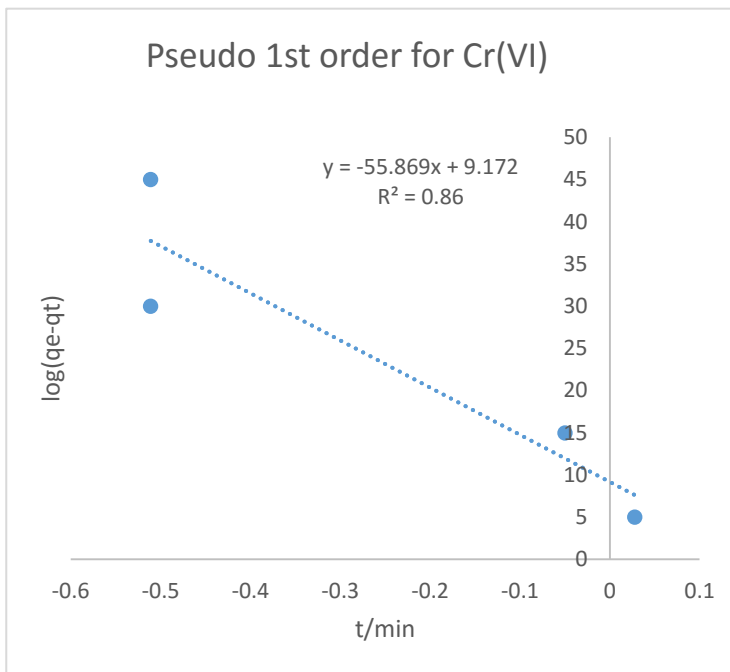


Figure 4.22: First and Second order kinetic model of Cr(VI) removal from aqueous solutions

If the 2nd order kinetics is applicable, the plot of $t/q(t)$ versus t should show a linear relationship. Figure 4.22 (b) shows the plot for pseudo-2nd-order model. The linear fit with correlation coefficient, $R^2 = 0.986$ for Cr(VI) and $R^2 = 1$ for As(III) which illustrates that the adsorption follows the pseudo-second-order model indicated in figure 4.21 (b). The correlation coefficients for the second-order kinetic model are greater than 0.9 indicating the applicability of this kinetic equation and the second-order nature of the adsorption process of Cr(VI) ions and As(III) on PPy-PvOH-Fe₃O₄ (56:42:2) polymer nanocomposites.

The rate constant for Cr(VI) adsorption was measured from the gradient of the straight line (Fig.4.22 b). The rate constant $k = 0.257 \text{ min}^{-1}$ was measured from the gradient of the straight line with a correlation factor of 0.9807. The mechanism suggests the assumption behind the pseudo-second-order model that the Cr(VI) removal process was because of chemisorption. The theory behind the pseudo-second-order kinetic model was that the rate-limiting step is a chemisorption involving valence forces through exchange of electrons between nanocomposite and Cr(VI). Similarly, The rate constant for As(III) adsorption was measured from the gradient of the straight line (Fig.4.21 b). The rate constant $k = 0.374 \text{ min}^{-1}$ was measured from the gradient of the straight line with a correlation factor equals to 1. The mechanism also suggested that the pseudo-second-order model was carried out for As(III) removal process due to chemisorption. The theory behind the pseudo-second-order kinetic model was that the rate-limiting step is a chemisorption involving valence forces through exchange of electrons between nanocomposite and As(III).

4.6. References

- [1] E. Vunain, A. Mishra and R. Krause, "Fabrication, characterization and of polymer nanocomposite for Arsenic (III) removal from water," *Journal of inorganic and organometallic polymer and materials*, vol. 23, no. 2, pp. 293-305, 2013.
- [2] T. Ramesan, "In-situ synthesis, characterization and conductivity of copper sulphide/polypyrrole/polyvinyl alcohol blend nanocomposite," *polymer-plastics technology and engineering*, vol. 51, no. 12, pp. 1223-1229, 2012.
- [3] L. Gai, X. Han, Y. Hou, J. Chen, H. Jianga and X. Chena, "Surfactant-free synthesis of Fe₃O₄@PANI and Fe₃O₄@PPy microspheres as adsorbents for isolation of PCR-ready DNA," *Royal Society of Chemistry*, vol. 42, p. 1820–1826, 2013.
- [4] H. Wang and J. Fernandez, "Blends of polypyrrole and polyvinyl alcohol," *Macromolecules*, vol. 26, pp. 3336-3339, 1993.
- [5] E. Karada, D. SaraydÖn and O. Güven, *Macromolecule Material Engeneering*, vol. 286, no. 42, 2011.
- [6] E. Karada and D. SaraydÖn, "Swelling studies of super water retainer acrylamide/crotonic acid hydrogels crosslinked by trimethylolpropane triacrylate and 1,4-butanediol dimethacrylate," *Polymer Bulletin*, vol. 48, pp. 299-307, 2002.
- [7] M. Muliwa, O. M.S. and A. Maity, "Magnetic adsorption separation process for industrial wastewater treatment using polypyrrole- magnetite nanocomposite," *Separation and Purification Technology*, vol. 158, pp. 250-258, 2016.
- [8] I. Langmuir, *Journal of the American Chemical Society*, vol. 38, p. 2221–2295, 1916.
- [9] D. Božić, V. Stanković, M. Gorgievski and G. Bogdanović, *Journal Hazard. Materials*, vol. 171, p. 684–692, 2009.
- [10] E. Alvarez-Ayuso and A. Garcia-Sanchez, *Clays Clay Minerals*, vol. 51, pp. 475-580, 2003.

- [11] A. Hosseini-Bandegharai, M. Hosseini, Y. Jalalabadi, M. Sarwghadi, M. Nedaie, A. Aherian, A. Ghaznavi and A. Eftekhari, *Chemical Engineering Journal*, vol. 168, pp. 1163-1173, 2010.
- [12] O. Bello, O. Adelaide, M. Abdul Hammed and O. Abdul Muiz Popoola, *Macedonian Journal of Chemical Engineering*, vol. 29, p. 77–85, 2010.
- [13] K. Hall, L. Eagleton, A. Acrivos and T. Vermeulen, *Journal of Industrial Engineering and Chemistry*, vol. 5, pp. 212-223, 1966.
- [14] K. Choy, G. McKay and J. Potter, *Journal of Resource Conservation Recycle*, vol. 27, pp. 57-71, 1999.

CHAPTER 5

4. Conclusions and Recommendations

4.1. Conclusions

This study demonstrates the application of nanocomposite for the removal of highly toxic hexavalent chromium [Cr (VI)] ions from aqueous solution using polypyrrole-poly (vinyl) alcohol-magnetite (PPy-PvOH-Fe₃O₄) nanocomposite as an adsorbent. First, Fe₃O₄ was prepared by coprecipitation, using FeCl₃ and FeCl₂ as precursors at a ratio 1:2. Furthermore, PPy-PvOH-Fe₃O₄ nanocomposite was synthesized via in situ polymerization in the presents of FeCl₃ as an oxidant. It was established that PPy loading in the nanocomposite depends on the ratios of the constituent components during synthesis. X-ray diffraction (XRD) characterization revealed that the nanocomposite is crystalline in nature regardless of the ratios alteration between the three components. Fourier transform infra-red (FTIR) spectrum confirmed that indeed Cr (VI) was adsorbed in the nanocomposite. SEM, TEM and Zeta potential confirmed the external, internal morphology, and surface charge of the PPy-PvOH-Fe₃O₄ nanocomposites, respectively. Adsorption kinetics studies were performed under batch operation mode and the influence of PvOH polymer and magnetic content in the nanocomposite, individual constituent components, adsorbent dose and initial Cr (VI) concentration were all explored at room temperature and constant pH 12. It was revealed that the ratios of constituent components in the polymer blend significantly increased the adsorption process whereby 56:42 PPy-PvOH nanocomposite performed better [96%, 30 ppm] than 74:26, 64:36, and 52:48 polymer blend. The 56:44 polymer blend performance was exemplary compared to its constituent components. Fe₃O₄ was introduced to the blend in order to increase the polymer blend efficiency. However, a slight decrease in the removal percentage was observed after adding 2% of Fe₃O₄ nanoparticle for Cr (VI) removal. This may be due to particle agglomeration of the nanoparticle. Adsorption capacity of the nanocomposite increased with increase in adsorbent dosage and increase in initial Cr(VI) concentration and reached maximum at 91% removal efficiency of Cr(VI), however, As(III) showed constant removal as the percentage of removal did not change drastically. When adsorption kinetic data was fitted to both linear and nonlinear kinetic models, it was established

that adsorption of Cr (VI) on PPy-PvOH-Fe₃O₄ is through a chemisorption process and that intraparticles played a key role in controlling the adsorption process. Furthermore, results revealed that by using 10 ml of 30ppm Cr (VI) aqueous solution with 0.12g at 45 minutes and pH 12 optimum conditions, the Cr (VI) removal of was sufficient to achieve 91.3%. And also using 10 ml of 150 ppm of As(III) aqueous solution with 0.10g at 30 minutes and pH 12 optimum conditions. The removal of As(III) from aqueous solution was also sufficient and 100% removal under the optimal conditions.

4.2. Recommendations

This research is at its early stages and therefore there were a number of challenges encountered throughout the experimental studies, which prompt us to recommend the following for future works. The morphology studies of the nanocomposites indicated that an incorporation of Fe₃O₄ NPs was not homogeneously dispersed among the polymer matrix. Hence, it is important to improve the surface chemistry properties of Fe₃O₄ NPs by incorporating nanomaterial such as functionalized carbon based material (graphene oxide and carbon nanotubes). This will result in Fe₃O₄ NPs with improved properties; these include surface area, active sites (surface chemistry) and their dispersion. These properties will minimize the agglomeration of Fe₃O₄ NPs within the polymer thus enhancing the adsorption capacity for removal of heavy metals in wastewater. Mostly, it is important to use real wastewater samples from the industries in order to gather more information regarding the adsorption ability and selectiveness of this nanocomposites towards removal of Cr (VI) ions and other heavy metals.